UNIVERSITY OF CALIFORNIA
RIVERSIDE

Neutral and Anionic Carboranes as Electronically and Sterically Diverse Phosphine Substituents

A Dissertation submitted in partial satisfaction
of the requirements for the degree of

Doctor of Philosophy

in

Chemistry

by

Christopher Alexander Lugo

June 2018

Dissertation Committee:
Dr. Vincent Lavallo, Chairperson
Dr. Hill Harman
Dr. Catharine Larsen

The Dissertation of Christopher Alexander Lugo is approved:

_____

_____

_____

Committee Chairperson

University of California, Riverside

Acknowledgements

First and foremost I would like to thank Dr. Vincent Lavallo for taking me in to his lab and giving me much guidance and support throughout the years. The experience gained from graduate school will most certainly shape my future and I can never say thank you enough. Thank you. I would also like to say thanks to all my lab mates who have battled the chemistry gods with me, for better and for worse. You guys made the lab a very entertaining place to be and I am very glad for the relationships that have been forged in Room 403 and 409. I would also like to thank all the helpful graduate students of the 4th floor chemical sciences building for helping me with random questions I had about everything. I would like to thank the faculty that I have encountered throughout my undergraduate and graduate years. You all taught in a way that displayed the pure passion you had for chemistry and that no doubt had a role to play in me pursuing this degree. May you continue to inspire others to pursue a path in chemistry. I would also like to thank Dr. Borchardt and Dr. Tham for dealing with me and assisting me through all my NMR and X-ray troubles. I would like to thank my friends and my family for supporting me throughout the years. Special thanks to my wife and my daughter who have been with me through the ups and downs. They have been a source of constant motivation and I would not be where I am today without them. Thank you.

The text, figures, and schemes for the following chapters have been reproduced, in part or in their entirety, from the following published or submitted manuscripts.

Chapter 2: “Synthesis of a Hybrid m-Terphenyl/o-Carborane Building Block: Applications in Phosphine Ligand Design” C. A. Lugo, C. Moore, A. Rheingold, V. Lavallo, *Inorg. Chem.,* **2015**, *54*2, 2094

Chapter 3: “The Inductive Effects of 10 and 12-Vertex *closo*-Carborane Anion Ligand Substituents: Cluster Size and Charge Make a Difference” J. Estrada, C. A. Lugo, S. G. McArthur, V. Lavallo, *Chem. Commun*., **2016,** *52*, 1824

ABSTRACT OF THE DISSERTATION

Neutral and Anionic Carboranes as Electronically and Sterically Diverse Phosphine Substituents

by

Christopher Alexander Lugo

Doctor of Philosophy, Graduate Program in Chemistry
University of California, Riverside, June 2018
Dr. Vincent Lavallo, Chairperson

The chemistry of carboranes has expanded greatly since their discovery in the 1960's. Displaying 3D aromaticity, superior thermal and chemical stability, and facile tunability, these molecules have seen a wide range of applications but little has been said for their potential as transition metal catalysts. We sought to remedy this rift by 1) constructing a library of ligands that integrate carboranes into phosphines as R-group substituents, 2) ligating the ligands to an array of transition metal centers, and 3) surveying the reactivity of the isolated metal complexes.

By substituting the inherently bulky *ortho*-carborane with a terphenyl moiety at the C-2 position, and a phosphine at the C-1 position, a massive ligand was created. The donor and steric properties were analyzed via a rhodium carbonyl complex. A nido version of the above terphenyl carboranyl phosphine was also synthesized and its behavior with iridium was investigated. Through preparation of phosphines of the anionic 12 and 10-vertex carboranes, rhodium carbonyl complexes were synthesized to quantitatively assess their donor properties. Through utilization of a carboranylphosphino iron complex, the ability to cyclically trimerize methylacrylate has been demonstrated through the isolation a phosphonium enolate species. Amongst the vast library of monoanionic carboranyl phosphines there are none containing a dianionic phosphine. Using PCl_3 as a launch pad, a variety of monoanionic and dianionic ligands were systematically prepared with ranging electronic and steric profiles.

Table of Contents

List of figures

List of Schemes

List of Supplemental Data

Chapter 1: Introduction

1.1 Birth of relevant carboranes

Designing a vast array of phosphines functionalized with the versatile carborane moiety is the focus of this dissertation. Carboranes have a unique three-dimensional structure (**Figure 1.1**) that features carbon and boron vertices that can be substituted with various functional groups. With a varying amount of carbon and boron content, cluster size, and overall associated charge, an arsenal of carborane clusters have been synthesized, but only a select few are relevant to this dissertation. For clarity in borane and carborane structures, B-H bonds are replaced with unlabeled vertices (**Figure 1.1**). Stemming from an attempt to develop boron based rocket fuels, the 1,2-dicarba-*closo*-dodecaborate carborane ($H_2C_2B_{10}H_{10}$), also commonly known as the *ortho*-carborane, was first synthesized in 1957 by Reaction Motors Inc. Six years later the cluster was published concurrently in 1963 by Thiokol and Olin-Mathieson.[1] Derived from the neutral *ortho*-carborane, also abbreviated as *o*-carborane, the monoanionic dicarba-*nido*-undecaborane was first reported in 1964 by Hawthorne ($H_2C_2B_9H_{10}^-$).[2] Quickly following the previously mentioned emerging carboranes, in 1967 Knoth synthesized the monoanionic carba-*closo*-dodecaborate ($HCB_{11}H_{11}^-$) and the monoanionic carba-*closo*-nonadecaborate ($HCB_9H_9^-$).[3] These four carborane clusters are the foundation of the chemistry explored in this dissertation (**Figure 1.2**).

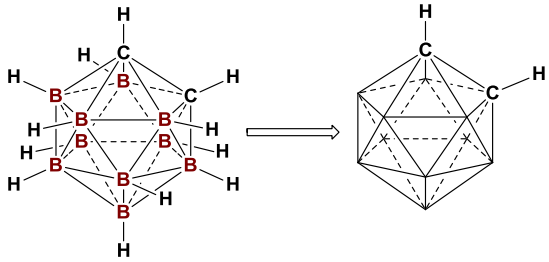

Figure 1.1 - *ortho*-carborane (left), simplified with unlabeled vertices equivalent to B-H bonds (right).

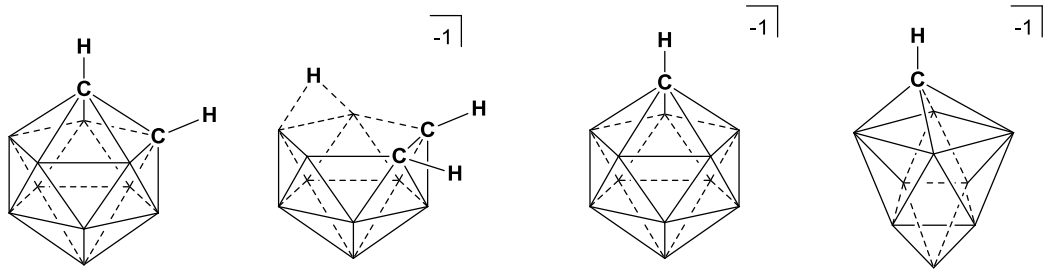

Figure 1.2 – Featured carboranes (left to right): $H_2C_2B_{10}H_{10}$, $H_2C_2B_9H_{10}^-$, $HCB_{11}H_{11}^-$, and the $CB_9H_9^-$. Fluxional bridging hydride noted with dashed lines to H atom in $H2C_2B_9H_{10}^-$.

1.2 Properties and bonding

Carboranes have come to be renowned for the excellent chemical and thermal stability, a superior property that is rooted in their non-classical electronic structure. Typical organic molecules follow the 2-center 2-electron (2c2e) bonding concept, where two electrons are shared between two atoms to constitute a single bond. Upon viewing the structure of a carborane, it can be seen that all the skeletal carbon and boron atoms appear to participate in at least five or six bonds, exceeding their typical valence and violating the 2c2e approach. Instead, skeletal bonding can be viewed more as a multi-centered 2-electron motif, in which an electron pair is delocalized over more than 2 atoms. Since the skeletal electrons are delocalized over the entire surface of the three-dimensional cluster, carboranes have been noted for being 3-D aromatics. This claim for 3-D aromaticity is supported through its correlation to the well established 2-D aromatic systems. Magnetic susceptibility exaltation values describe ring current associated with aromatic systems, where a high negative value is aromatic, a near zero value is non-aromatic, and a highly positive value is anti-aromatic. The $H_2C_2B_{10}H_{10}$ and the $HCB_{11}H_{11}^-$ carboranes have magnetic exaltation values of -155.86 ppm cgs and -153.48 ppm cgs,[4] compared to benzene -13.4 ppm cgs. Nucleus-independent chemical shift

(NICS) gauge the absolute magnetic shielding at the center of a ring with NICS values following the same trend as magnetic susceptibility exaltation values. Once again the $H_2C_2B_{10}H_{10}$ and the $HCB_{11}H_{11}^-$clusters have highly negative values, -35.4 ppm and -34.36 ppm respectively,[4] suggesting aromaticity. Also, akin to an aromatic benzene ring, the cage can undergo electrophilic substitution, in which B-H vertices are able to undergo substitution to B-X vertices (X being a suitable electrophile), with cluster halogenations being extremely prevalent in our lab.[5]

As previously mentioned, the classical 2c2e bonding motif is insufficient in describing carborane cluster bonding. This explanation void was filled when an ingenious and elegant method for determining the skeletal electron count was formulated by Kenneth Wade and further elaborated on by Michael Mingos. The now well established Wade's rules (or also Wade-Mingos) rules clearly relate borane cluster geometry and vertex count with the number of skeletal electrons. To determine the number of electrons participating in skeletal bonding in a deltahedron cage with *n* vertices, the number of skeletal electron pairs is *n* + 1. If there is a *nido* geometry, a *closo* cluster having a one vertex removed, or an arachno geometry, corresponding to two vertices removed, the number of skeletal electron pairs is (n + 1) + 1 and (n + 2) + 1 respectively. For the dianionic $B_{12}H_{12}^{2-}$ cluster which has a total of 50 electrons, 24 electrons are involved in 12 B-H bonds, 24 electrons corresponding to 12 boron vertices, leaving 2 additional electrons for an overall -2 charge. Replacing a B-H vertex with a C-H vertex, to make the $HCB_{11}H_{11}^-$, adds an additional electron to the cage from carbon, in turn decreasing the

overall charge of the cluster from -2 to -1. Replacing an additional B-H vertex with a C-H vertex then affords the charge-free neutral $H_2C_2B_{10}H_{10}$.

1.3 $H_2C_2B_{10}H_{10}$

In 1963 the *o*-carborane was first reported in literature[1] and has since then been the most studied carborane. The initial synthesis utilized decaborane, $B_{10}H_{14}$, a weak lewis base, commonly acetonitrile, and acetylene, which were refluxed to lose an equivalent of H_2 gas and produce $H_2C_2B_{10}H_{10}$ (**Scheme 1.1**). Early on it was observed that a wide variety of alkynes could be tolerated including mono and di-substituted alkynes with varying functional groups, excluding acids or alcohols that can degrade decaborane, giving a convenient avenue in which to tune the subsequently produced *o*-carborane.[5] It was also reported that the C-H proton was acidic enough to be deprotonated by *n*-butyl lithium to give the mono or dianionic carborane, depending on the number of available C-H protons. This renders the cluster nucleophilic enough to attack a sufficiently available electrophile. In 1963 Schroeder reported the synthesis of the first carboranyl phosphine through this route,[6] using the dianionic lithium salt of the *o*-carborane and two equivalents of $P(Ph)_2Cl$ as the electrophile (**Scheme 1.2**). He built upon this work further in 1965 through the reaction of the recently isolated bisphosphinocarborane with $NiCl_2$ to give the first transition metal complex with a carboranyl phosphine ligand.[7] Since then, a plethora of *o*-carborane based phosphines

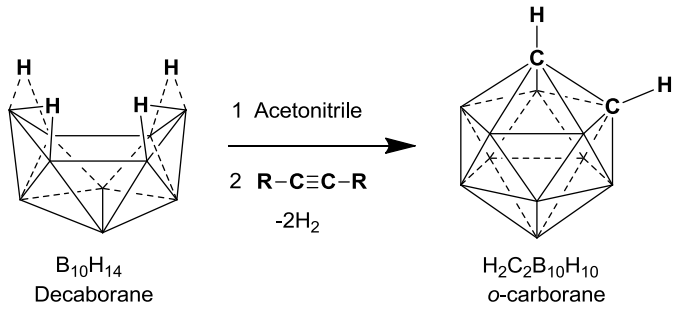

Scheme 1.1- Synthesis of the $H_2C_2B_{10}H_{10}$.[1]

ligands have been made and their catalytic ability demonstrated.[8] Despite this, typical hydrocarbon based phosphines are still superior in regards to catalytic applications, overshadowing the *o*-carborane's unrealized potential in this field.

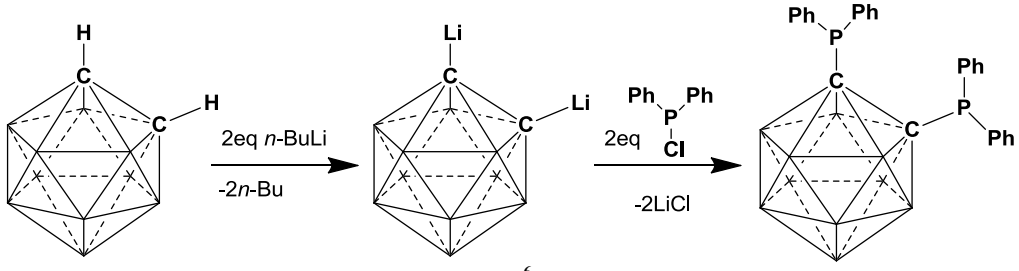

Scheme 1.2 – Synthesis of first carboranyl phosphine.[6]

1.4 *nido*-$H_2CB_9H_{10}^-$

The superior chemical stability of the carborane cluster is one of its prized properties that have been taken advantage of in its many applications. Still, the cage can undergo degradation when exposed to an alcoholic base. In 1964, Hawthorne synthesized the first *nido*- $H_2CB_9H_{10}^-$ carborane by extruding a boron vertex from the $C_2B_{10}H_{12}$ cage with potassium hydroxide in methanol (**Scheme 1.3**).[2] He also was able to clearly determine that a boron from the upper pentagonal belt was extruded, specifically the borons adjacent to both carbon atoms, through elegant labeling studies. Importantly, the degradation can also be achieved in alcohol-free conditions, where piperdine is used as a nucleophilic base and benzene as a solvent.[9] Although *o*-carboranyl phosphine was prepared quickly

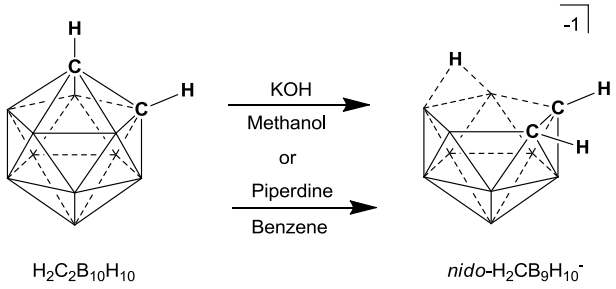

Scheme 1.3 – Methods for synthesizing *nido*-$H_2CB_9H_{10}^-$ from $H_2CB_{10}H_{10}$.[2,9]

after its precursor, it wasn't until 1995 that Teixidor was able to make the *nido*-carbonyl phosphines.[10] Derived from the *o*-carboranyl phosphines, it was seen that boron extrusion was not exclusive in the presence of an alcoholic base due to C_{carb}-P bond cleavage. Instead, success was obtained through the alternate previously reported method, utilizing piperdine and aromatic hydrocarbon solvents (**Scheme 1.4**). *nido*-Carboranyl phosphines and their reactivity with transition metals has been well documented,[11] but the overall utility of this cluster as a ligand is still in its infancy.

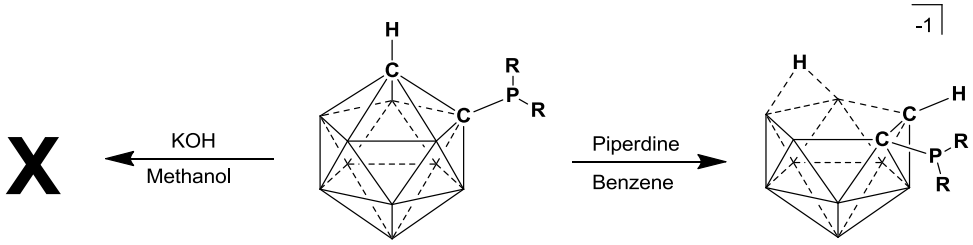

Scheme 1.4 – Clean synthesis of *nido*-carboranyl phosphine achieved when using piperdine instead of potassium hydroxide.[10]

1.5 $HCB_{11}H_{11}^-$

Along with the emergence of the $H_2C_2B_{10}H_{10}$ and the $H_2C_2B_9H_{10}^-$ carboranes, the 12-vertex monoanionic $HCB_{11}H_{11}^-$ cluster was synthesized by Knoth in 1967,[3] also starting from decaborane. A more efficient overall synthesis had been achieved from the work of Reed in 2010[12] and is frequently used (**Scheme 1.5**) in our lab where the $HCB_{11}H_{11}^-$ carborane is a main focal point. In addition to retaining all the stability benefits of being a carborane, this specific class of carboranes is also ubiquitous for its role as a weakly coordination anion. Complete halogenation of the boron vertices

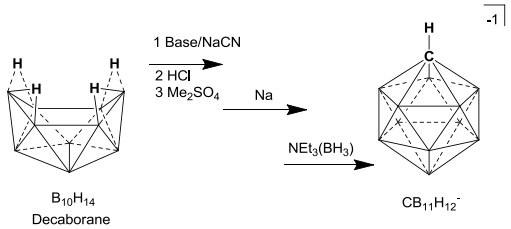

Scheme 1.5 – Preparation of $CB_{11}H_{12}$ cluster.[12]

represents one method of tuning the steric and electronic properties of the carborane, which was achieved in 1997 by Xie.[13] Although computational studies place a larger negative charge density around the more electronegative carbon atom,[14] the electrophilic aromatic substitution like reaction places halogens first at the B-12 position (antipodal to the carbon), then to boron vertices at ascending pentagonal belts there from (**Scheme 1.6**). This process greatly enhances the stability and its ability to act as an extremely weakly coordinating anion which has been exploited to create super acids[15] and isolate highly reactive cationic species.[16a,b,c] C-H functionalization is still a facile method in which new species can be produced. In 1993 Reed took advantage of this to produce the first $HCB_{11}H_{11}^-$ phosphines with the intention of enhancing the overall solubility of the cluster.[17] Two decades later, our lab reported the first transition metal complex containing the fully chlorinated $HCB_{11}Cl_{11}^-$ phosphine by synthesizing a Au(THT) complex and applied it as a hydroamination catalyst for amines and alkynes.[18] In contrast to its *o*-carborane cousin, for which evidence of catalytic potency is lacking, the gold catalyst showed unprecedented turnover numbers in this realm, taking advantage of the clusters weakly coordinating ability to enhance the reactivity at the metal center. Other transition metal complexes and catalysts have been reported utilizing the $HCB_{11}H_{11}^-$cluster and its

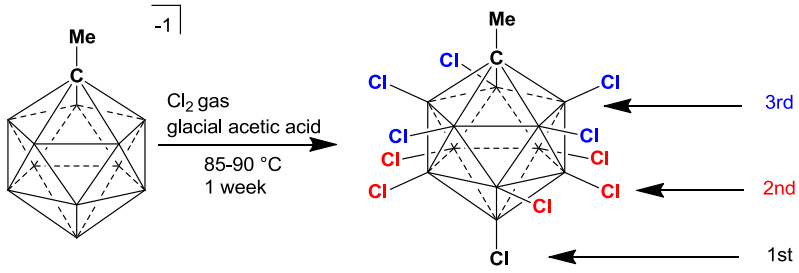

Scheme 1.6 – Chlorination of Me-1-$CB_{11}H_{11}^-$.[13] The order in which Cl atoms are also substituted is indicated.

derivatives,[19] with many other avenues being pursued in addition to its use as an anionic, sterically bulky, extremely weakly coordinating phosphines substituent.

1.6 $HCB_9H_9^-$

Alongside the larger 12-vertex $HCB_{11}H_{11}^-$, the 10-vertex $HCB_9H_9^-$ carborane was synthesized in 1967 by Knoth.[3] This carborane can alternatively be made through a Brellochs reaction, where an optimized three-stage procedure was developed by Ringstrand in 2009.[20] Starting from decaborane, $B_{10}H_{14}$, a boron vertex is replaced with a carbon atom by addition of formaldehyde to a hexane and aqueous sodium hydroxide mixture (**Scheme 1.3**).. This open cluster can be closed through oxidation with I_2 to give the 2-closo-HCB_9H_9 product. The carbon can thermally isomerize from the 2 to the 1 position by refluxing in DME for 5 days, giving the 1-closo-HCB_9H_9 desired product.

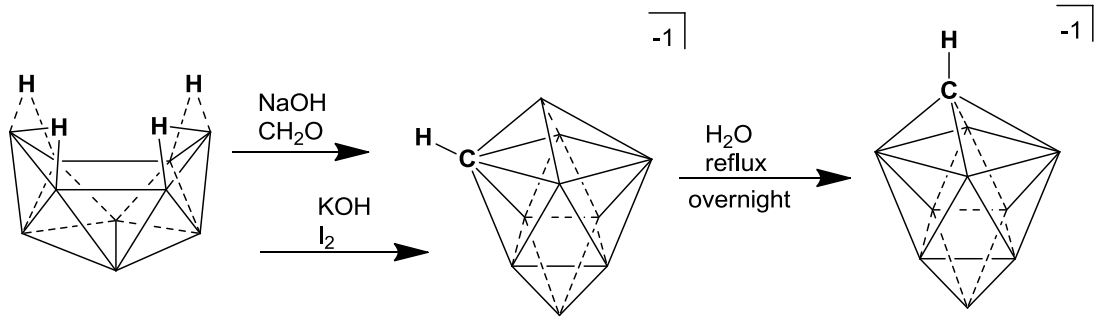

Scheme 1.7- The synthesis of $CB_9H_9^-$ with optimized 3rd step.

This procedure has been the method of choice in our lab, with a massive amount of decaborane being converted on 10 gram scales or more. Through our labs work with the 10-vertex carborane an alternative, more environmentally friendly, optimization was discovered. Instead by refluxing in water instead of DME, not only is a hazardous organic solvent waste avoided, the reaction time decreases from five days to less than 10 hours. Analogous to the $HCB_{11}H_{11}^-$ in properties and reactivity, $HCB_9H_9^-$ can also undergo

stepwise halogenations to form the halo-derivatives. This was first demonstrated in 2000 by Xie, by taking the $HCB_9H_9^-$ and adding triflic acid plus iodine monochloride to a sealed reaction vessel and heating at 230 °C for 2 days.[21] The afforded $HCB_9Cl_9^-$, commonly used as the trimethylammonium salt, is frequently prepared in our lab. Extreme caution is always taken as the reaction container is a pressure vessel, showcasing one of the most dangerous aspects of operating in a chemistry lab. C-H functionalization is also achieved through reaction with *n*-butyl lithium and subsequent treatment with a chlorophosphine to give the ensuing $CB_9H_9^-$ phosphine. Its first reported use as a ligand was seen in our lab in 2016, where its rhodium complex will be discussed later in this dissertation.

1.7 Preview of dissertation

The four above mentioned carboranes have established their ever expanding roles in chemistry, some more so than others, and also have played the lead in my work here at the University of California Riverside. The construction of a terphenyl *o*-carboranyl phosphine and its nido derivative has been achieved and the analysis of their steric and electronic properties is reported. The electronic properties of the 12 and 10-vertex anionic carboranyl phosphines were assessed through the synthesis of rhodium carbonyl complexes. The reactivity of the $HCB_9H_9^-$ phosphine with iron sources was also investigated with some interesting results with methylacrylate. Using PCl_3 as an electrophile, a variety of mono substituted and disubstituted phosphines could be prepared and comparisons between the hydridic and chlorinated 10-vertex phosphines could be drawn.

1.8 References

1. M. M. Fein, J. Bobinski, N. Mayes, N. Schwartz, M. S. Cohen, *Inorg. Chem*., **1963**, *2*, 1111.

2. R. Wiesbock, M. F. Hawthorne, *J. Am. Chem. Soc.,* **1964**, *86*, 1962.

3. W. H. Knoth, *J. Am. Chem. Soc.,* **1967,** *89*, 1274.

4. P. Schleyer, K. Najafian, *Inorg. Chem.,* **1998**, *37*, 3454.

5. M. M. Fein, D. Grafstein, J. E. Paustian, J. Bobinski, B. M. Lichstein, N. Mayes, *Inorg. Chem.*, **1963**, *2*, 1115.

6. R. P. Alexander, H. Schroeder, *Inorg. Chem.,***1963**, *2*, 1107.

7. H. D. Smith, *J. Am. Chem. Soc.,* **1965**, *87*, 1817.

8. M. Kumada, K. Sumitani, Y. Kiso, K. Tamao, *J. Organomet. Chem*., **1973,** *50*, 319.

9. L. I. Zakharkin, G. G. Zhigareva, *lzv. Akad. Nauk SSSR,Ser. Khim.,* **1965**, *5,* 932.

10. F. Teixidor, C. Vinas, M. M. Abad, R. Nunez, R. Kivekas, R. Sillanpaa, *J. Organomet. Chem*., **1995**, *503*, 193.

11. A. R. Popescu, F. Teixidor, C. Vinas, *Coord. Chem. Rev*., **2014**, *269*, 54.

12 C. A. Reed, *Acc. Chem. Res,* **2010,** *43*, 121.

13. Z. Xie, C. Tsang, F. Xue, T. C. W. Mak, *Inorg. Chem.,* **1997,** *36,* 2246.

14. I. Zharov, T. Weng, A. Orendt, D. Barich, J. Penner-Hahn, D. Grant, Z. Havlas, J. Michl, *J. Am. Chem. Soc.,* **2004**, *126*, 12033.

15. C. A. Reed, *Acc. Chem. Res.,* **1998,** *31* , 133.

16. (a) M. Nava,I. V. Stoyanova, S. Cummings, E. S. Stoyanov, C. A. Reed, *Angew. Chem. Int. Ed,* **2014**, *53*, 1131. (b) A. S. Jalilov, L. Han, S. F. Nelsen, I. A. Guzei, *J. Org. Chem,* **2013**, *78*, 1137. (c) K. C. Kim, F. Hauke, A. Hirsch, P. D. W. Boyd, E. Carter, R. S. Armstrong, P. A. Lay, C. A. Reed, *J. Am. Chem. Soc.,* **2003**, *125*, 4024.

17. T. Jelinek, P. Baldwin, W. R. Scheidt, C. A. Reed, *Inorg. Chem.* **1993, *32,*** 1982.

18. V. Lavallo, J. H. Wright II, F. S. Tham, S. Quinlivan, *Angew. Chem. Int. Ed.,* **2013**, *52*, 3172.

19. (a) A. El-Hellani, C. E. Kefalidis, F. S. Tham, L. Maron, V. Lavallo, *Organometallics***, 2013**, *32*, 6887. (b) J. Estrada, D. H. Woen, F. S. Tham, G. M. Miyake, V. Lavallo, *Inorg. Chem.***, 2015**, *54*, 5142. (c) S. P. Fisher, A. El-Hellani, F. Tham, V. Lavallo, *Dalton Trans*., **2016,** *45*, 9762. (d) A. L. Chan, J. Estrada, C. E. Kefalidis, V. Lavallo, *Organometallics***, 2016,** *35*, 3257.

20. A. Franken, C. A. Kilner, M. Thornton-Pett, J. D. Kennedy, *Chem. Commun.,* **2002,** *18*, 2048.

21. C. Tsang, Q. Yang, E. T. Sze, T. C. W. Mak, D. T. W. Chan, and Z. Xie, *Inorg. Chem.,* **2000,** *39,* 3582.

Chapter 2: Terphenyl carboranyl phosphines

2.1 Abstract

A hybrid terphenyl/o-carborane ligand building block has been synthesized by the reaction of a $B_{10}H_{14}$ with a *m*-terphenylalkyne. This substituent was used to prepare an extremely sterically demanding carboranylphosphine. Reaction of the bulky phosphine with $[ClRh(CO)_2]_2$ produces the mono phosphine complex $ClRhL(CO)_2$, which subsequently extrudes CO under vacuum to afford the dimeric species $[ClRhL(CO)]_2$. The latter complex does not react with excess phosphine and is resistant to toward cyclometalation, which is in contrast to related *o*-carborane phosphine complexes. A *nido* counterpart had also been derived from the previous ligand through boron extrusion with piperdine. From the *nido* phosphine an iridium complex was prepared, who structural characteristics bear a remarkable resemblance with the previously reported $CB_{11}H_{11}^-$ iridium complex.

2.2 Introduction

Bulky hydrocarbon substituents are key components in ligand design. Sterically demanding groups both favor the formation of low-coordinate species and kinetically protect reactive metal centers. Low-coordinate transition-metal complexes are of practical importance because of their prominent role in catalysis and the formation of M−M multiply bonded species. One of the bulkiest ligand substituent families is derivatives of the m-terphenyl 1 (**Figure 2.1**). The coordinating atom or group is typically attached at position A^1 or B^2 on the central terphenyl aromatic ring. Alternatively, as exemplified by

the elegant work of Power and co-workers,[3] the terphenyl itself can be used as a massive X-type ligand when coordinated directly to a metal center at position B.

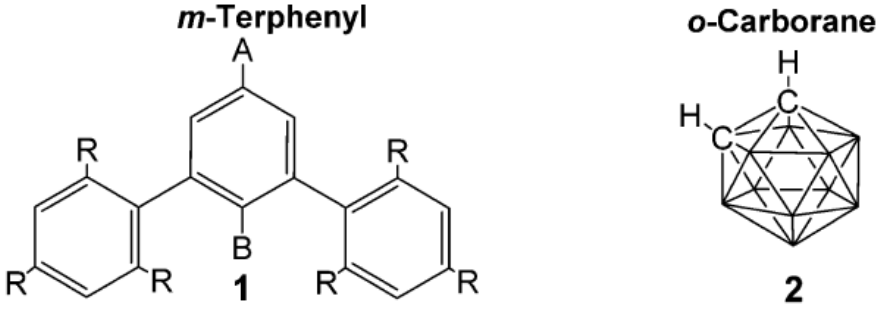

Figure 2.1- Representations of *m*-terphenyl **1** and *o*-carborane **2**.

Interesting alternatives to bulky hydrocarbon groups are the carborane and boron cluster compounds.[4] Because of their unusual electronic structure and distinct polyhedral geometries, these ligand substituents produce unique coordination environments.[4a,b] Particular progress has been made in the design of carboranylphosphine ligands[5] and, more recently, N-heterocyclic carbenes (NHCs).[6] Most investigations have focused on the utilization of icosahedral dicarbaborane clusters ($H_2C_2B_{10}H_{10}$) or anionic nido derivatives ($H_2C_2B_9H_{10}^-$) as hydrocarbon surrogates.[4a,b] Because of their accessibility,[7] derivatives of the *o*-carborane **2** are most often implemented in ligand design (Figure 1, top right). *o*-Carborane clusters can be assembled by the reaction of functionalized alkynes with decaborane ($B_{10}H_{14}$).[7] We envisioned utilizing this reaction methodology to couple a substituted m-terphenyl 1 with an o-carborane motif **2** to create a superbulky ligand building block. Furthermore, *o*-carboranylphosphines undergo facile transformation to anionic *nido* derivatives[8], providing two analogous but distinct species for investigation. Here we report the synthesis of such a hybrid m-terphenyl/o-carborane

architecture its derivatization to a phosphine ligand, production of its *nido* cousin, and subsequent studies of their reactivity with rhodium(I) and iridium(I) metal centers.

2.3 Results and discussion

2.3.1 *o*-carborane terphenyl

As a starting *m*-terphenylalkyne, we chose the triisopropylphenyl-substituted derivative **3**, whose isopropyl resonances provide a convenient NMR signature (**Scheme 2.1**). Installation of the alkyne moiety at position A on the *m*-terphenyl was strategically chosen to project the massive aromatic ring system in the coordination sphere of subsequent transition-metal complexes, vide infra. The novel alkyne **3** is readily prepared from the corresponding bromo-*m*-terphenyl[1a] via Sonogashira coupling (see the Supporting Information for details). The subsequent reaction of **3** with $B_{10}H_{14}$ in acetonitrile affords the corresponding hybrid m-terphenyl/o-carborane **4** in 75% yield. Deprotonation of the C−H vertex of **4** with n-butyllithium, followed by the reaction with $ClP(iPr)_2$ affords the corresponding air-stable phosphine **5**.

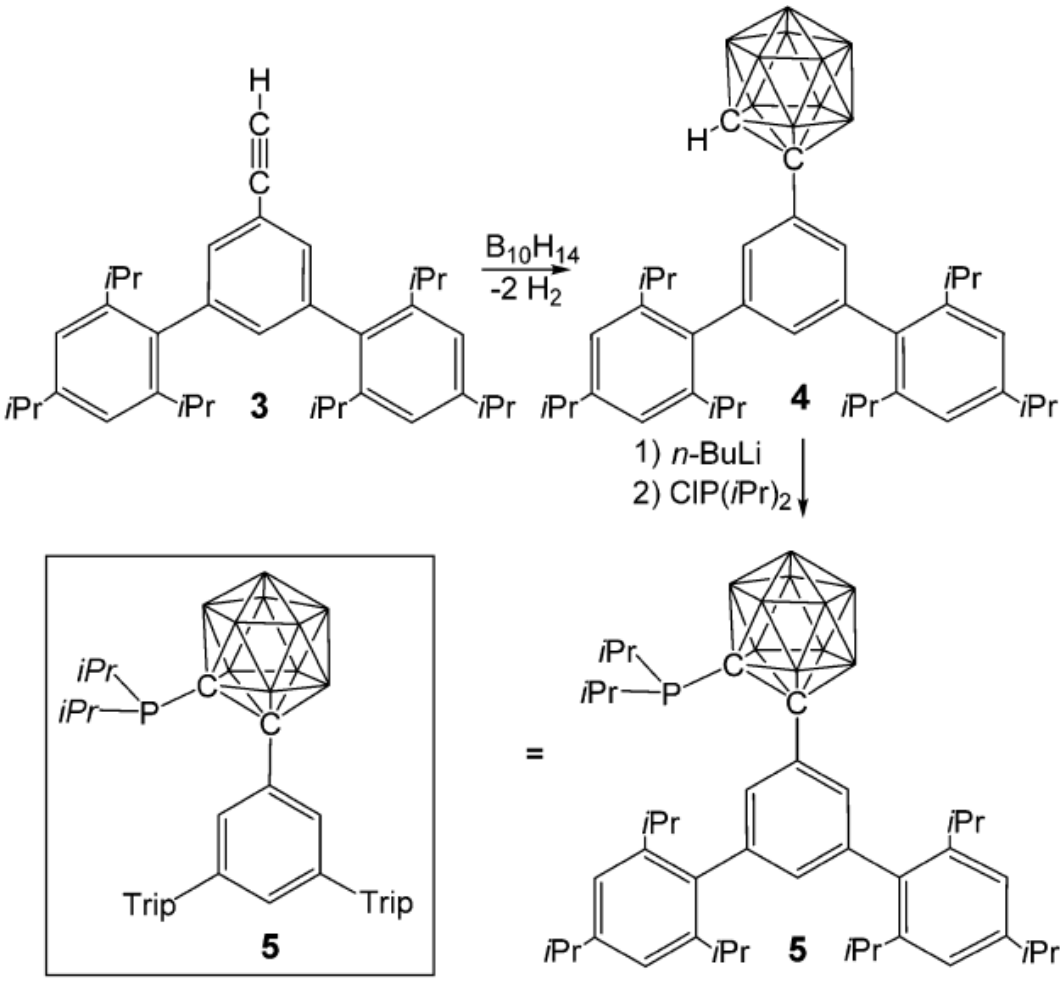

Scheme 2.1 - Synthesis of the hybrid *m*-terphenyl/*o*-carborane building block **4** and its derivatization to a phosphine ligand **5**. Unlabeled carborane vertices = B−H.

We next turned our attention to the coordinative ability of ligand **5** with rhodium(I). The carbonyl complex $[ClRh(CO)_2]_2$ was chosen as a starting material because IR analysis of the CO stretching frequencies of the ensuing complex would provide insight into the donor ability of the ligand. The reaction of ligand **5** with $[ClRh(CO)_2]_2$ at 60 °C very slowly (6 days) produces the corresponding *cis*-dicarbonyl complex **6** (**Scheme 2.2**), as confirmed by multinuclear NMR (^{31}P, δ = 88.4 ppm, d, $^{1}J_{Rh,P}$ = 190.5 Hz) and IR [ν(CO) = 2089 and 2022 cm^{-1}] analysis. Complex **6** is stable in

solution but extrudes CO under vacuum to produce the monocarbonyl chloro-bridged dimer **7**, as indicated by multinuclear NMR (^{31}P, δ = 96.7 ppm, d, $^{1}J_{Rh,P}$ = 194.3 Hz) and IR [ν(CO) = 1987 cm^{-1}] analysis. Bubbling CO through a solution of **7** reforms **6**, which indicates that the process is reversible. Comparison of the CO stretching frequencies of **6** with reported analogous ClRhL(CO)$_2$ species supported by P(*t*Bu)$_3$ [ν(CO) = 1960 cm^{-1}][9] and PPh$_3$ [ν(CO) = 1979 cm^{-1}][10] shows that ligand **5** is a relatively poor electron donor. This observation is in agreement with Röhrscheid and Holm's[5b] and Teixidor et al.'s[5m,n] reports, which demonstrate that o-carborane acts as a strong electron-withdrawing group when bound to phosphines by the carbon vertex.

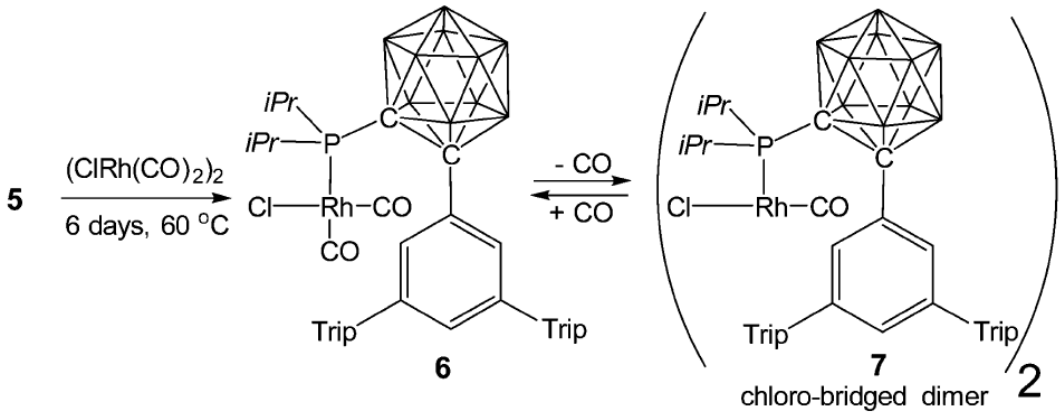

Scheme 2.2 – Synthesis of complexes **6** and **7**. Unlabeled verticies = B-H.

Many classical phosphines behave similarly to **5** to produce analogous dimeric [ClRhL(CO)]$_2$ species.[10] Such complexes readily react with an additional phosphine ligand to produce ClRhL$_2$(CO) species. What is unusual in this case is that the addition of excess (5 equiv, 60 °C, 24 h) phosphine ligand **5** to **7** does not result in the formation of a diphosphine adduct, as indicated by ^{31}P NMR and IR spectroscopy. Additionally, in contrast to related [ClRhL(CO)]$_2$ complexes containing *o*-carborane phosphines that

feature an unsubstituted C−H vertex,[5i] **7** is indefinitely stable in solution and does not undergo decomposition by B−H cyclometalation. The resistance of **7** toward additional phosphine coordination and cyclometalation is likely due to the steric influence of the *m*-terphenyl substituent.

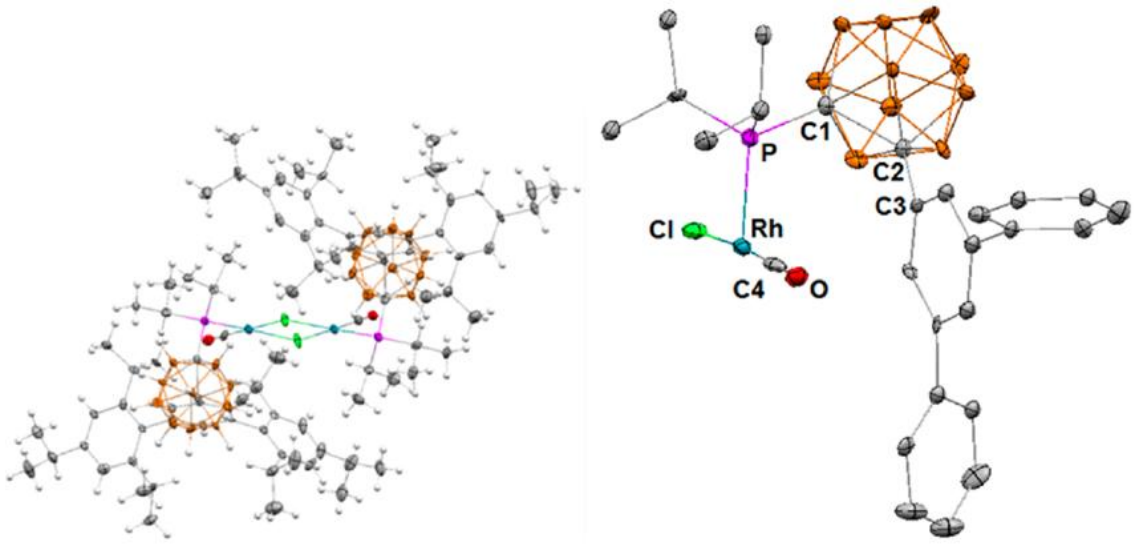

Figure 2.2 - Full molecular structure of complex **7** (left). Simplified view of half of dimer **7** (right; hydrogen atoms and Trip isopropyl groups are omitted for clarity). Thermal ellipsoids drawn at the 50% probability level. Color code: C, gray; B, brown; O, red; H, white; P, violet; Rh, blue; Cl, green. Selected bond lengths (Å; average from both halves of the dimer): P−Rh = 2.2297(19), P−C1 = 1.895(9), C1−C2 = 1.775(10), C2−C3 = 1.513(10), Rh−C4 = 1.785(8), C4−O = 1.156(8).

To gain insight into the steric parameters of ligand **5**, we carried out a single-crystal X-ray diffraction study of complex **7** (**Figure 2.2**). In the solid state, the m-terphenyl substituents are projected above and below each of the square-planar rhodium centers (**Figure 2.2**, left). The geometric parameters of each half of the dimer are essentially identical; thus, a simplifed view of **7** is provided for further discussion (**Figure 2.2**, right). The Rh−P−C1−C2 dihedral angle is 47.7(5)°, which skews the *m*-terphenyl group to the side of the square plane containing the carbonyl substituent. This

observation reveals that the P−C1 bond can rotate to some extent even with the presence of two gearing P−*i*Pr groups that direct the *m*-terphenyl substituent toward the metal center. While the unusual shape of the ligand renders the cone angle description of the steric parameter uninstructive, the percent buried volume (% V_{bur}) approach[11] provides a better gauge of the steric impact of this ligand. In the observed conformation, % V_{bur} of ligand **5** in complex **7** is 45.7%. Comparatively, %V_{bur} for uncoordinated P(*i*Pr)$_3$ is 37.6%.[11] This means that replacement of a single *i*Pr substituent of P(*i*Pr)$_3$ with the m-terphenyl/o-carborane substituent leads to an increase in % V_{bur} of at least 8.1%. When % V_{bur} of ligand **5** in complex **7** is calculated with the Rh−P−C1−C2 torsional angle set to 0°, which rotates the central benzene ring of the m-terphenyl group directly underneath the square-planar rhodium atom, a significant increase in steric impact is observed (% V_{bur} = 52.1). On the basis of the symmetry of the ^{1}H NMR spectra of **7**, this is a likely conformation in solution because the m-terphenyl substituent swings back and forth underneath the rhodium square plane (via partial P−C1 rotation). Therefore, the actual steric effect resulting from *i*Pr substitution by the m-terphenyl/ocarborane substituent is an increase of +8.1−14.5% V_{bur}, depending on the conformation adopted in solution.

2.3.2 *nido*-Carboranyl terphenyl

To complement the neutral compound **5**, we sought to synthesize an anionic nido counterpart, whose altered electronics would complement the exploration of this ligand scaffold. The conversion of *o*-carboranyl phosphines into their corresponding nido species has been shown to be accomplished with piperidine as the boron extrusion agent[8] and thus inspired our synthetic methodology (**Scheme 2.3**).

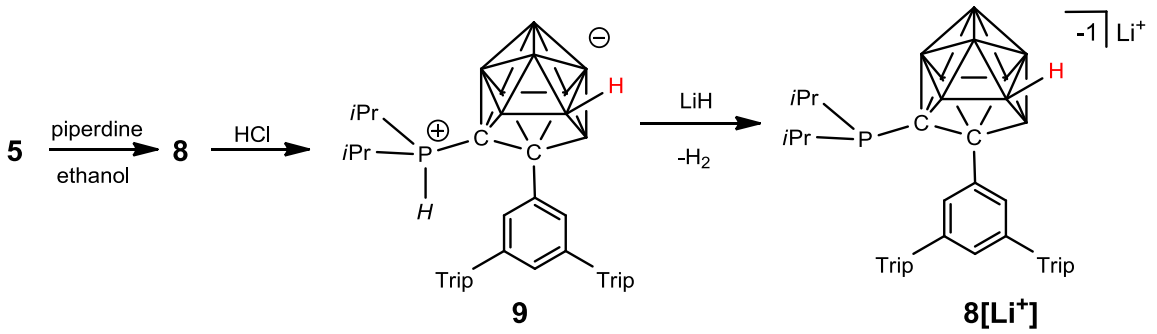

Scheme 2.3 - Synthesis of *nido*-carboranyl ligand **8[Li$^+$]** from deprotonation of zwitterion **9**. Unlabled boron verticies = B-H. Hydrogen in red represents the fluxional bridging hydride.

Treatment of **5** with piperdine in refluxing ethanol produced the the *nido*-carboranyl terphenyl phosphine **8** as the major product (^{31}P NMR 17.2 ppm), along with a minor species. Subsequent addition of aqueous HCl afforded the cleanly isolated, protonated zwitterion **9**. This is supported by the ^{31}P NMR which shows a doublet at 38.14 ppm (^1J(P-H) = 445.4 Hz) and a doublet of doublets at 4.63 ppm (^{1}H NMR dd, ^1J(P-H) = 445.4 Hz, ^2J(H-H) = 7.4 Hz). This zwitterionic compound was then treated with LiH to give the lithium salt **8[Li$^+$].** Destruction of cluster symmetry is apparent as the ^{11}BNMR displays multiple broad signals (-7.39, -9.10, -13.75,-17.20, -23.71, -30.55, -34.38 ppm). The fluxional bridging hydride of the nido species **8[Li$^+$]** is observed in the ^{1}HNMR as an upfield broad singlet at -2.30 ppm, characteristic of *nido*-carboranyl bridging hydrides.

Preliminary attempts in ligating **5** with various metal complexes including $[ClIrCOD]_2$ were met with much resistance. Due to its vast steric profile and weak coordinative ability, **5** does not react with $[ClIrCOD]_2$ even at elevated temperatures for extended time periods. In contrast to the *o*-carborane group that is considered electron withdrawing,[12] *nido*-carboranyl substituents are considered to be electron releasing,[13]

enhancing the ensuing phosphine's coordinative ability. In addition, the lithium counter cation on **8[Li$^+$]** serves as a built-in chloride abstraction tool, which can produce vacant coordination sites for the ligand to approach the metal. With these properties in mind, reaction of **8[Li$^+$]** with $[ClIrCOD]_2$ in DCM produced a single new downfield phosphorus resonance at 38.14 ppm, suggesting formation of a new complex **10** (**Scheme 2.4**). ^{1}H NMR analysis displayed two broad resonances suggesting coordinated cyclooctadiene at (4.68 and 4.76 ppm). In addition to the expected bridging hydride resonance, there were additional upfield broad singlets (-1.55 to -2.03), suggestive of B-H hydridic interactions. This is not uncommon as we had also reported an iridium cyclooctadiene complex containing a $CB_{11}H_{11}^-$ functionalized diisopropylphosphine, **11**, which observed double B-H agostic-like interactions in solution albeit below room temperature.[14]

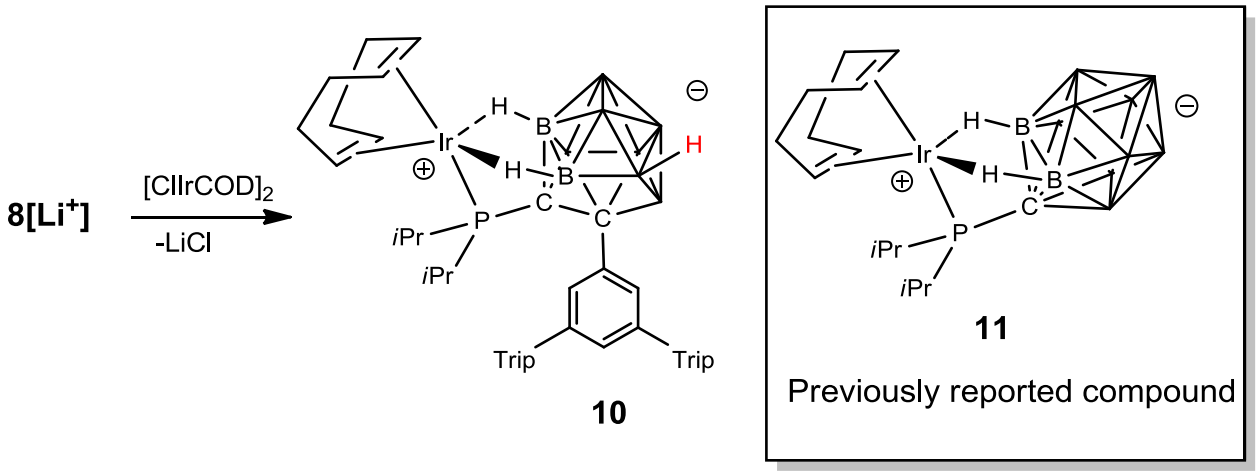

Scheme 2.4 – Synthesis of zwitterionic iridium complex **10**. Unlabled verticies = B-H. Hydrogen in red represents the fluxional bridging hydride. Schematic of iridium complex **11** utilizing the $CB_{11}H_{11}^-$ substituent.[14]

X-ray crystallographic data confirm ligation of anionic phosphine **8** to the iridium metal center (**Figure 2.3**). Though the B-H hydrogen locations are unreliable, the iridium-boron-boron triangle is nearly identical to the previous iridium complex (**10**: Ir-

B2 = 2.488 Å, Ir-B4 = 2.430 Å, B2-B4 = 1.720 Å; **11**: Ir-B2 = 2.467 Å, Ir-B4 = 2.491 Å). The suggested agostic like B-H interactions are further supported by a C-C double bond elongation of the olefin trans to the B-H bonds (1.449 Å) versus the C-C double bond trans to the phosphorus atom (1.392 Å), a characteristic also observed in **11** (1.451 Å vs 1.362 Å respectively). Incorporating the above information, the overall geometry can be considered to be a distorted-trigonal-bipyramidal geometry with two B-H hydrides directly interacting with the iridium metal center. Of the various coordination modes possible from ligand **8**, the strong interaction of the B-H bonds of the carborane project the terphenyl substituent far from the iridium metal center in stark contrast to the complex **7** containing the *ortho*-carboranyl terphenyl ligand **5**.

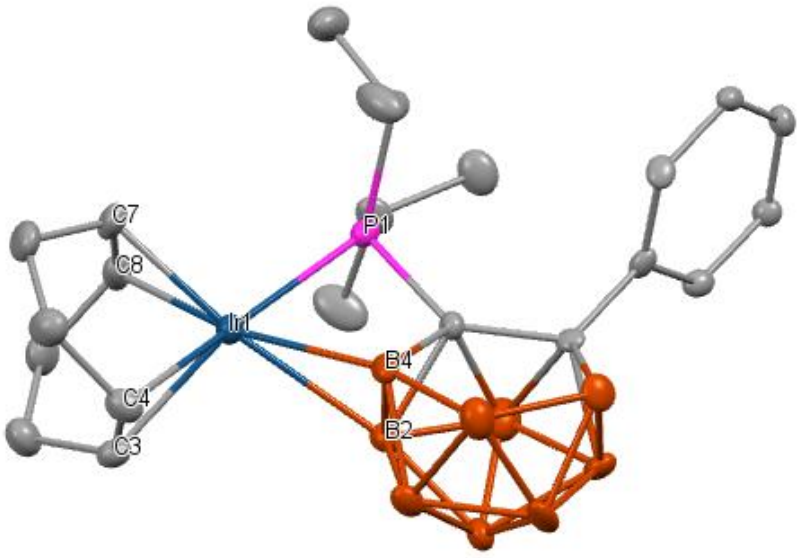

Figure 2.3 – Solid state structure of **10**. Hydrogens and Trip groups omitted for clarity. Color code: C, gray; B, brown; Ir, blue; P, violet.

2.4. Conclusion

The results described above demonstrate the facile and efficient synthesis of a hybrid m-terphenyl/o-carborane ligand building block. Its utility as a sterically demanding ligand substituent is demonstrated by the preparation of phosphine **5** and subsequent reaction with $[ClRh(CO)_2]_2$. The carborane substituent bestows unusual stability to the ensuing chloro-bridged dimer **7**, as shown by its unreactivity with additional phosphine and resistance to B−H cyclometalation. The analogous *nido*-carboranyl phosphine **8** was also synthesized, displaying enhanced coordination towards metal centers, $[ClIrCOD]_2$ in this study, in comparison to **5**. The ensuing zwitterionic iridium complex **10** showed similar structural features to the previously reported iridium complex utilizing a $CB_{11}H_{11}^-$ substituent instead, including a double B-H hydride agostic-like interaction. The unique properties of the corresponding clusters give value to the exploration of this particular ligand framework.

2.5 Experimental

Experimental data in regards to the compounds **3 - 7** can be observed online at DOI: 10.1021/ic5030636. For compounds **8[Li$^+$]**, **9**, and **10**, data is contained below. Unless otherwise stated, all manipulations were carried out using standard Schlenk or glovebox techniques (O_2, H_2O < 1ppm) under a dinitrogen or argon atmosphere. piperdine and ethanol were bubbled with N_2 for 15 minutes prior to use. Solvents were dried on K or CaH_2, and distilled under argon before use. Reagents were purchased from commercial vendors and used without further purification. NMR spectra were recorded on Bruker Avance 300/600 MHz or Varian Inova 300-500 MHz spectrometers. NMR

chemical shifts are reported in parts per million (ppm). ^{1}H NMR and ^{13}C NMR chemical shifts were referenced to residual solvent. ^{11}B NMR chemical shifts were externally referenced to BF_3OEt_2. ^{31}P NMR chemical shifts were externally referenced to 80% H_3PO_4 in H_2O.

2.5.1 Synthesis of **9**

To a 100 mL three necked round bottom flask **5** (500 mg, 0.675 mmol) and deoxygenated piperdine (1.44 mL, 14.6 mmol) was added, followed by addition of deoxygenated ethanol (10 mL). This solution was was refluxed for 16 hours under a N_2 atomosphere. Concentrated aqueous HCl (5 mL) was added to precipitate out a white solid, which was filtered, washed with water (3 x 5 mL) and hexanes (3 x 5 mL), and then dried in vacuo. 432 mg of compound **9** was obtained (0.591 mmol, 87% yield). ^{1}H NMR (600 MHz, $CDCl_3$, 25 °C) δ = 7.33 (br s, 2H, CH_{aryl}), 7.05 (s, 4H, CH_{aryl}), 6.96 (t, 1H, ^{4}J(*H-H*) = 1.4 Hz), 5.03 (ddd, 1H, ^{1}J(*P-H*) = 441.9 Hz, ^{3}J(*H-H*) = 6.9 Hz, ^{4}J(*H-H*) = 1.4 Hz), 2.93 (sep, 2H, C$H_{i\text{Pr}}$, ^{3}J (*H-H*) = 6.9 Hz), 2.61 (sep, 4H, C$H_{i\text{Pr}}$, ^{3}J (*H-H*) = 6.9 Hz), 2.53 (d-sep, 4H, C$H_{i\text{Pr}}$, ^{2}J (*P-H*) = 1.4 Hz, ^{3}J (*H-H*) = 6.9 Hz), 1.42 (dd, 3H, CH_3, ^{2}J (*P-H*) = 2.2 Hz, ^{3}J (*H-H*) = 6.9 Hz) 1.39 (d, 3H, CH_3, ^{2}J (*H-H*) = 7.4 Hz), 1.27-1.37 (m, 6H, CH_3) 1.29 (d, 12H, CH_3, ^{3}J (*H-H*) = 7.4 Hz), 1.16 (d, 12H, CH_3, ^{3}J (*H-H*) = 7.4 Hz), 1.04 (d, 12H, CH_3, ^{3}J (*H-H*) = 7.4 Hz), -2.30 (br s, 1H, *nido*-bridging *H*). ^{11}B-(^{1}H-dec) NMR (192 MHz, $CDCl_3$, 25 °C) δ = -6.49, -8.68, -13.58, -14.87, -16.70, -23.39, -30.09, -33.97. ^{13}C-(^{1}H-dec) NMR (151 MHz, $CDCl_3$, 25 °C) δ = 148.3 (C_{aryl}), 140.96 (C_{aryl}), 136.7 (C_{aryl}), 135.8 (C_{aryl}), 131.3 (C_{aryl}), 120.6 (C_{aryl}), 34.2 (*C*H), 30.6 (*C*H), 30.5 (*C*H), 24.6 (*C*H_3), 24.2 (*C*H_3), 24.1 (*C*H_3), 24.0 (*C*H_3), 23.9 (*C*H_3), 23.6 (*C*H_3), 23.3 (*C*H_3), 23.0

(CH_3), 19.4 (CH_3), 19.1 (CH_3), 17.9 (CH_3), 16.7 (CH_3). ^{31}P-(^{1}H-coup) NMR (151 MHz, $CDCl_3$, 25 °C). δ = 35.26 (d, ^{1}J (*P-H*) = 441.9 Hz).

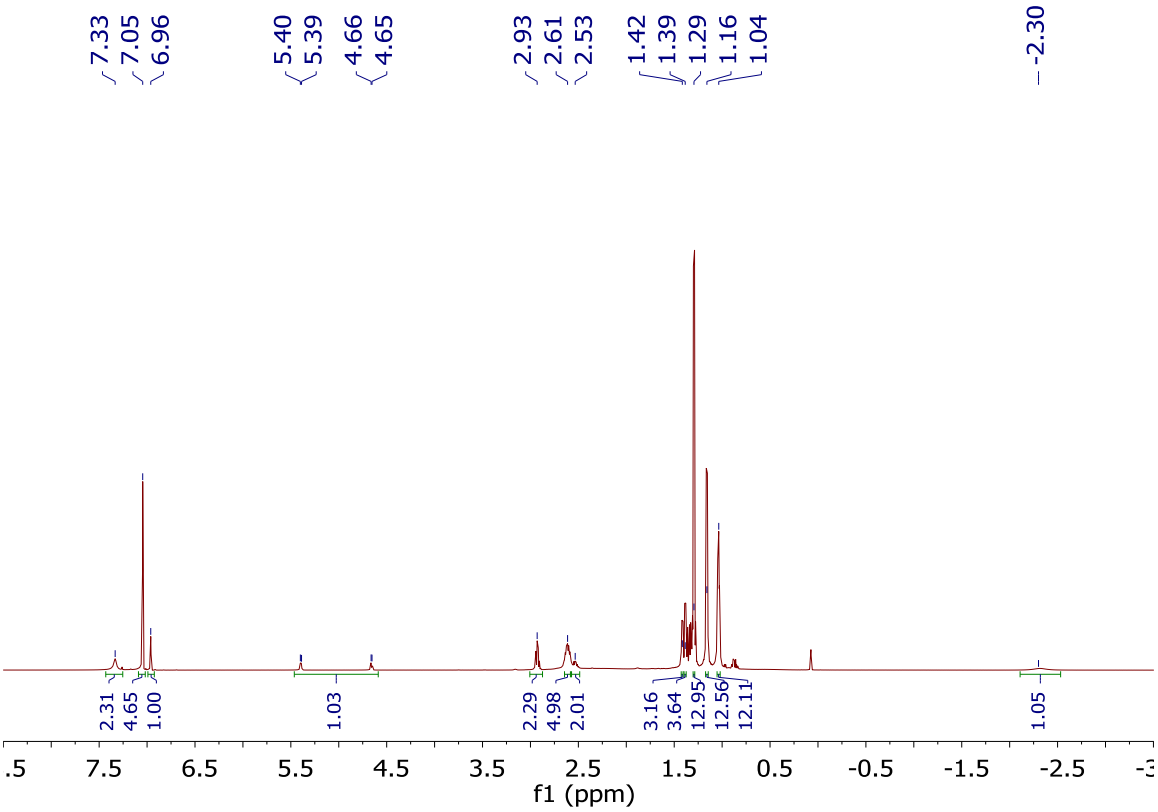

S-2.1 ^{1}H NMR of **9** (600 MHz, $CDCl_3$).

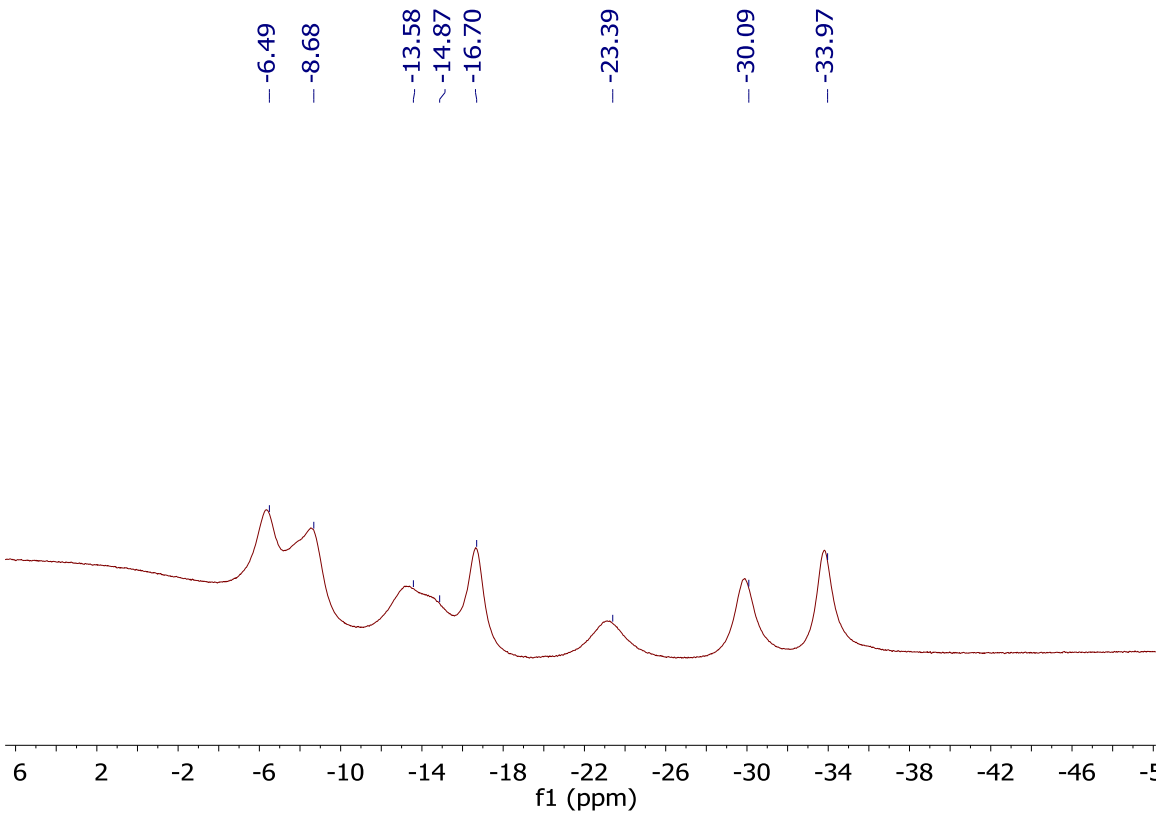

S-2.2 ^{11}B-(^{1}H-dec) NMR of **9** (192 MHz, $CDCl_3$).

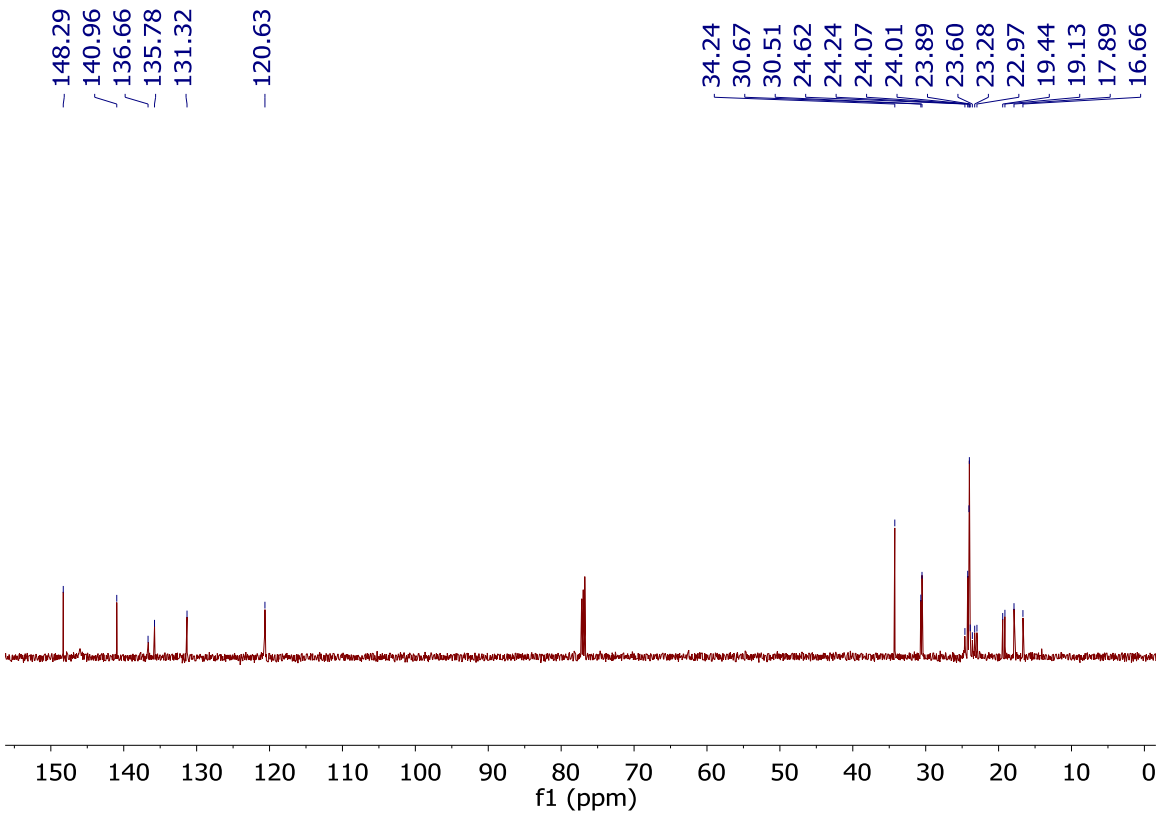

S-2.3 ^{13}C-(^{1}H-dec) NMR of **9** (151 MHz, $CDCl_3$).

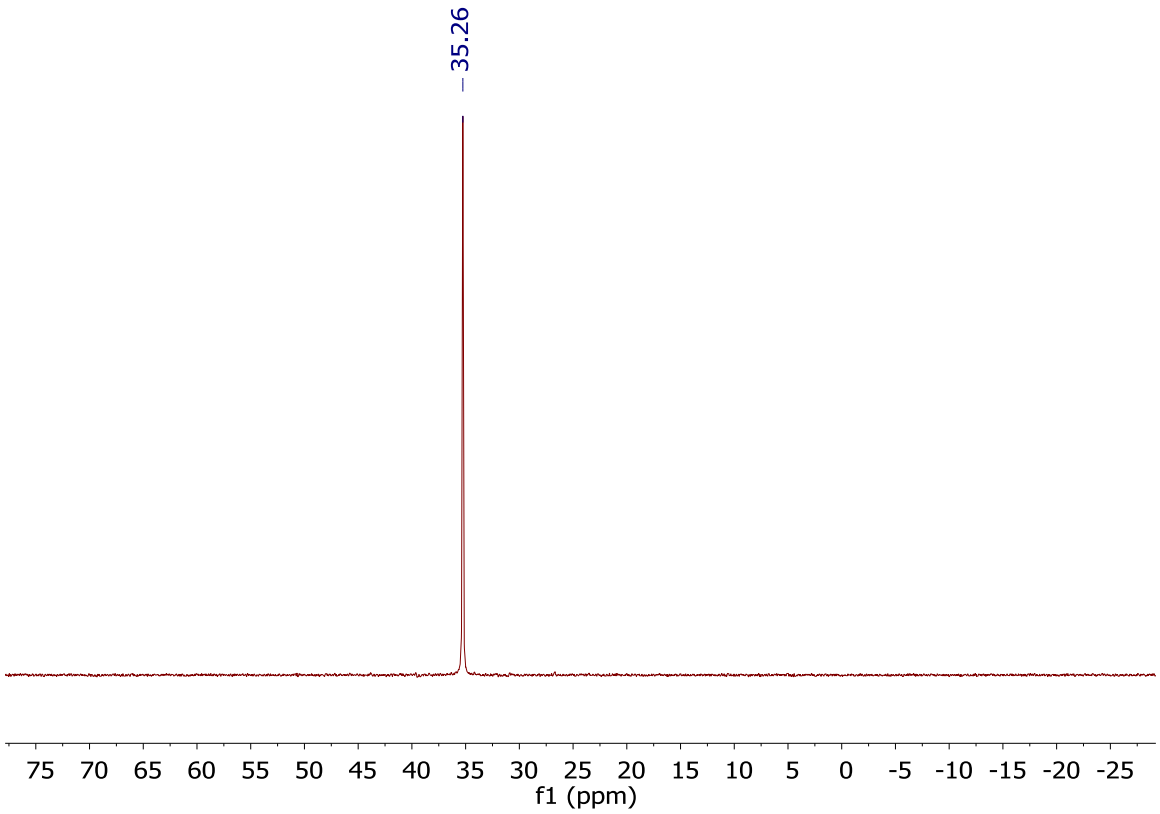

S-2.4 ^{31}P-(^{1}H-dec) NMR of **9** (151 MHz, $CDCl_3$).

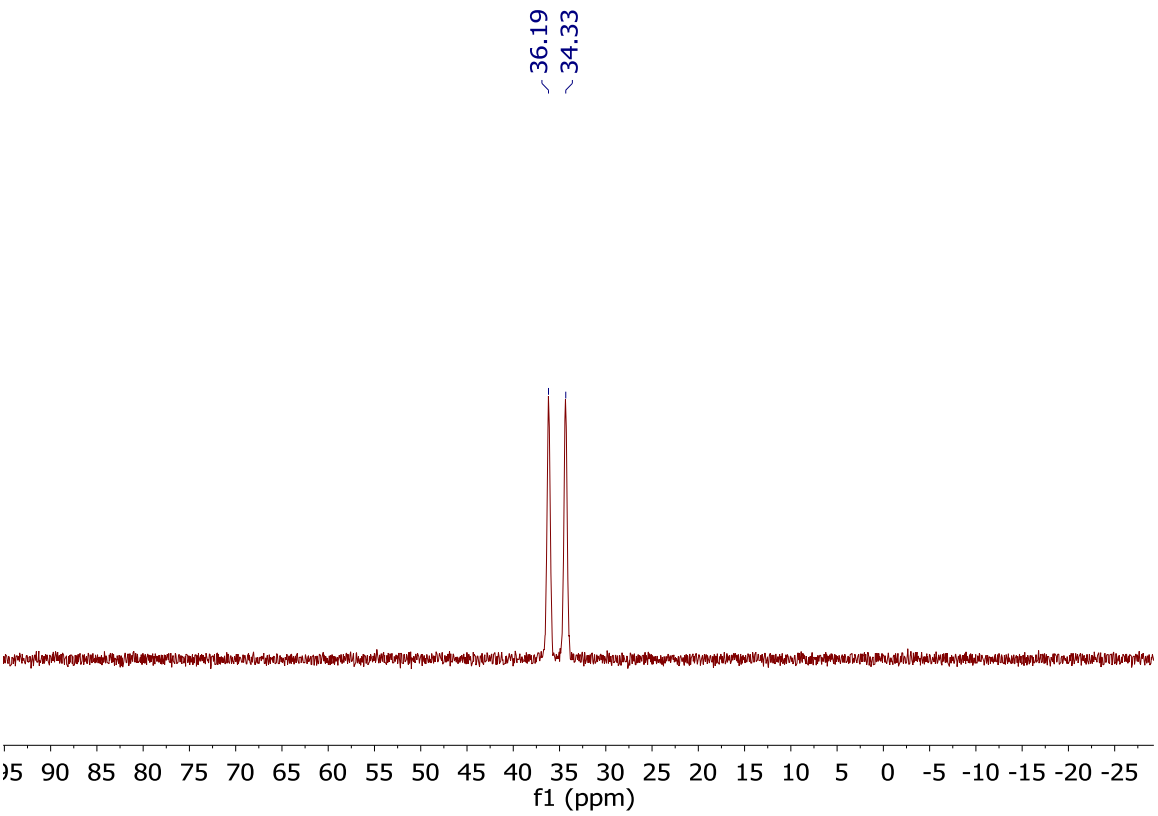

S-2.5 ^{31}P-(^{1}H-coup) NMR of **9** (151 MHz, $CDCl_3$).

2.5.2 Synthesis of **8[Li$^+$]**

Compound **9** (50 mg, 0.068 mmol) was dissolved in THF (2 mL) inside a 20 mL scintillation vial, to which LiH (50 mg, 6.3 mmol) was subsequently added. After 1 hour of stirring, LiH was filtered off through a wool fiber plugged glass pipette. The filtrate was then pipetted slowly to a stirring solution of pentane (10 mL) to precipate the product. Solvent was removed under reduced pressure to afford 48 mg of pure **8[Li$^+$]** (0.059 mmol, 86.7 % yield). ^{1}H NMR (400 MHz, d_8-THF, 25 °C) δ = 7.15 (br s, 2H, CH_{aryl}), 7.00 (s, 2H, CH_{aryl}) 6.99 (s, 2H, CH_{aryl}), 6.55 (t, 1H, ^{4}J(*H-H*) = 1.5 Hz), 3.62 (m, 4H, THF), 2.99 (m, 4H, C$H_{i\mathrm{Pr}}$,), 2.87 (sep, 2H, C$H_{i\mathrm{Pr}}$, ^{3}J (*H-H*) = 7.4 Hz), 2.02 (m, 4H, C$H_{i\mathrm{Pr}}$,), 1.77 (m, 4H, THF) 1.26 (d, 12H, CH_3, ^{3}J (*H-H*) = 7.4 Hz), 1.17 (d, 6H, CH_3, ^{3}J

(*H-H*) = 7.4 Hz), 1.12 (d, 6H, C*H*$_3$, ^3J (*H-H*) = 7.4 Hz), 1.02-1.09 (m, 9H, C*H*$_3$), 1.03 (d, 6H, C*H*$_3$, ^3J (*H-H*) = 7.4 Hz), 1.00 (d, 6H, C*H*$_3$, ^3J (*H-H*) = 7.4 Hz), 0.87 (dd, 3H, C*H*$_3$, ^3J (*P-H*) = 14.3 Hz, ^3J (*H-H*) = 6.7 Hz), -2.30 (br s, 1H, *nido*-bridging *H*). ^{11}B-(^{1}H-dec) NMR (128 MHz, d_8-THF, 25 °C) δ = -8.60, -14.94, -16.82, -20.06, -32.70, -35.05. ^{13}C-(^{1}H-dec) NMR (151 MHz, d_8-THF, 25 °C) δ = 147.6 (C_{aryl}), 147.1 (C_{aryl}), 143.72 (C_{aryl}), 139.2 (C_{aryl}), 138.4 (C_{aryl}), 134.5 (C_{aryl}), 138.5 (C_{aryl}), 120.6 (C_{aryl}), 120.5 (C_{aryl}), 67.21 (THF) 35.2 (*C*H), 30.7 (*C*H), 30.5 (*C*H), 26.2 (*C*H$_3$), 26.1 (*C*H$_3$), 25.3 (THF), 24.7 (*C*H$_3$), 24.4 (*C*H$_3$), 24.0 (*C*H$_3$), 23.9 (*C*H$_3$), 23.7 (*C*H$_3$), 22.81 (*C*H$_3$), 21.4 (*C*H$_3$), 21.2 (*C*H$_3$), 17.8 (*C*H$_3$). ^{31}P-(^{1}H-dec) NMR (243 MHz, d_8-THF, 25 °C). δ = 16.84.

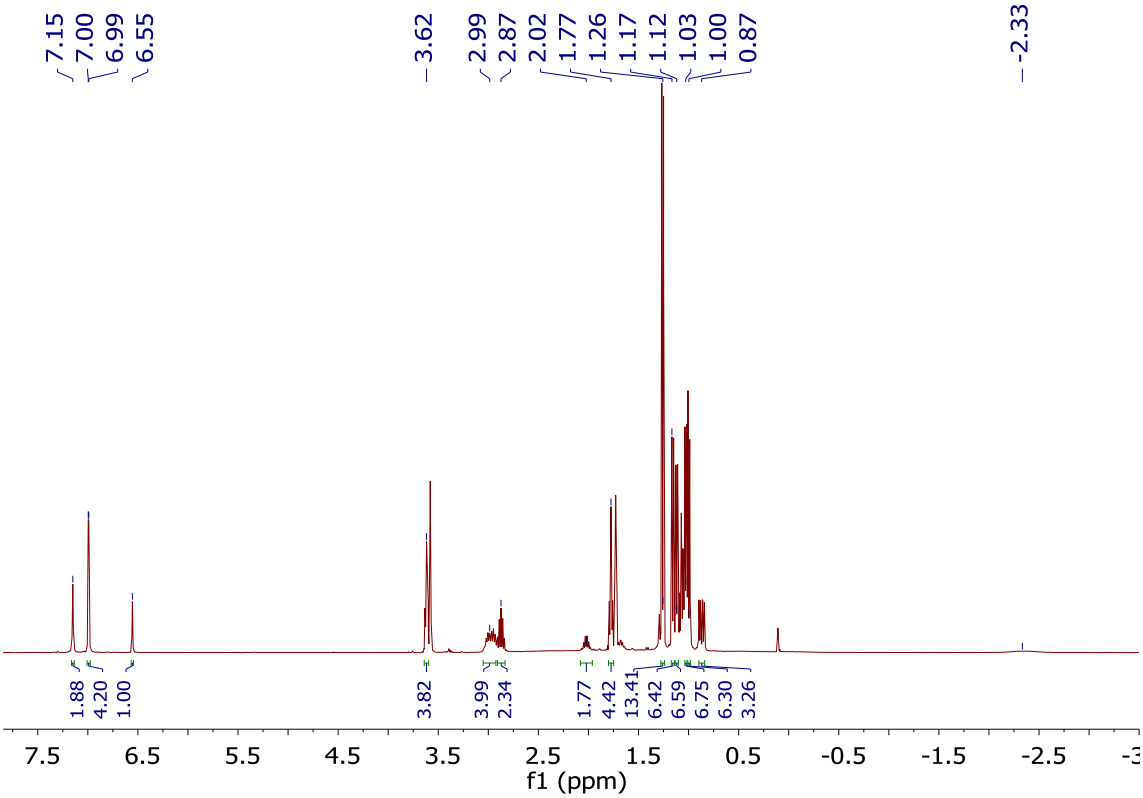

S-2.6 ^{1}H NMR of **8[Li$^+$]** (400 MHz, d_8-THF).

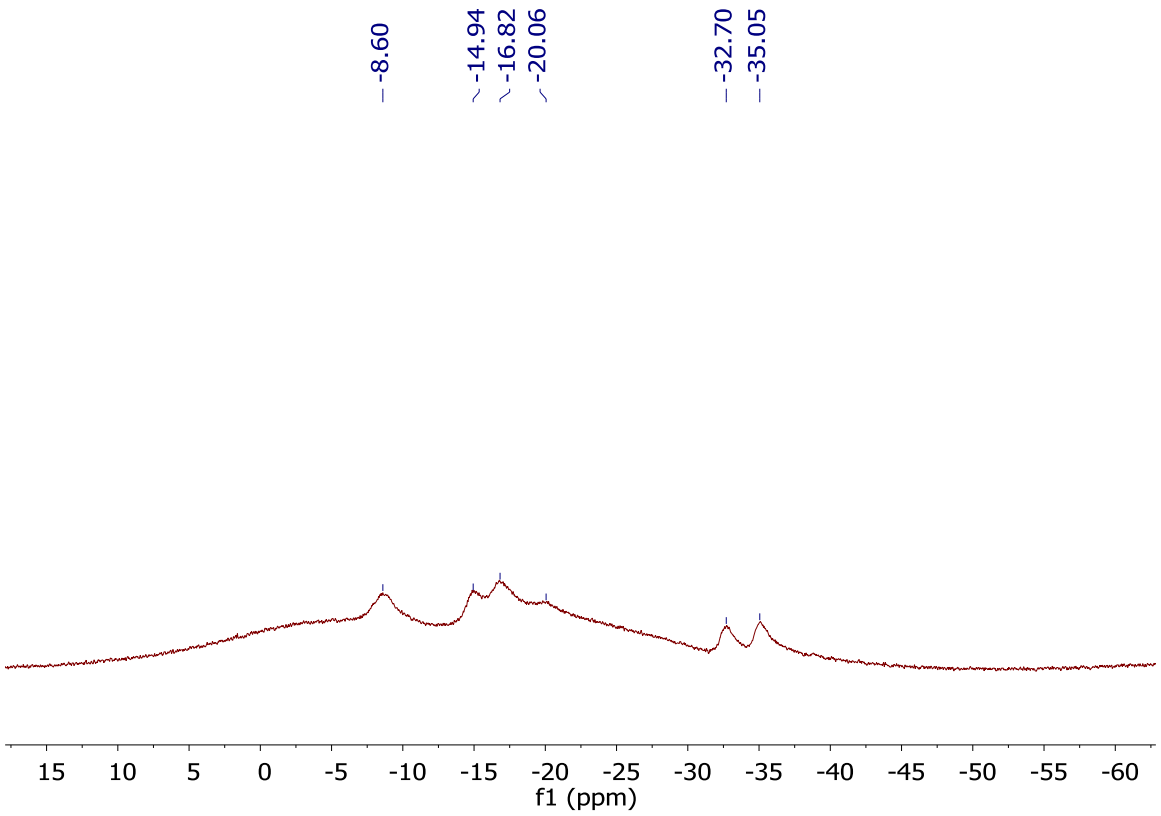

S-2.6 ^{11}B-(^{1}H-dec) NMR of **8[Li^{+}]** (128 MHz, d_8-THF).

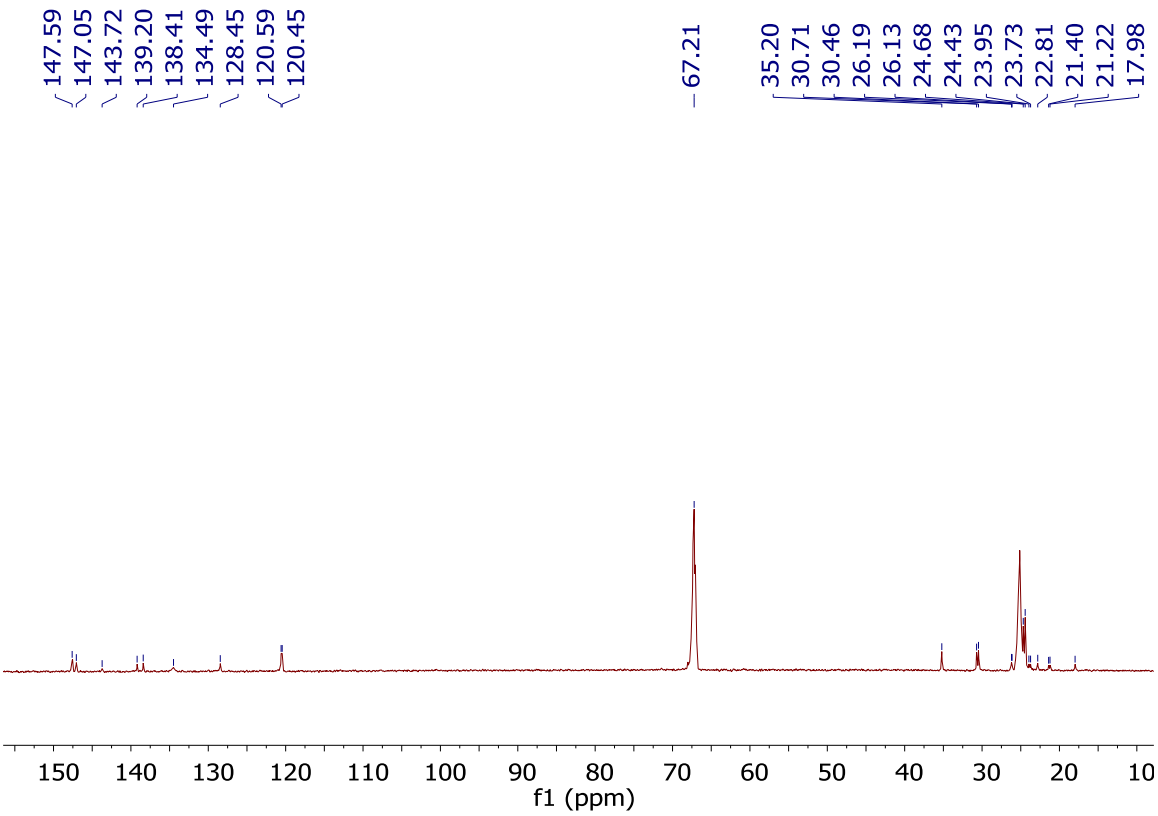

S-2.7 ^{13}C-(^{1}H-dec) NMR of **8[Li^{+}]** (151 MHz, d_8-THF).

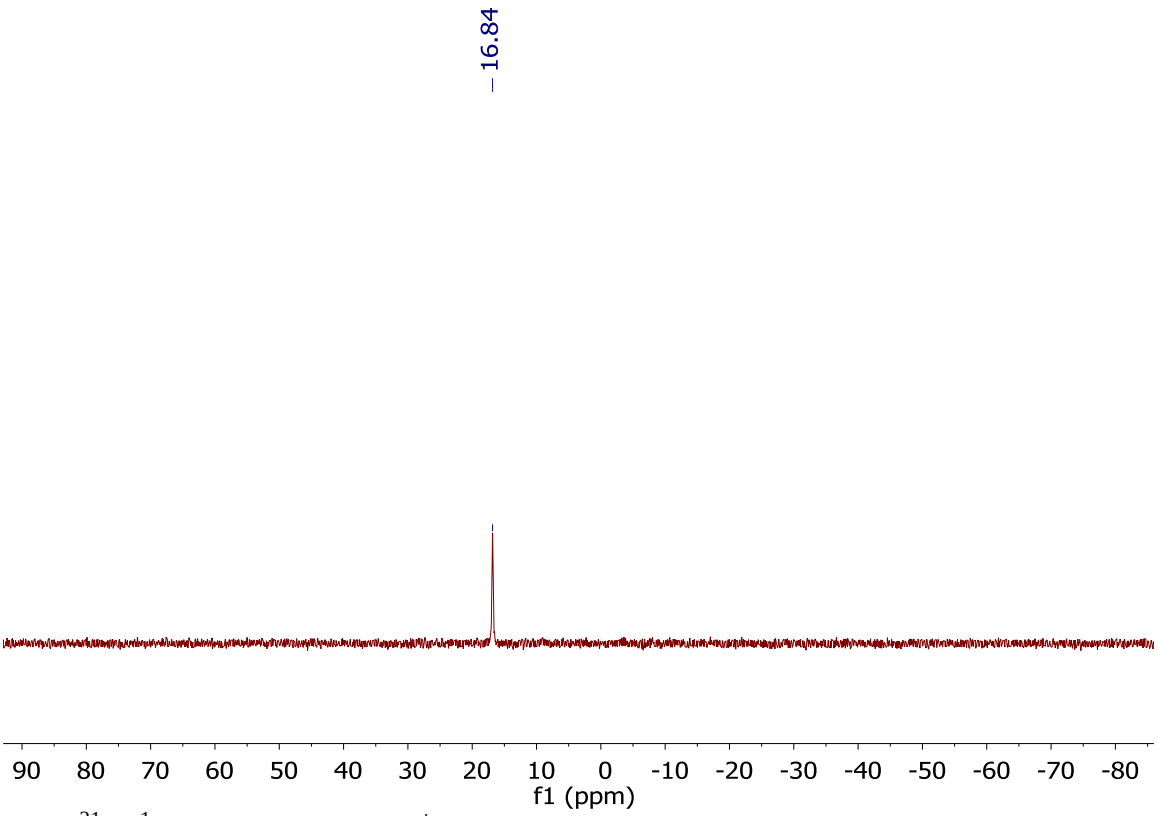

S-2.8 ^{31}P-(^{1}H-dec) NMR of **8[Li^{+}]** (243 MHz, d_8-THF).

2.5.3 Synthesis of **10**

Compound **8[Li^{+}]** (34 mg, 0.041 mmol) was dissolved in benzene (1 mL) inside a 20 mL scintillation vial charged with a magnetic stir bar. [ClIrCOD]2 (14 mg, 0.021 mmol) was dissolved in benzene (1mL) in a separate 20 mL scintillation vial. The iridium solution was then slowly pipetted to the ligand solution. After 2 hours of stirring, the cloudy brownish orange solution was filtered, with the solvent removed in vacuo. Compound **10** was recrystallized in boiling hexanes to give 41 mg of a yellowish orange powder, (0.039 mmol, 95% yield) . ^{1}H NMR (400 MHz, C_6D_6, 25 °C) δ = 7.44 (d, 2H, CH_{aryl}, ^{4}J(*H-H*) = 1.5 Hz), 7.1 (s, 24, CH_{aryl}), 6.84 (t, 1H, ^{4}J(*H-H*) = 1.4 Hz), 4.76 (br s, 2H, COD-C*H*), 4.68 (br s, 2H, COD-C*H*), 2.82 (sep, 6H, C$H_{i\mathrm{Pr}}$, ^{3}J (*H-H*) = 7.4 Hz,), 2.27

(sep, 2H, C$H_{i\text{Pr}}$, ^{3}J (*H*-*H*) = 7.4 Hz), 2.03 (br m, 2H, COD-CH_2), 1.91 (br m, 2H, COD-CH_2), 1.70 (br m, 2H, COD-CH_2), 1.55 (br m, 2H, COD-CH_2), 1.25 (d, 12H, CH_3, ^{3}J (*H*-*H*) = 7.4 Hz), 1.22 (d, 6H, CH_3, ^{3}J (*H*-*H*) = 7.4 Hz), 1.18 (d, 6H, CH_3, ^{3}J (*H*-*H*) = 7.4 Hz), 1.08-1.15 (m, 15H, CH_3), 1.01 (dd, 3H, CH_3, ^{3}J (*P*-*H*) = 16.2 Hz, ^{3}J (*H*-*H*) = 7.3 Hz), 0.59 (dd, 3H, CH_3, ^{3}J (*P*-*H*) = 16.2 Hz, ^{3}J (*H*-*H*) = 7.3 Hz), 0.52 (dd, 3H, CH_3, ^{3}J (*P*-*H*) = 16.2 Hz, ^{3}J (*H*-*H*) = 7.3 Hz), -1.55 (br s, 1H, B-*H*), -1.79 (br s, 1H, B-*H*), -2.30 (br s, 1H, *nido*-bridging *H*). ^{11}B-(^{1}H-dec) NMR (96 MHz, d_8-THF, 25 °C) δ = 24.64, 21.89, -2.99, -4.86, -7.06. ^{13}C-(^{1}H-dec) NMR (101 MHz, C_6D_6, 25 °C) δ = 148.5 (C_{aryl}), 146.8 (C_{aryl}), 146.61 (C_{aryl}), 140.98 (C_{aryl}), 136.8 (C_{aryl}), 132.3 (C_{aryl}), 131.1 (C_{aryl}), 128.6 (C_{aryl}), 120.9 (C_{aryl}), 120.6 (C_{aryl}), 88.3 (COD-*C*H), 87.1 (COD-*C*H), 45.6 (COD-*C*H$_2$), 44.4 (COD-*C*H$_2$), 36.9 (*C*H), 36.1 (*C*H), 34.7 (*C*H), 30.9 (*C*H), 30.7 (*C*H), 28.6 (*C*H), 28.4 (*C*H), 25.9 (*C*H$_3$), 25.7 (*C*H$_3$), 24.6 (THF), 24.6 (*C*H$_3$), 24.3 (*C*H$_3$), 24.2 (*C*H$_3$), 23.9 (*C*H$_3$), 23.6 (*C*H$_3$), 20.8 (*C*H$_3$), 19.1 (*C*H$_3$), 18.3 (*C*H$_3$), 17.4 (*C*H$_3$). ^{31}P-(^{1}H-dec) NMR (121 MHz, C_6D_6, 25 °C). δ = 39.03.

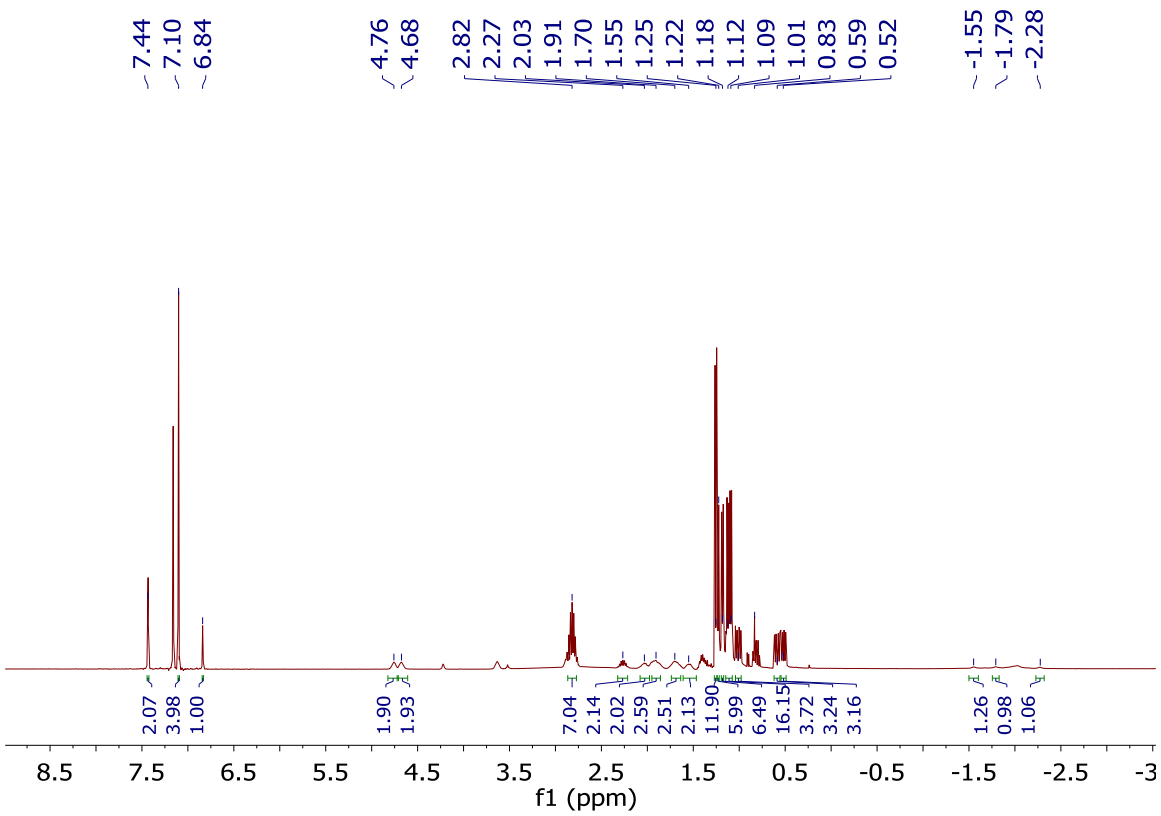

S-2.9 ^{1}H NMR of **10** (400 MHz, C_6D_6).

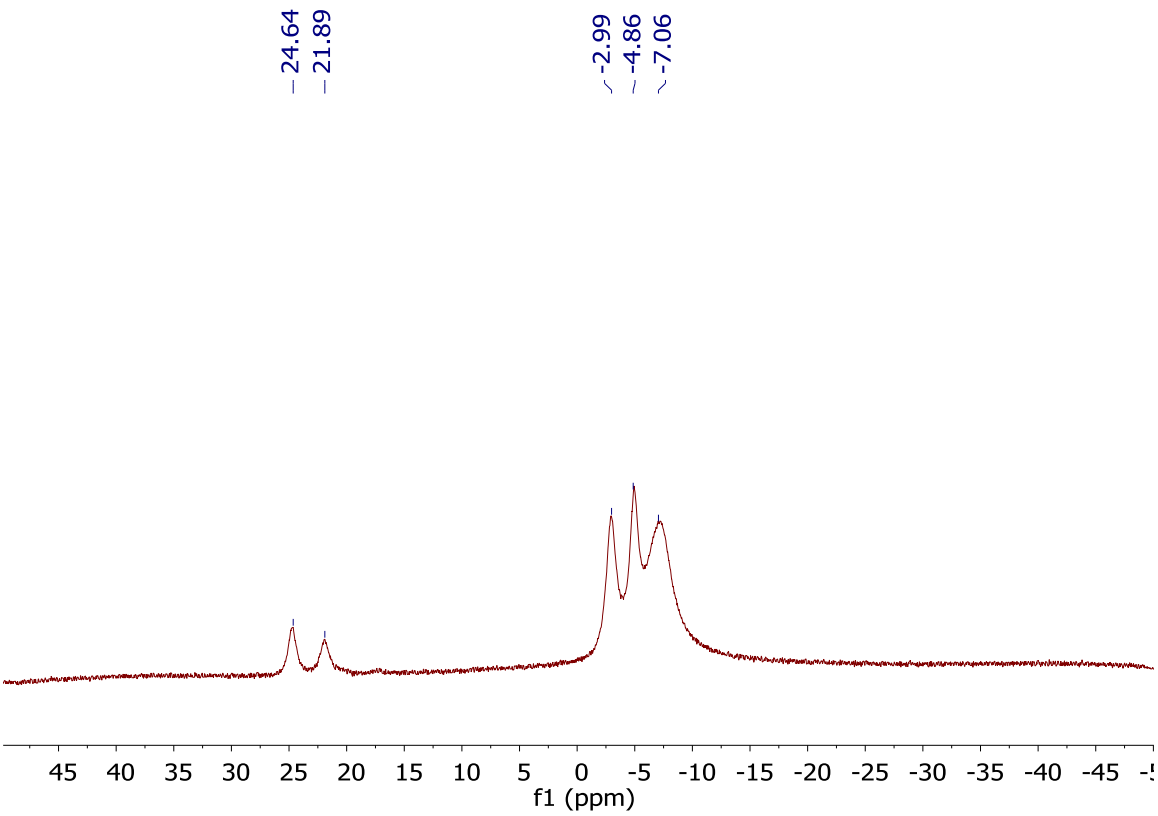

S-2.10 ^{11}B-(^{1}H-dec) NMR of **10** (96 MHz, d_8-THF).

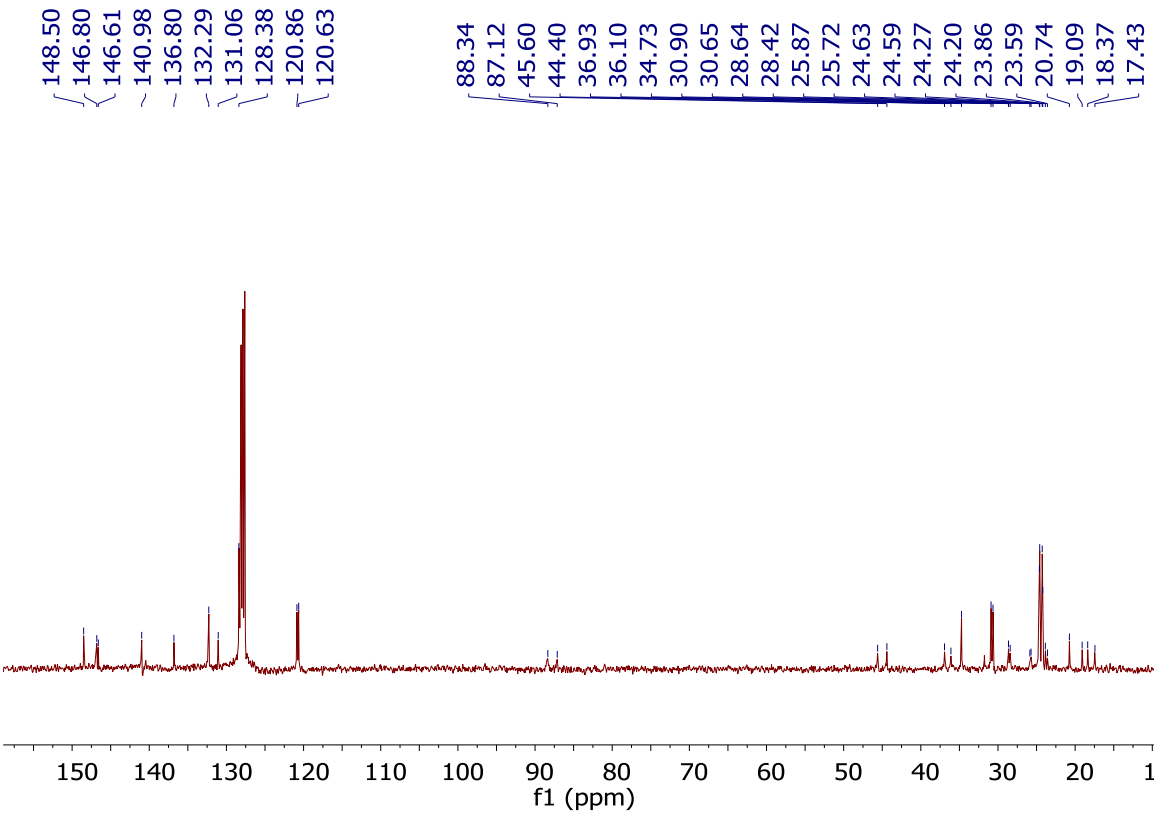

S-2.11 ^{13}C-(^{1}H-dec) NMR of **10** (101 MHz, C_6D_6).

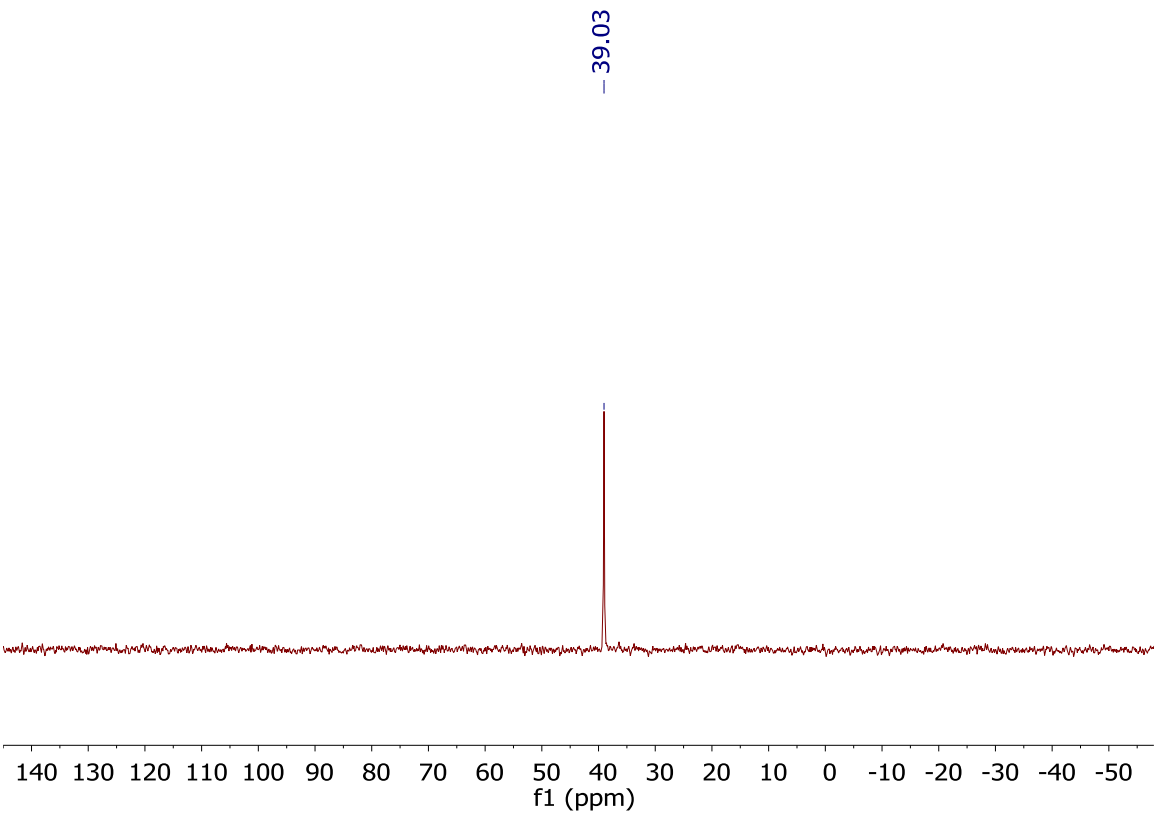

S-2.11 ^{31}P-(^{1}H-dec) NMR of **10** (121 MHz, C_6D_6).

2.5.4 X-ray crystallographic data for compound **10**

Table 1. Crystal data and structure refinement for lavallo15.

Identification code	lavallo15	
Empirical formula	C55 H85 B9 Ir P	
Formula weight	1066.68	
Temperature	100(2) K	
Wavelength	0.71073 Å	
Crystal system	Triclinic	
Space group	P -1	
Unit cell dimensions	a = 10.0150(8) Å	a= 104.856(3)°.
	b = 15.5333(11) Å	b= 103.048(3)°.
	c = 18.4013(14) Å	g = 96.367(3)°.
Volume	2651.8(4) $Å^3$	
Z	2	

Density (calculated)	1.336 Mg/m^3
Absorption coefficient	2.583 mm^{-1}
F(000)	1104
Crystal size	0.300 x 0.090 x 0.050 mm^3
Theta range for data collection	2.122 to 25.378°.
Index ranges	-12<=h<=12, -18<=k<=14, -22<=l<=22
Reflections collected	41899
Independent reflections	9709 [R(int) = 0.0873]
Completeness to theta = 25.000°	99.9 %
Absorption correction	Semi-empirical from equivalents
Max. and min. transmission	0.900 and 0.499
Refinement method	Full-matrix least-squares on F^2
Data / restraints / parameters	9709 / 0 / 584
Goodness-of-fit on F^2	1.045
Final R indices [I>2sigma(I)]	R1 = 0.0471, wR2 = 0.1021
R indices (all data)	R1 = 0.0648, wR2 = 0.1081
Extinction coefficient	n/a
Largest diff. peak and hole	1.551 and -1.644 $e.Å^{-3}$

Table 2. Atomic coordinates (x 10^4) and equivalent isotropic displacement parameters ($Å^2$x 10^3)
for lavallo15. U(eq) is defined as one third of the trace of the orthogonalized U^{ij} tensor.

	x	y	z	U(eq)
Ir(1)	5419(1)	2917(1)	3593(1)	14(1)
P(1)	6834(2)	3004(1)	4808(1)	14(1)
C(1)	6579(7)	2352(5)	2185(4)	29(2)
C(2)	5033(7)	2243(5)	1788(4)	27(2)
C(3)	4143(6)	2353(4)	2360(4)	18(1)
C(4)	3751(7)	3168(4)	2682(4)	22(2)
C(5)	4236(7)	4054(5)	2534(4)	29(2)
C(6)	5824(7)	4276(5)	2671(4)	31(2)
C(7)	6625(7)	3859(5)	3262(4)	23(2)
C(8)	6994(7)	2974(5)	3018(4)	24(2)
C(9)	6096(6)	2409(4)	6499(4)	14(1)
C(10)	6653(6)	1696(4)	6717(4)	15(1)
C(11)	7658(6)	1849(4)	7417(3)	14(1)
C(12)	8093(6)	2727(4)	7913(3)	16(1)
C(13)	7535(6)	3458(4)	7728(3)	14(1)
C(14)	6520(6)	3280(4)	7016(3)	16(1)
C(15)	8184(6)	1096(4)	7705(3)	15(1)
C(16)	7423(6)	648(4)	8090(3)	14(1)
C(17)	7984(6)	4(4)	8419(3)	16(1)
C(18)	9282(6)	-198(4)	8370(3)	16(1)
C(19)	9994(6)	240(4)	7968(4)	19(1)
C(20)	9488(6)	887(4)	7636(4)	17(1)
C(21)	4840(7)	122(5)	7566(4)	29(2)
C(22)	5988(6)	854(4)	8161(4)	18(1)
C(23)	5788(7)	967(5)	8983(4)	31(2)
C(24)	10042(8)	-1710(5)	8136(4)	29(2)

C(25)	9909(7)	-875(4)	8752(4)	21(2)
C(26)	11311(8)	-433(5)	9347(4)	35(2)
C(27)	10651(7)	663(4)	6530(4)	24(2)
C(28)	10363(6)	1344(4)	7214(4)	19(1)
C(29)	11736(7)	1907(5)	7774(4)	27(2)
C(30)	7898(6)	4367(4)	8321(4)	17(1)
C(31)	8964(6)	5036(4)	8323(4)	16(1)
C(32)	9261(7)	5869(4)	8893(4)	19(1)
C(33)	8554(6)	6063(4)	9465(3)	16(1)
C(34)	7528(7)	5375(4)	9464(4)	20(1)
C(35)	7203(7)	4534(4)	8917(4)	20(1)
C(36)	6047(7)	3814(4)	8949(4)	24(2)
C(37)	9832(7)	4842(4)	7737(4)	20(1)
C(38)	10259(8)	5660(5)	7475(4)	32(2)
C(39)	10212(7)	7568(4)	10163(4)	26(2)
C(40)	8823(7)	6974(4)	10073(4)	22(2)
C(41)	7626(7)	7488(5)	9884(4)	32(2)
C(42)	6188(8)	3735(5)	9771(4)	34(2)
C(43)	11098(7)	4485(5)	8076(4)	36(2)
C(44)	4606(7)	3997(5)	8601(5)	37(2)
C(45)	8956(8)	4503(5)	5402(4)	36(2)
C(46)	7606(6)	4104(4)	5536(4)	19(1)
C(47)	6588(8)	4771(5)	5543(4)	35(2)
C(48)	8923(7)	2282(5)	5657(4)	28(2)
C(49)	8277(6)	2357(5)	4842(4)	22(2)
C(50)	7943(8)	1449(5)	4208(4)	36(2)
C(51)	5294(6)	2522(4)	5042(3)	14(1)
C(52)	4984(6)	2248(4)	5754(3)	12(1)
B(1)	4985(9)	1392(6)	4938(5)	32(2)
B(2)	4346(7)	1808(5)	4154(4)	15(2)
B(3)	2628(8)	2848(6)	4969(5)	26(2)
B(4)	4024(8)	2879(5)	4511(4)	17(2)
B(5)	3700(7)	1326(5)	5444(4)	18(2)
B(6)	2622(7)	1967(5)	4133(4)	20(2)

B(7)	3396(8)	2448(5)	5807(4)	20(2)
B(8)	3218(8)	1017(5)	4392(4)	20(2)
B(9)	2225(7)	1682(6)	4954(4)	22(2)

Table 3. Bond lengths [Å] and angles [°] for lavallo15.

Ir(1)-C(7)	2.090(6)
Ir(1)-C(8)	2.095(6)
Ir(1)-C(4)	2.229(6)
Ir(1)-C(3)	2.230(6)
Ir(1)-P(1)	2.3222(16)
Ir(1)-B(4)	2.430(7)
Ir(1)-B(2)	2.488(7)
P(1)-C(51)	1.825(6)
P(1)-C(46)	1.838(6)
P(1)-C(49)	1.848(6)
C(1)-C(8)	1.524(9)
C(1)-C(2)	1.526(9)
C(2)-C(3)	1.516(9)
C(3)-C(4)	1.392(8)
C(4)-C(5)	1.520(9)
C(5)-C(6)	1.537(9)
C(6)-C(7)	1.526(9)
C(7)-C(8)	1.449(9)
C(9)-C(14)	1.395(8)
C(9)-C(10)	1.400(8)
C(9)-C(52)	1.501(8)
C(10)-C(11)	1.391(8)
C(11)-C(12)	1.390(8)
C(11)-C(15)	1.502(8)
C(12)-C(13)	1.404(8)
C(13)-C(14)	1.405(8)
C(13)-C(30)	1.494(8)
C(15)-C(16)	1.394(8)

C(15)-C(20)	1.405(8)
C(16)-C(17)	1.402(8)
C(16)-C(22)	1.533(8)
C(17)-C(18)	1.387(8)
C(18)-C(19)	1.382(9)
C(18)-C(25)	1.524(8)
C(19)-C(20)	1.388(8)
C(20)-C(28)	1.526(9)
C(21)-C(22)	1.522(9)
C(22)-C(23)	1.539(9)
C(24)-C(25)	1.529(9)
C(25)-C(26)	1.532(9)
C(27)-C(28)	1.528(8)
C(28)-C(29)	1.533(9)
C(30)-C(31)	1.404(8)
C(30)-C(35)	1.411(8)
C(31)-C(32)	1.393(8)
C(31)-C(37)	1.525(8)
C(32)-C(33)	1.387(8)
C(33)-C(34)	1.397(9)
C(33)-C(40)	1.515(8)
C(34)-C(35)	1.383(9)
C(35)-C(36)	1.540(9)
C(36)-C(42)	1.526(10)
C(36)-C(44)	1.529(10)
C(37)-C(43)	1.511(9)
C(37)-C(38)	1.521(9)
C(39)-C(40)	1.532(9)
C(40)-C(41)	1.537(9)
C(45)-C(46)	1.522(9)
C(46)-C(47)	1.532(9)
C(48)-C(49)	1.532(9)
C(49)-C(50)	1.529(9)
C(51)-C(52)	1.561(8)

C(51)-B(4)	1.659(9)
C(51)-B(1)	1.701(10)
C(51)-B(2)	1.714(9)
C(52)-B(7)	1.673(9)
C(52)-B(5)	1.694(9)
C(52)-B(1)	1.731(10)
B(1)-B(2)	1.749(11)
B(1)-B(5)	1.759(11)
B(1)-B(8)	1.774(12)
B(2)-B(4)	1.721(9)
B(2)-B(6)	1.765(10)
B(2)-B(8)	1.780(10)
B(3)-B(6)	1.776(10)
B(3)-B(4)	1.790(10)
B(3)-B(9)	1.803(12)
B(3)-B(7)	1.848(11)
B(4)-B(6)	1.754(10)
B(5)-B(9)	1.770(10)
B(5)-B(7)	1.785(10)
B(5)-B(8)	1.805(10)
B(6)-B(8)	1.786(11)
B(6)-B(9)	1.794(11)
B(7)-B(9)	1.776(10)
B(8)-B(9)	1.808(10)

C(7)-Ir(1)-C(8)	40.5(3)
C(7)-Ir(1)-C(4)	81.2(3)
C(8)-Ir(1)-C(4)	96.6(3)
C(7)-Ir(1)-C(3)	89.5(2)
C(8)-Ir(1)-C(3)	80.3(2)
C(4)-Ir(1)-C(3)	36.4(2)
C(7)-Ir(1)-P(1)	101.07(19)
C(8)-Ir(1)-P(1)	97.40(19)
C(4)-Ir(1)-P(1)	160.62(16)

C(3)-Ir(1)-P(1)	160.86(16)
C(7)-Ir(1)-B(4)	139.5(2)
C(8)-Ir(1)-B(4)	167.1(2)
C(4)-Ir(1)-B(4)	95.9(2)
C(3)-Ir(1)-B(4)	111.9(2)
P(1)-Ir(1)-B(4)	69.72(17)
C(7)-Ir(1)-B(2)	170.5(2)
C(8)-Ir(1)-B(2)	135.9(2)
C(4)-Ir(1)-B(2)	108.3(2)
C(3)-Ir(1)-B(2)	98.6(2)
P(1)-Ir(1)-B(2)	69.74(16)
B(4)-Ir(1)-B(2)	40.9(2)
C(51)-P(1)-C(46)	108.7(3)
C(51)-P(1)-C(49)	116.4(3)
C(46)-P(1)-C(49)	104.2(3)
C(51)-P(1)-Ir(1)	88.25(19)
C(46)-P(1)-Ir(1)	121.0(2)
C(49)-P(1)-Ir(1)	118.0(2)
C(8)-C(1)-C(2)	112.8(5)
C(3)-C(2)-C(1)	112.8(5)
C(4)-C(3)-C(2)	123.6(6)
C(4)-C(3)-Ir(1)	71.8(4)
C(2)-C(3)-Ir(1)	112.2(4)
C(3)-C(4)-C(5)	123.6(6)
C(3)-C(4)-Ir(1)	71.9(4)
C(5)-C(4)-Ir(1)	109.2(4)
C(4)-C(5)-C(6)	113.2(6)
C(7)-C(6)-C(5)	113.1(6)
C(8)-C(7)-C(6)	121.2(6)
C(8)-C(7)-Ir(1)	69.9(4)
C(6)-C(7)-Ir(1)	115.6(4)
C(7)-C(8)-C(1)	125.3(6)
C(7)-C(8)-Ir(1)	69.6(4)
C(1)-C(8)-Ir(1)	113.5(4)

C(14)-C(9)-C(10)	118.7(6)
C(14)-C(9)-C(52)	119.5(5)
C(10)-C(9)-C(52)	121.7(5)
C(11)-C(10)-C(9)	121.3(6)
C(12)-C(11)-C(10)	118.9(5)
C(12)-C(11)-C(15)	117.9(5)
C(10)-C(11)-C(15)	122.8(5)
C(11)-C(12)-C(13)	121.7(6)
C(12)-C(13)-C(14)	117.9(5)
C(12)-C(13)-C(30)	119.7(5)
C(14)-C(13)-C(30)	122.0(5)
C(9)-C(14)-C(13)	121.5(6)
C(16)-C(15)-C(20)	120.0(5)
C(16)-C(15)-C(11)	119.9(5)
C(20)-C(15)-C(11)	119.9(5)
C(15)-C(16)-C(17)	119.4(5)
C(15)-C(16)-C(22)	120.9(5)
C(17)-C(16)-C(22)	119.7(5)
C(18)-C(17)-C(16)	121.4(6)
C(19)-C(18)-C(17)	117.8(6)
C(19)-C(18)-C(25)	120.9(5)
C(17)-C(18)-C(25)	121.3(6)
C(18)-C(19)-C(20)	123.0(6)
C(19)-C(20)-C(15)	118.4(6)
C(19)-C(20)-C(28)	119.1(5)
C(15)-C(20)-C(28)	122.6(5)
C(21)-C(22)-C(16)	110.4(5)
C(21)-C(22)-C(23)	109.8(6)
C(16)-C(22)-C(23)	113.6(5)
C(18)-C(25)-C(24)	110.8(5)
C(18)-C(25)-C(26)	111.0(5)
C(24)-C(25)-C(26)	111.6(6)
C(20)-C(28)-C(27)	112.1(5)
C(20)-C(28)-C(29)	111.5(5)

C(27)-C(28)-C(29)	110.1(5)
C(31)-C(30)-C(35)	119.5(6)
C(31)-C(30)-C(13)	121.4(6)
C(35)-C(30)-C(13)	119.0(5)
C(32)-C(31)-C(30)	118.9(6)
C(32)-C(31)-C(37)	120.3(5)
C(30)-C(31)-C(37)	120.7(5)
C(33)-C(32)-C(31)	122.6(6)
C(32)-C(33)-C(34)	117.3(6)
C(32)-C(33)-C(40)	123.6(6)
C(34)-C(33)-C(40)	119.2(5)
C(35)-C(34)-C(33)	122.4(6)
C(34)-C(35)-C(30)	119.2(6)
C(34)-C(35)-C(36)	119.3(5)
C(30)-C(35)-C(36)	121.4(5)
C(42)-C(36)-C(44)	111.3(6)
C(42)-C(36)-C(35)	112.3(6)
C(44)-C(36)-C(35)	110.8(6)
C(43)-C(37)-C(38)	110.7(6)
C(43)-C(37)-C(31)	109.6(5)
C(38)-C(37)-C(31)	113.2(5)
C(33)-C(40)-C(39)	113.8(5)
C(33)-C(40)-C(41)	110.2(5)
C(39)-C(40)-C(41)	109.5(6)
C(45)-C(46)-C(47)	110.6(6)
C(45)-C(46)-P(1)	110.8(4)
C(47)-C(46)-P(1)	111.8(5)
C(50)-C(49)-C(48)	112.9(6)
C(50)-C(49)-P(1)	114.1(4)
C(48)-C(49)-P(1)	113.5(4)
C(52)-C(51)-B(4)	116.3(5)
C(52)-C(51)-B(1)	63.9(4)
B(4)-C(51)-B(1)	114.2(5)
C(52)-C(51)-B(2)	114.2(5)

B(4)-C(51)-B(2)	61.3(4)
B(1)-C(51)-B(2)	61.6(4)
C(52)-C(51)-P(1)	135.9(4)
B(4)-C(51)-P(1)	102.4(4)
B(1)-C(51)-P(1)	118.9(4)
B(2)-C(51)-P(1)	102.1(4)
C(9)-C(52)-C(51)	121.9(5)
C(9)-C(52)-B(7)	118.6(5)
C(51)-C(52)-B(7)	108.0(5)
C(9)-C(52)-B(5)	120.2(5)
C(51)-C(52)-B(5)	110.2(5)
B(7)-C(52)-B(5)	64.0(4)
C(9)-C(52)-B(1)	119.7(5)
C(51)-C(52)-B(1)	62.0(4)
B(7)-C(52)-B(1)	114.0(5)
B(5)-C(52)-B(1)	61.8(4)
C(51)-B(1)-C(52)	54.1(4)
C(51)-B(1)-B(2)	59.6(4)
C(52)-B(1)-B(2)	104.4(5)
C(51)-B(1)-B(5)	101.0(5)
C(52)-B(1)-B(5)	58.1(4)
B(2)-B(1)-B(5)	108.6(6)
C(51)-B(1)-B(8)	104.8(6)
C(52)-B(1)-B(8)	106.1(5)
B(2)-B(1)-B(8)	60.7(4)
B(5)-B(1)-B(8)	61.5(4)
C(51)-B(2)-B(4)	57.7(4)
C(51)-B(2)-B(1)	58.8(4)
B(4)-B(2)-B(1)	108.8(5)
C(51)-B(2)-B(6)	103.2(5)
B(4)-B(2)-B(6)	60.4(4)
B(1)-B(2)-B(6)	108.7(5)
C(51)-B(2)-B(8)	104.0(5)
B(4)-B(2)-B(8)	109.2(5)

B(1)-B(2)-B(8)	60.4(4)
B(6)-B(2)-B(8)	60.5(4)
C(51)-B(2)-Ir(1)	85.5(3)
B(4)-B(2)-Ir(1)	67.7(3)
B(1)-B(2)-Ir(1)	133.0(5)
B(6)-B(2)-Ir(1)	108.6(4)
B(8)-B(2)-Ir(1)	166.6(4)
B(6)-B(3)-B(4)	58.9(4)
B(6)-B(3)-B(9)	60.1(4)
B(4)-B(3)-B(9)	104.5(5)
B(6)-B(3)-B(7)	105.0(5)
B(4)-B(3)-B(7)	101.4(5)
B(9)-B(3)-B(7)	58.2(4)
C(51)-B(4)-B(2)	60.9(4)
C(51)-B(4)-B(6)	106.0(5)
B(2)-B(4)-B(6)	61.0(4)
C(51)-B(4)-B(3)	105.8(5)
B(2)-B(4)-B(3)	110.8(5)
B(6)-B(4)-B(3)	60.1(4)
C(51)-B(4)-Ir(1)	88.6(4)
B(2)-B(4)-Ir(1)	71.3(3)
B(6)-B(4)-Ir(1)	111.5(4)
B(3)-B(4)-Ir(1)	164.7(5)
C(52)-B(5)-B(1)	60.1(4)
C(52)-B(5)-B(9)	104.8(5)
B(1)-B(5)-B(9)	108.0(5)
C(52)-B(5)-B(7)	57.4(4)
B(1)-B(5)-B(7)	107.4(5)
B(9)-B(5)-B(7)	59.9(4)
C(52)-B(5)-B(8)	106.4(5)
B(1)-B(5)-B(8)	59.7(4)
B(9)-B(5)-B(8)	60.7(4)
B(7)-B(5)-B(8)	108.4(5)
B(4)-B(6)-B(2)	58.6(4)

B(4)-B(6)-B(3)	60.9(4)
B(2)-B(6)-B(3)	109.5(5)
B(4)-B(6)-B(8)	107.5(5)
B(2)-B(6)-B(8)	60.2(4)
B(3)-B(6)-B(8)	111.5(5)
B(4)-B(6)-B(9)	106.4(5)
B(2)-B(6)-B(9)	107.1(5)
B(3)-B(6)-B(9)	60.7(4)
B(8)-B(6)-B(9)	60.7(4)
C(52)-B(7)-B(9)	105.4(5)
C(52)-B(7)-B(5)	58.6(4)
B(9)-B(7)-B(5)	59.6(4)
C(52)-B(7)-B(3)	108.4(5)
B(9)-B(7)-B(3)	59.6(4)
B(5)-B(7)-B(3)	108.5(5)
B(1)-B(8)-B(2)	58.9(4)
B(1)-B(8)-B(6)	106.7(5)
B(2)-B(8)-B(6)	59.3(4)
B(1)-B(8)-B(5)	58.9(4)
B(2)-B(8)-B(5)	105.2(5)
B(6)-B(8)-B(5)	106.4(5)
B(1)-B(8)-B(9)	105.7(5)
B(2)-B(8)-B(9)	105.8(5)
B(6)-B(8)-B(9)	59.9(4)
B(5)-B(8)-B(9)	58.7(4)
B(5)-B(9)-B(7)	60.5(4)
B(5)-B(9)-B(6)	107.6(5)
B(7)-B(9)-B(6)	107.3(5)
B(5)-B(9)-B(3)	111.2(5)
B(7)-B(9)-B(3)	62.2(4)
B(6)-B(9)-B(3)	59.2(4)
B(5)-B(9)-B(8)	60.6(4)
B(7)-B(9)-B(8)	108.7(5)
B(6)-B(9)-B(8)	59.4(4)

B(3)-B(9)-B(8)	109.2(5)

Symmetry transformations used to generate equivalent atoms:

2.6 References

1. For select examples of coordinating atoms tethered to m-terphenyl position A, see: (a) B. Jung, A. H. Hoveyda, *J. Am. Chem. Soc.,* **2012**, *134*, 1490. (b) S. Schenk, M. Reiher, *Inorg. Chem.*, **2009**, *48*, 1638. (c) A. L. Kenward, J. A. Ross, W. E. Piers, M. Parvez, *Organometallics,* **2009**, *28*, 3625. (d) D. V. Yandulov, R. R. Schrock, A. L. Rheingold, C. Ceccarelli, W. M. Davis, *Inorg. Chem*., **2003**, *42*, 796. (e) D. V. Yandulov, R. R. Schrock, *Science,* **2003**, *301*, 76. (f) D. V. Yandulov, R. R. Schrock, *J. Am. Chem. Soc.,* **2002**, *124*, 6252.

2. For select examples of coordinating atoms tethered to m-terphenyl position B, see: (a) B. Jung, A. H. Hoveyda, *J. Am. Chem. Soc*., **2012**, *134*, 1490. (b) B. R. Barnett, C. E. Moore, A. L. Rheingold, J. S. Figueroa, *J. Am. Chem. Soc.*, **2014**, *136*, 10262. (c) T. B. Ditri, A. E. Carpenter, D. S. Ripatti, C. E. Moore, A. L. Rheingold, J. S. Figueroa, *Inorg. Chem.*, **2013**, *52*, 13216. (d) B. M. Emerich, C. E. Moore, B. J. Fox, A. L. Rheingold, J. S. Figueroa, J. S. *Organometallics*, **2011**, *30*, 2598. (e) B. P. Johnson, S. Almstätter, F. Dielmann, M. Bodensteiner, M. Scheer, *Z. Anorg. Allg. Chem.*, **2010**, *636*, 1275. (f) G. W. Margulieux, N. Weidemann, D. C. Lacy, C. E. Moore, A. L. Rheingold, J. S. Figueroa, *J. Am. Chem. Soc.,* **2010**, *132*, 5033. (g) S.T. Liddle, P. L. Arnold, *Dalton Trans.*, **2007**, 3305. (h) J. Gavenonis, T. D. Tilley, *Organometallics,* **2003**, *23*, 31. (i) N. J. Hardman, C. Cui, H. W. Roesky, W. H. Fink, P. P. Power, *Angew. Chem., Int. Ed.* **2001**, *40*, 2172. (j) B. Twamley, C. S. Hwang, N. J. Hardman, P. P. Power, *J. Organomet. Chem*., **2000**, *609*, 152. (k) B. Twamley, C.D. Sofield, M. M. Olmstead, P. P. Power, *J. Am. Chem. Soc.,* **1999**, *121*, 3357.

3. For reviews on applications of terphenyls as superbulky anionic ligands, see: (a) P. P. Power, *Acc. Chem. Res.,* **2011**, *44*, 627. (b) E. Rivard, P. P. Power, *Inorg. Chem.,* **2007**, *46*, 10047.

4. For reviews on carboranes and boron clusters as ligand substituents, see: (a) A. R. Popescu, F. Teixidor, C. Vinas, *Coord. Chem. Rev*., **2014**, *269*, 54. (b)A. M. Spokoyny, *Pure Appl. Chem.*, **2013**, *85*, 903. For reviews on icosahedral carboranes, see: (c) D.Olid, R. Nunez, C. Vinas, F. Teixidor, *Chem. Soc. Rev.*, **2013**, *42*, 3318. (d) C. Douvris, J. Michl, *Chem. Rev.*, **2013**, *113*, 179. (e) M. Scholz, E. Hey-Hawkins, *Chem. Rev.,* **2011**, *111*, 7035.

5. For classic examples of phosphines containing carborane ligand substituents, see: (a) E. Hoel, M. F. Hawthorne, *J. Am. Chem. Soc.,* **1975**, *97*, 6388. (b) F. Rohrscheid, R. H. Holm, *J. Organomet. Chem.,* **1965**, *4*, 335. (c) F. Teixidor, J. A. Ayllon, C. Vinas, R. Kivekas, R. Sillanpaa, J. Casabo, *J. Chem. Soc.*, *Chem. Commun.,* **1992**, 1281. (d) F. Teixidor, C. Vinas, M. Mar Abad, M. Lopez, J. Casabo, *J. Organometallics,* **1993**, *12*, 3766. For recent examples of phosphines containing carborane substituents, see: (e) V. Lavallo, J. H. Wright II, F. S. Tham, and S. Quinlivan, *Angew. Chem. Int. Ed.*, **2013**, *52*, 3172. (f) A. El-Hellani, C. E. Kefalidis, F. S. Tham, L. Maron, V.

Lavallo, *Organometallics*, **2013**, 32, 6887. (g) A. M. Spokoyny, C. D. Lewis, G. Teverovskiy, S. L. Buchwald, *Organometallics*, **2012**, *31*, 8478. (h) A. M. Spokoyny, C. W. Machan, D.J. Clingerman, M. S. Rosen, M. J. Wiester, R. D. Kennedy, C. L. Stern, A. A. Sarjeant, C. A. Mirkin, *Nat. Chem.,* **2011**, *3*, 590. (i) N. Fey, M. F. Haddow, R. Mistry, N. C. Norman, A. G. Orpen, T. J. Reynolds, P. G. Pringle, *Organometallics* **2012**, *31*, 2907. (j) P. Farras, F. Teixidor, I. Rojo, R. Kivekas, R. Sillanpaa, P. Gonzalez-Cardoso, C. Vinas, *J. Am. Chem. Soc.,* **2011**, *133*, 16537. (k) P. Farras, D. Olid-Britos, C. Vinas, F. Teixidor, *Eur. J. Inorg. Chem*., **2011**, 2011, 2525. (l) A. R. Popescu, A. Laromaine, F. Teixidor, R. Sillanpaa, R. Kivekas, J. I. Llambias, C. Vinas, *Chem. Eur. J.,* **2011**, *17*, 4429. (m) R. Nunez, P. Farras, F. Teixidor, C. Vinas, R. Sillanpaa, R. Kivekas, *Angew. Chem., Int. Ed.*, **2006**, *45*, 1270. (n) F. Teixidor, R. Nunez, C. Vinas, R. Sillanpaa, R. Kivekas, *Angew. Chem., Int. Ed.,* **2000**, *39*, 4290.

6. (a) M. J. Asay, S. P. Fisher, S. E. Lee, F. S. Tham, D. Borchardt, V. Lavallo, *Chem. Commun.*, **2015**, *51*, 5359. (b) A. El-Hellani, V. Lavallo, *Angew. Chem., Int. Ed.*, **2014**, *53*, 4489.

7. (a) Y. Li, P. J. Carroll, L. G. Sneddon, *Inorg. Chem.,* **2008**, *47*, 9193. (b) U. Kusari, Y. Li, M. G. Bradley, L. G. Sneddon, *J. Am. Chem. Soc.*, **2004**, *126*, 8662.

8. F. Teixidor, C. Vinas, M. M. Abad, R. Nunez, R. Kivekas, R. Sillanpaa, *J. Organomet. Chem*., **1995**, *503*, 193.

9. H. Schumann, M. Heisler, J. Pickardt, *Chem. Ber.* 1977, 110, 1020.

10. A. Maisonnat, P. Kalck, R. Poilblanc, *Inorg. Chem*., **1974**, *13*, 661.

11. H. Clavier, S. P. Nolan, *Chem. Commun.*, **2010**, *46*, 841.

12. V. I. Bregadze, *Chem. Rev.* **1992**, *92*, 209.

13. (a) B. A. Adler, M. F. Hawthorne, *J. Am. Chem. Soc.* **1970**, *92*, 6174, (b) L. A. Leites,

Chem. Rev. **1992**, *92*, 312.

14. A. El-Hellani, C. E. Kefalidis, F. S. Tham, L. Maron, V. Lavallo, *Organometallics***,**

2013, *32*, 6887.

Chapter 3: Inductive effects of the monoanionic 12 and 10-vertex carboranes

3.1 Abstract

A phosphine containing a 10-vertex carborane anion substituent and its subsequent ligation to a Rh(I) carbonyl complex is reported. The complex is characterized by NMR spectroscopy and a single crystal X-ray diffraction study. In addition, the inductive effects of both 10 and 12 vertex C-functionalized closo-carborane anions are elucidated via I.R. analysis of the CO stretching frequencies of two Rh carbonyl complexes. Unlike C-functionalized neutral o-carborane the 10 and 12-vertex carborane anions are both strong electron donor substituents.

3.2 Introduction

An intriguing alternative to ubiquitous hydrocarbon ligand R-groups are the organomimetic[1] closo-carboranes,[2] which can be thought of as 3-dimensional analogues of Huckel aromatics.[2g] The most common closo-carboranes utilized in ligand design are derived from neutral icosahedral dicarbaborane clusters ($C_2B_{10}H_{12}$).[2f] Due to its facile synthesis,[3] the ortho-carborane (o-carborane) isomer **1** (**Figure 3.1**) has been the most frequently utilized. When functionalized at a C-vertex **1** acts as a strong electron withdrawing group, more so than a benzene ring.[4] Spokoyny,[1,5] has elegantly shown that functionalization at B-vertices renders such clusters strong donor substituents. Although **1** offers many distinct characteristics, such as a unique steric profile and the ability to form H–H hydrogen bonds,[2f] it exhibits reactivity that is perhaps undesirable for catalysis, such as facile B–H cyclometalation[6] and cluster opening reactions[7] to afford nido-carboranes. The latter reactions have been exploited by Teixidor and Vinas to

produce novel anionic ligands, featuring nido-cluster substituents.[2a,d,e,4b,c,8] These *nido*-cluster substituents have also been shown to be strong donors when attached to ligands via the B-vertices.[8o]

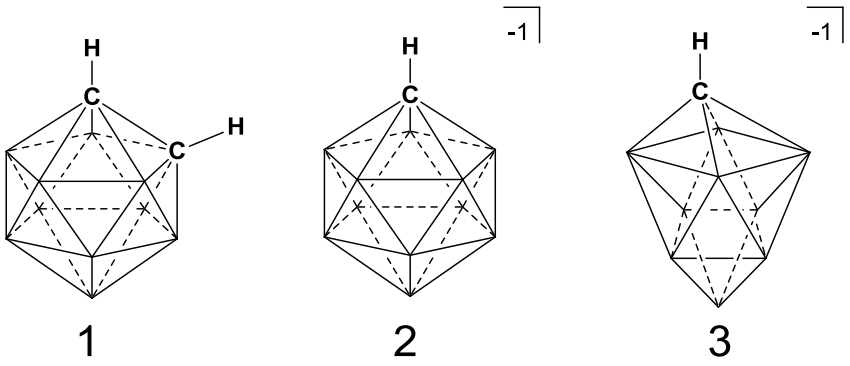

Figure 3.1- Representations of carborane clusters **1** ($C_2B_{10}H_{12}$), **2** ($CB_{11}H_{12}^-$), and **3** ($CB_9H_{10}^-$).

The carba-closo-dodecaborate anion **2** $CB_{11}H_{12}^{-1}$ is isoelectronic with 1.[2c] As a result of the negative charge of **2** being delocalized over the 12 cage atoms, this carborane is rendered a weakly coordinating anion. This characteristic has led to the utilization of **2** and its derivatives as spectator anions to stabilize exotic cations.[9] We recently reported the first examples of C-functionalized carborane anions **2** in ligand and transition metal-based catalyst design.[10] It was demonstrated that **2** and its polyhalogenated variants are competent substituents for phosphine[10a,d–f] and N-heterocyclic carbene ligands,[10b,c] which produce unusual zwitterionic and anionic complexes. Importantly, it was shown that the introduction of a closo-carborane anion substituent can lead to dramatically improved catalytic performance compared to systems containing traditional ligands.[10d] In addition, we have shown that as a ligand substituent **2** is intrinsically more resistant to B–H cyclometalation compared to **1**.[10f]

Another closo-carborane anion is the ten vertex species **3** $CB_9H_{10}^-$, which has a slightly less delocalized charge. In contrast to **2**, cluster **3** and its derivatives have rarely[11] been exploited as weakly coordinating anions. Recently, improved synthetic protocols have made **3** readily accessible on a reasonable scale.[12] We became interested in the possibility of utilizing **3** as a ligand substituent,[13] which could complement our investigations into **2** by providing a smaller group with distinct electronic properties. Here we report the first example of the utilization of cluster **3** as a ligand substituent. In addition, a comparative study on the inductive effects of closocarborane anions **2** and **3** reveals that in contrast to C-functionalized o-carborane **1** these anionic clusters are strong electron donors.

3.3 Results and discussion

To begin this investigation we chose to target a simple phosphine **4[Li$^+$]** (Fig. 2) with a 10-vertex carborane anion substituent **3**. Similar to carboranes **1** and **2**, cluster **3** contains a mildly acidic C–H vertex that can be deprotonated with strong bases and subsequently functionalized with electrophiles. Thus, reaction of **3[HNMe$_3^+$]** with two equivalents of *n*-BuLi followed by the addition of ClP(*i*Pr)$_2$ results in rapid formation of the desired ligand **4[Li$^+$]** as evidenced by multinuclear NMR spectroscopy (Fig. 2). The ^{31}P and ^{11}B NMR spectra of the anionic carboranyl phosphine **4[Li$^+$]** display a single peak at 22.0 ppm and a set of three broad singlets (11B{1H}: 32.6, -16.4, -23.4 ppm; 1 : 4 : 4 ratio), respectively. Similar to the known carboranyl phosphine containing the 12-vertex cluster **2**, which is air sensitive when dissolved in organic solvents,[14] THF

solutions of ligand **4[Li$^+$]** are oxidized to the corresponding phosphine oxide in two hours.

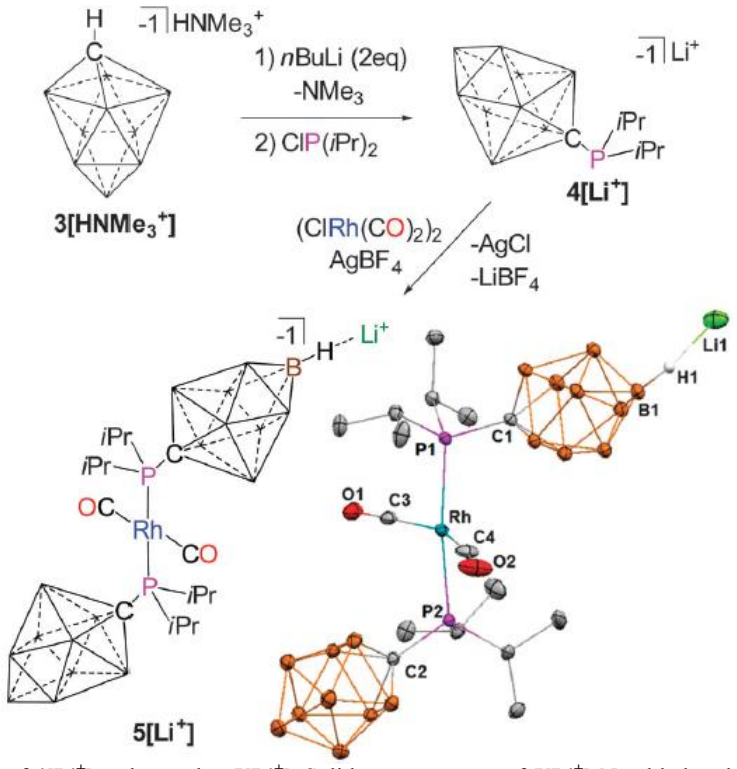

Fig. 3.2 - Synthesis of **4[Li$^+$]** and complex **5[Li$^+$]**. Solid-state structure of **5[Li$^+$]**. Notable bond lengths (Å): Rh–P1 = 2.3534(3), Rh–P2 = 2.3554(3), Rh–C3 = 1.9024(11), Rh–C4 = 1.9166(12), C4–O2 = 1.1321(15), C3–O1 = 1.1354(14), H1–Li1 = 1.997. Selected bond angles (°): C3–Rh–C4 = 154.4, P1–Rh–P2 = 171.9. Color code: C = grey, B = brown, Rh = blue, Li = green, O = red. Unlabeled vertices = B–H.

In order to gain insight into the inductive effects of anionic carborane substituent **3**, we targeted the carbonyl complex **5[Li$^+$]** for I.R. analysis. Although anionic because of the presence of two charged phosphine ligands, **5[Li$^+$]** has an iso-electronic coordination environment with cationic species $RhL_2(CO)_2^{+1}$ for which there is a significant amount of I.R. data available for comparison. Thus, reaction of **4[Li$^+$]** with a mixture of $(ClRh(CO)_2)_2$ and $AgBF_4$ dissolved in CH_2Cl_2 results in rapid formation of the anionic diphosphine complex **5[Li$^+$]**. The ^{31}P and ^{11}B NMR spectra of **5[Li$^+$]** display a doublet at

56.1 ppm ($^{31}P\{1H\}$; d, ^{1}J(Rh–P) = 102.4 Hz) and a set of three broad singlets ($^{11}B\{^{1}H\}$: 35.9, -15.7, -23.5 ppm; 1 : 4 : 4 ratio), respectively. The ^{11}B proton coupled spectrum shows three doublet resonances, which indicates the presence of hydrides at each cluster vertex and rules out the possibility of cyclometalation at Rh. A single crystal X-ray diffraction study confirms the identity of **5[Li^{+}]**, which displays a slightly distorted square planar geometry (sum of the L–M–L angles = 363.61°). The cone angle of ligand **4[Li^{+}]**, as determined from the crystallographic data, is 168°. Notably, the Li^{+} counter cation in **5[Li^{+}]** is coordinated to the most electron rich B–H vertex that is antipodal to carbon. Two THF molecules and an additional B–H interaction from a different molecule in the unit cell complete the tetrahedral coordination environment at Li^{+}. The solution I.R. spectrum of **5[Li^{+}]** shows a prominent absorbance for the B–H architecture (I.R. = 2553 cm^{-1}; CH_2Cl_2) as well as an intense stretch for the carbonyl ligands (I.R. = 1997 cm^{-1}; CH_2Cl_2). For comparison, the isoelectronic complexes $Rh(P(iPr)_3)_2(CO)_2^{+1}$ and $Rh(P(Ph)_3)_2(CO)_2^{+1}$ display CO stretching frequencies at 2010 cm^{-1} and 2047 cm^{-1} (CH_2Cl_2), respectively.[15] Therefore, in contrast to C-functionalized *o*-carborane **1**, **3** is a potent electron donor substituent, more so than an isopropyl group.

For further comparison we next sought to elucidate the inductive effects of the larger 12-vertex carborane anion **2**. We hypothesized that because the negative charge in **2** is more delocalized it should be a weaker donor than **3** but still a stronger donor than neutral C-functionalized *o*-carborane **1**. Reaction of phosphine **6[Li^{+}]**, which is isostructural with **4[Li^{+}]**, with a mixture of $(ClRh(CO)_2)_2$ and $AgBF_4$ dissolved in CH_2Cl_2 results in the formation of the anionic diphosphine complex **7[Li^{+}]** as determined by

multinuclear NMR spectroscopy (Fig. 3). However, **7[Li$^+$]** rapidly extrudes a CO ligand to afford the mono-CO complex **8[Li$^+$]**. The difference in stability between **7[Li$^+$]** and isoelectronic **5[Li$^+$]** can perhaps be explained by the greater steric bulk of the 12-vertex carborane anion as well as electronic effects, vide infra. The structure of **8[Li$^+$]** was confirmed by NMR spectroscopy as well as a single crystal X-ray diffraction study. In the solid-state **8[Li$^+$]** displays a square planar geometry with a B–H ‘‘agostic-like’’[10e] interaction with the coordination site where CO was liberated. The cone angle for phosphine ligand **6[Li$^+$]** is slightly larger (171°) compared to the 10-vertex ligand **4[Li$^+$]**, vide supra. Interestingly, in contrast to **5[Li$^+$]** the Li^+ cation in **8[Li$^+$]** is sequestered by four THF molecules and shows no interaction with the 12-vertex carborane anion. This feature highlights the reduced coordinative ability, due to enhanced charge delocalization, of **2** compared to **3**. The I.R. spectrum of a CH_2Cl_2 solution of 8[Li+] shows a single CO stretch at 1991 cm^{-1}.

Seeking to generate **7[Li$^+$]** in pure form and obtain I.R. data for an isoelectronic comparison we charged a J-young tube, containing a solution of **8[Li$^+$]**, with one atmosphere of CO. Gratifyingly, under these conditions **8[Li$^+$]** is completely converted back to **7[Li$^+$]**, which is stable under a CO atmosphere. Analysis of the I.R. spectrum of **7[Li$^+$]** dissolved in CH_2Cl_2 reveals a strong CO stretch at 2012 cm^{-1}. The increased CO stretching frequency relative to **8[Li$^+$]**, is consistent with the formation of **7[Li$^+$]**, since both of the trans-CO ligands are engaged in competitive π-backbonding with the same Rh d-orbital. This data also suggests that the lability of CO in **7[Li$^+$]** compared to **5[Li$^+$]** is not only the result of increased steric pressure, but also perhaps a result of reduced π-

backbonding from the less electron rich Rh-center of **7[Li$^+$].** From this analysis we can conclude that the 12-vertex carborane anion substituent **2** is an electron donor, nearly as strong as an isopropyl group but not as potent as **3**. The observed electronic differences between **2** and **3** mirror classical Hammet studies by Zakharkin,[16a,b] which showed that isoelectronic 10-vertex neutral dicarbaboranes are less electron withdrawing than their 12-vertex analogues.

3.4 Conclusion

The manuscript above demonstrates for the first time that 10-vertex closo-carborane anion **3** is a viable ligand substituent with distinct electronic and steric properties. In addition, the inductive effects of both the parent hydrido 10 and 12-vertex C-functionalized closo-carborane anions **3** and **2** have been elucidated. Unlike C-functionalized neutral o-carborane **1** both **2** and **3** are strong electron donor substituents. The fact that C-functionalized **2** is a much stronger donor than **1** highlights the effect that cluster charge has on the inductive effects of 12-vertex closo-carboranes. Likewise, the increase in donor ability of **3** relative to **2** shows that implementing smaller clusters with less delocalized charge dramatically influences the inductive effects of carborane ligand substituents. These results are not only fundamentally important but should be instructive for future investigations into ligand design for implementation in homogenous catalysis.

3.5 Experimental

Experimental data can be observed online at DOI: 10.1039/C5CC08377J.

3.6 References

1 For a discussion of the organomimetic properties of carboranes, see: A. M. Spokoyny, *Pure Appl. Chem.,* **2013**, *85*, 903.

2 For recent reviews on carboranes, see: (a) A. R. Popescu, F. Teixidor, C. Vinas, *Coord. Chem. Rev.,* **2014**, *269*, 54; (b) J. Zhang, Z. Xie, *Acc. Chem. Res.*, **2014**, *47*, 1623; (c) C. Douvris, J. Michl, *Chem. Rev.*, **2013**, *113*, 179; (d) D. Olid, R. Nunez, C. Vinas, F. Teixidor, *Chem. Soc. Rev.,* **2013**, *42*, 3318; (e) P. Farras, E. J. Juarez-Perez, M. Lepsik, R. Luque, R. Nunez, F. Teixidor, *Chem. Soc. Rev*., **2012**, *41*, 3445; (f) M. Scholz, E. Hey-Hawkins, *Chem. Rev.,* **2011**, *111*, 7035; (g) J. Poater, M. Sola`, C. Vin˜as, F. Teixidor, *Angew. Chem., Int. Ed*., **2014**, *53*, 12191.

3 Y. Li, P. J. Carroll, L. G. Sneddon, *Inorg. Chem.*, **2008**, *47*, 9193.

4 (a) F. Rohrscheid, R. H. Holm, *J. Organomet. Chem.*, **1965**, *4*, 335; (b) R. Nunez, P. Farra`s, F. Teixidor, C. Vin˜as, R. Sillanpaa, R. Kivekas, *Angew. Chem., Int. Ed*., **2006**, *45*, 1270; (c) F. Teixidor, R. Nu´n˜ez, C. Vin˜as, R. Sillanpaa,R. Kivekas, Angew. *Chem., Int. Ed.*, **2000**, 39, 4290.

5 (a) A. M. Spokoyny, C. D. Lewis, G. Teverovskiy, S. L. Buchwald, *Organometallics*, **2012**, *31*, 8478; (b) A. M. Spokoyny, C.W.Machan, D. J. Clingerman, M. S. Rosen, M. J. Wiester, R. D. Kennedy, C. L. Stern, A. A. Sarjeant, C. A. Mirkin, *Nat. Chem.*, **2011**, *3*, 590.
6 E. L. Hoel, M. F. Hawthorne, *J. Am. Chem. Soc*., **1975**, *97*, 6388.

7 R. A. Wiesboeck, M. F. Hawthorne, *J. Am. Chem. Soc.,* **1964**, *86*, 1642.

8 (a) D. Brusselle, P. Bauduin, L. Girard, A. Zaulet, C. Vinas, F. Teixidor, I. Ly, O. Diat, *Angew. Chem., Int. Ed*., **2013**, *52*, 12114; (b) A. R. Popescu, A. Laromaine, F. Teixidor, R. Sillanpaa, R. Kivekas, J. I. Llambias, C. Vinas, *Chem. Eur. J.,* **2011**, *17*, 4429; (c) P. Farras, F. Teixidor, I. Rojo, R. Kiveka¨s, R. Sillanpaa, P. Gonzalez-Cardoso, C. Vinas, *J. Am. Chem. Soc.*, **2011**, *133*, 16537; (d) P. Farra`s, D. Olid-Britos, C. Vinas, F. Teixidor, *Eur. J. Inorg. Chem.,* **2011**, 2525; (e) F. Teixidor, R. Nunez, M. A. Flores, A. Demonceau, C. Vinas, *J. Organomet. Chem.,* **2000**, *614–615*, 48–56; (f) F. Teixidor,M. A. Flores, C. Vinas, R. Sillanpaa, R. Kivekas, *J. Am. Chem. Soc.,* **2000**, *122*, 1963; (g) R. Nunez, C. Vinas, F. Teixidor, R. Sillanpaa, R. Kivekas, *J. Organomet. Chem.,* **1999**, *592*, 22; (h) F. Teixidor, M. A. Flores, C. Vinas, R. Kivekas, R. Sillanpaa, *Organometallics*, **1998**, *17*, 4675; (i) C. Vinas, R. Nunez, F. Teixidor, R. Kivekas, R. Sillanpaa, *Organometallics*, **1996**, *15*, 3850; (j) F. Teixidor, J. A. Ayllon, C. Vinas, R. Kivekas, R. Sillanpaa, J. Casabo, *J. Organomet. Chem.,* **1994**, *483*, 153; (k) F. Teixidor, J. A. Ayllon, C. Vinas, R. Kivekas, R. Sillanpaa, J. Casabo, *Inorg. Chem*., **1994**, *33*, 1756; (l) F. Teixidor, J. A. Ayllon, C. Vinas, R. Kivekas, R. Sillanpaa, J. Casabo, *Organometallics*, **1994**, *13*, 2751; (m) F. Teixidor, C. Vinas, M. Mar Abad, M. Lopez, J. Casabo,

Organometallics, **1993**, *12*, 3766; (n) F. Teixidor, J. A. Ayllon, C. Vinas, R. Kivekas, R. Sillanpaa, J. Casabo, *J. Chem. Soc., Chem. Commun.,* **1992**, 1281; (o) F. Teixidor, G. Barbera, A. Vaca, R. Kivekas, R. Sillanpaa, J. Oliva, C. Vinas, *J. Am. Chem. Soc.*, **2005**, *127*, 10158.

9 For a review on the use of 12-vertex carborane anions to stabilize reactive cations, see: C. A. Reed, *Acc. Chem. Res*., **2009**, *43*, 121.

10 (a) J. Estrada, D. H. Woen, F. S. Tham, G. M. Miyake, V. Lavallo, *Inorg. Chem.,* **2015**, *54*, 5142; (b) M. J. Asay, S. P. Fisher, S. E. Lee, F. S. Tham, D. Borchardt, V. Lavallo, *Chem. Commun*., **2015**, *51*, 5359; (c) A. El-Hellani, V. Lavallo, *Angew. Chem., Int. Ed*., **2014**, *53*, 4489; (d) V. Lavallo, J. H. Wright, F. S. Tham, S. Quinlivan, *Angew. Chem., Int. Ed.,* **2013**, *52,* 3172; (e) A. El-Hellani, C. E. Kefalidis, F. S. Tham, L. Maron, V. Lavallo, *Organometallics*, **2013**, *32*, 6887; (f) J. Estrada, S. E. Lee, S. G. McArthur, A. El-Hellani, F. S. Tham, V. Lavallo, *J. Organomet. Chem.*, **2015**, *798*, 214.; for an example of a ligand containing a 12-vertex carborane anion tethered via a B-vertex, see: (g) A. Himmelspach, M. Finze, S. Raub, *Angew. Chem., Int. Ed.,* **2011**, *50*, 2628.

11 (a) Z. Xie, T. Jelinek, R. Bau, C. A. Reed, *J. Am. Chem. Soc.*, **1994**, *116*, 1907; (b) Z. Xie, D. J. Liston, T. Jelinek, V. Mitro, R. Bau, C. A. Reed, *J. Chem. Soc., Chem. Commun*., **1993**, 384.

12 B. Ringstrand, D. Bateman, R. K. Shoemaker, Z. Janousek, *Collect. Czech. Chem. Commun.*, **2009**, *74*, 419.
13 For an example of the 10-vertex anion 3 used as a ligand itself, bound to a metal via the C-vertex, see: M. Finze, J. A. P. Sprenger, *Chem. Eur. J.*, **2009**, *15*, 9918.

14 M. Drisch, J. A. P. Sprenger, M. Finze, *Z. Anorg. Allg. Chem.*, **2013**, *639*, 1134.

15 (a) O. Nurnberg, H. Werner, *J. Organomet. Chem*., **1993**, *460*, 163; (b) E. W. Evans, M. H. Howlader, M. Atlay, *Transition Met. Chem*., **1994**, *19*, 37.

16 (a) L. I. Zakharkin, V. N. Kalinin, E. G. Rys, B. A. Kvasov, *Izv. Akad. Nauk SSSR*, **1972**, 507; (b) L. I. Zakharkin, V. N. Kalinin, A. P. Snyakln, B. A. Kvasov, *J. Organomet. Chem*., **1969**, *18*, 19.

Chapter 4: Synthesis and reactivity of iron(II) carboranyl phosphines

4.1 Abstract

Methyl acrylate is a valuable feedstock that can be readily polymerized by simple amines and phosphines. However, production of discrete oligomers is quite rare. Utilizing the known 10-vertex carboranyl diisopropylphosphine, the synthesis of two iron complexes was achieved. The bismesitylphosphino iron(II) complex was reacted with three equivalents of methylacrylate to produce a novel phosphonium enolate containing a cyclicly trimerized methyl acrylate motif. A similar iron-carboranylphosphine salt was reacted with various acrylates and showed divergent reactivity from the above iron complex.

4.2 Introduction

Activated alkenes are a substrate class that can undergo synthetically useful carbon-carbon bond forming reactions, such as the atom-economically efficient Rahut-Currier and Morita-Baylis Hillman (MBH) reactions. Catalytic dimerization of methyl acrylate had been first demonstrated as early as 1963 using tris(2-ethylphenyl)phosphine in dioxane[1] and over the years the efficiency has been dramatically improved upon.[2] Catalytic trimerization has also been observed as a side product in dimerization reactions[2b,c] with up to 15% yield.[2b] In spite of these low yields this is currently the sole method in which industrial production of trimerized methyl acrylate, due it being a useful building block towards other organic molecules.[3] Typically simple neutral amines and phosphines are used for oligomerization and even polymerization, though anionic oligomerization has been demonstrated with NaOMe/EtOH albeit uncontrolled.[4] We have

recently developed a library of carboranyl phosphines that have displayed novel reactivity and properties using the 12 and 10-vertex carboranes **(Figure 4.1)** as R-group substituents.[5] Thus far all our reported transition metal complexes with these ligands contain 2nd or 3rd row transition metals, with no representation from the first row. This report investigates known phosphine **1 (Figure 4.1)** and its ligation to an iron(II) metal center and the following reactivity with methyl acrylate.

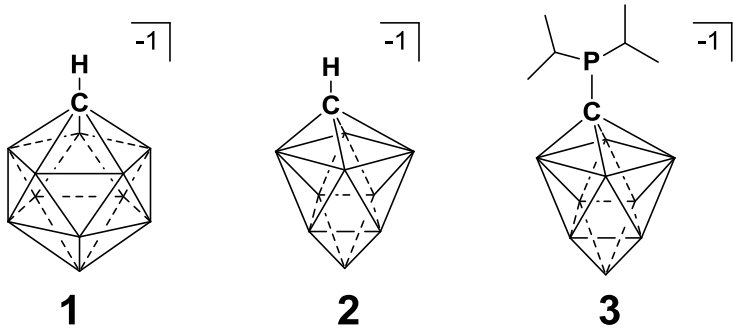

Figure 4.1- 12 and 10-vertex anionic carboranes (left and middle respectively) as well as the known diisopropylcarboranyl phosphine (right).

4.3 Results and discussion

Compound **3[Li$^+$]** was mixed with a $[FeMes_2]_2$ dimer in THF at room temperature to quickly generate product **4 (Scheme 4.1).** The newly produced dark red powder was characterized by multi-nuclear NMR spectroscopy. ^{1}H NMR data showed disappearance of $[FeMes_2]_2$ mestiyl resonances and appearance of broad extremely downfield resonances (129.80, 112.93, and 54.93 ppm) corresponding to the new mestiyl signals. **3** has a ^{31}P NMR signal at 22.0 ppm whereas **4** is silent suggesting the phosphorus atom is directly attached to the paramagnetic iron metal center. The ^{11}B NMR spectrum displayed three broad resonances at 37.38, -5.58, -19.45 ppm, signifying cluster symmetry is not broken in the reaction. Crystallization of the lithium salt of **4** proved difficult, but by

replacing the lithium with a sodium counter cation crystals suitable for diffraction could be obtained.

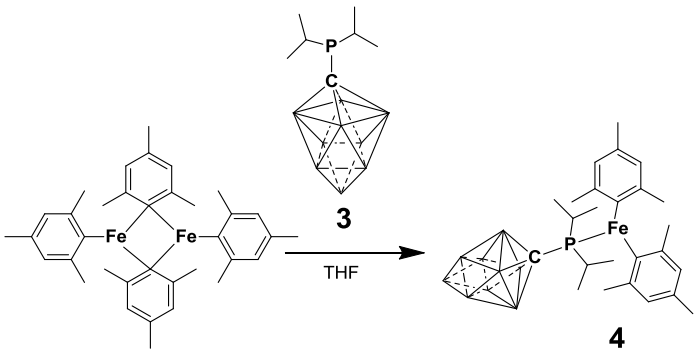

Scheme 4.1 – Synthesis of **4**.

The structure was unambiguously identified from the X-ray crystallographic data as a distorted trigonal planar dimesitylcarboranylphosphino iron(II) complex with a sodium cation with an η^6 coordination with a mesityl ring **(Figure 4.2)**. The sum of the angles at the iron center is essentially 360° (observed 359.82°) solidifying its planarity. The individual angles differ by up to roughly 20° (C1-Fe1-P1 = 110.74°, C2-Fe1-P1 = 119.98° C1-Fe1-C2 = 129.10°) producing the observed distortion. Both ipso mesityl carbon-iron bonds are nearly identical (2.043 Å and 2.046 Å) and the P-Fe bond length is typical (2.475 Å).

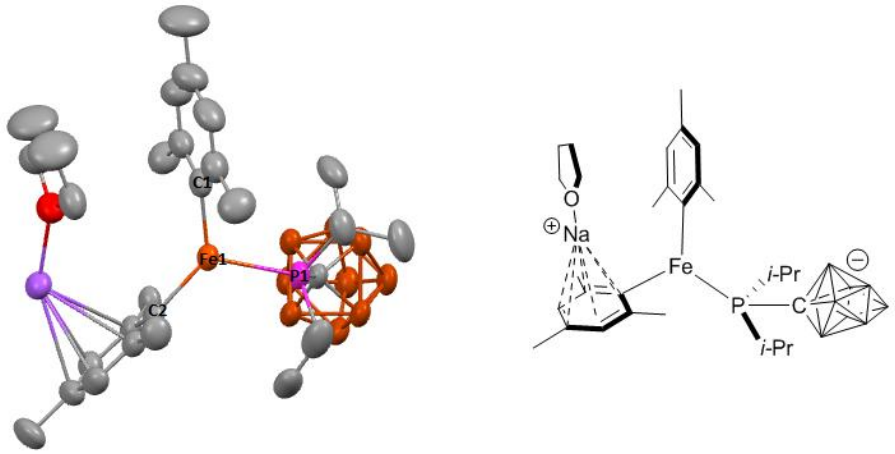

Figure 4.2 – Solid state structure of **4** (left) with a graphical representation (right). Hydrogens atoms and a single pentane molecule omitted for clarity. Color code: C, gray; B, brown; Fe, orange; P, violet; Na, lavender; O, red.

With compound **4** in hand, we then sought to investigate its reactivity with activated olefins, methyl acrylate being the simplest of its kind. Unexpectedly, upon addition of one equivalent of methyl acrylate we saw formation of a new compound by ^{11}B NMR, but presence of initial **4** was still observed suggesting an incomplete reaction. After three equivalents was added, no traces of **4** were observed and only a single set of boron resonances were observed at 46.74, -12.61, -20.44 ppm. Interestingly a new single phosphorus resonance was observed at 43.4 ppm in the ^{31}P NMR spectrum. Appearance of this signal corresponds to the phosphorus atom no longer bound to a paramagnetic iron metal center and also to be noted is that this does not belong to free ligand **3[Li$^+$]** (^{31}P = 22.0 ppm**)** . When catalyzing MBH reactions an intermediate in the reaction involves the initial addition of the phosphine to the beta carbon of an activated olefin to form a phosphonium enolate. These intermediates have escaped isolation until 2007 when the first phosphonium enolate was observed.[6] After production of yellow needle-like crystals,

crystallographic data obtained revealed the presence of a interesting phosphonium enolate complex.

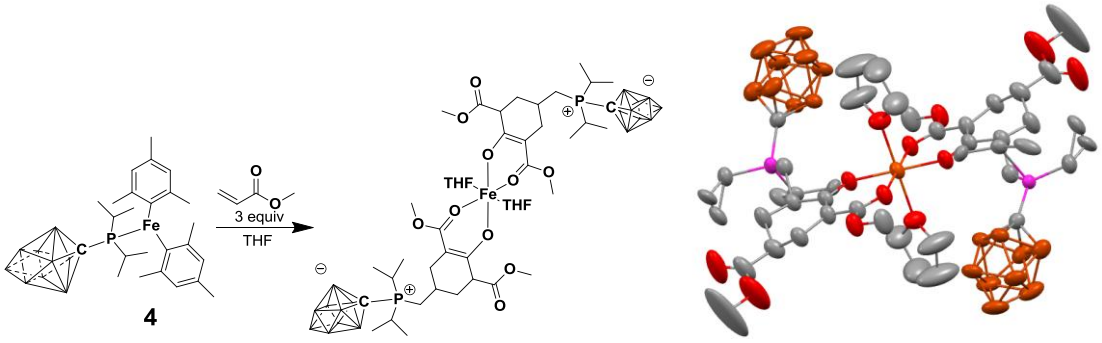

Scheme 4.2 - Synthesis of **5** and the solid state structure. Hydrogens atoms omitted for clarity. Color code: C, gray; B, brown; Fe, orange; P, violet; Na, lavender; O, red.

To our surprise the structure has two phosphonium enolates which contain a cyclicly trimerized methyl acrylate moiety, with coordination to an iron(II) metal center through two of the carbonyl oxygen atoms from separate methyl acrylate units. All iron coordinated O-C bond lengths showed slight elongation (1.279 Å or 1.234 Å) versus non-coordinated carbonyl O-C bond lengths (1.127 Å), but which were noticeably shorter than methoxy O-C single bonds (1.457 Å) suggesting double bond character. In 1966 the cyclic trimerization of methyl acrylate and ethyl acrylate was observed where the only evidence provided was a single NMR spectrum (^{13}C NMR for the methyl acrylate trimer and a ^{1}H NMR for the ethyl acrylate trimer).[7] A cyclotetramerization of various acrylates has also been performed by the Kwon group utilizing an N-heterocyclic carbene catalyst.[8] The crystallographic data shows that a cyclic trimer of methyl acrylate can potentially be synthesized with the assistance of compound **4.** Unfortunately these results were not

reproduced and further investigation is required to verify the production of this unique compound.

The crystal structure of **5** shows a net loss of both mesityl groups from the iron metal center, hinting at the possibility that a similar reactivity might be achieved from a mesityl-free starting complex. This prompted us to attempt synthesis of a bisphosphine iron complex using protonated zwitterion **6**. It is known in our lab that most carboranyl phosphines can undergo protonation upon treatment with HCl, typically as a means of purification. In the same vein, **3[Li$^+$]** was treated with aqueous HCl to precipitate the white powder **6** with a near quantitative yield. This zwitterion was reacted with $[FeMes_2]_2$ in hopes of protonating off the mesityl groups and subsequently producing a bisphosphino complex. The ^{31}P NMR spectrum fell silent, similar to compound **5**, suggesting phosphine ligation and the ^{11}B NMR also had a set of resonances (48.9, 39.6, and -9.5 ppm) drastically different from **3[Li$^+$]** or **6** in terms of chemical shift. Amazingly, needle like silver crystals started to precipitate out of the THF solution minutes after addition. From the produced crystals single-crystal X-ray crystallographic data was obtained which revealed that **7** was an octahedral iron(II) cation with six coordinating THF molecules and two carboranyl phosphine counter anions. Likely upon formation of the expected bisphosphine iron complex there is an equilibrium with **7**, possibly attributed to the carboranes weakly coordinating ability, and due to poor solubility it gradually precipitates out of solution.

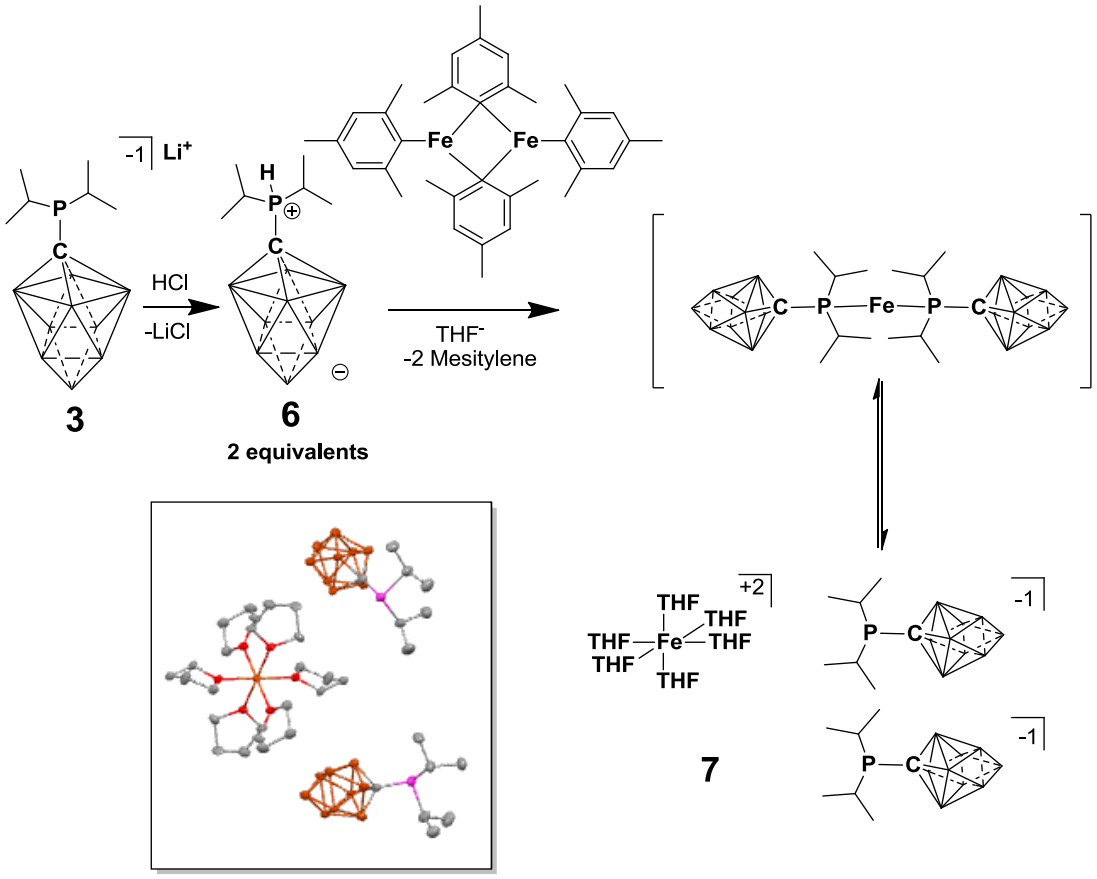

Scheme 4.3 - Synthesis of **6** and **7** as well as a solid state structure of **7** (bottom left). Hydrogens atoms omitted for clarity. Color code: C, gray; B, brown; Fe, orange; P, violet; Na, lavender; O, red.

With this interesting salt in hand we then decided to react it with methyl acrylate as well as other activated alkenes and alkynes. Unfortunately these studies produced none of the interesting reactivity of the previous iron complex **4** and isolated products were typically protonated versions of the corresponding phosphonium enolates.

4.4 Conclusion

The above studies demonstrate the novel reactivity of iron carboranyl phosphine complex **4** in its ability to potentially generate a cyclic trimer of methyl acrylate suspended as a phosphonium enolate in compound **5**, though results were not reproduced. With the expected reactivity of a phosphine to give a methyl acrylate dimer or in some

cases an acyclic trimer, it is intriguing that the cyclic trimer was observed. Synthesized iron salt **7** could produce any cyclic trimerized products and in nearly all cases only protonated phoshponium enolates with one acrylic monomer were observed from cryastal structures. Despite the similar contents of **4** and **7**, both containing a iron(II) metal center and the presence of carboranyl phosphine **3[Li$^+$]**, their divergent chemistry reveals that there is a more intricate dynamic between the components in solution that warrants further investigation into these unique molecules.

4.5 Experimental

Unless otherwise stated, all manipulations were carried out using standard Schlenk or glovebox techniques (O_2, H_2O < 1ppm) under a dinitrogen or argon atmosphere. Piperdine and ethanol were bubbled with N_2 for 15 minutes prior to use. Solvents were dried on K or CaH_2, and distilled under argon before use. Reagents were purchased from commercial vendors and used without further purification. Compound **3** was prepared according to literature.[5d] NMR spectra were recorded on Bruker Avance 300/600 MHz or Varian Inova 400 MHz spectrometers. NMR chemical shifts are reported in parts per million (ppm). ^{1}H NMR and ^{13}C NMR chemical shifts were referenced to residual solvent. ^{11}B NMR chemical shifts were externally referenced to BF_3OEt_2. ^{31}P NMR chemical shifts were externally referenced to 80% H_3PO_4 in H_2O.

4.5.1 Synthesis of **4**

3[Li$^+$] (27 mg, 0.070 mmol) and THF (1 mL) was added to a 20 mL scintillation vial and a separate solution of $[FeMes_2]_2$ (24 mg, 0.040 mmol) and THF (1mL) was also prepared in a 20 mL scintillation vial. The ligand solution was slowly added to the iron

solution and stirred for 30 minutes. Solvent was then removed under reduced pressure and the residue was recrystallized in hexanes to give 30 mg of **4**. ^{11}B-(^{1}H-dec) NMR (96 MHz, d_8-THF, 25 °C) δ = 37.38, -5.58, -19.45. ^{13}C-(^{1}H-dec) NMR (101 MHz, C_6D_6, 25 °C) silent. ^{31}P-(^{1}H-dec) NMR (121 MHz, C_6D_6, 25 °C). silent.

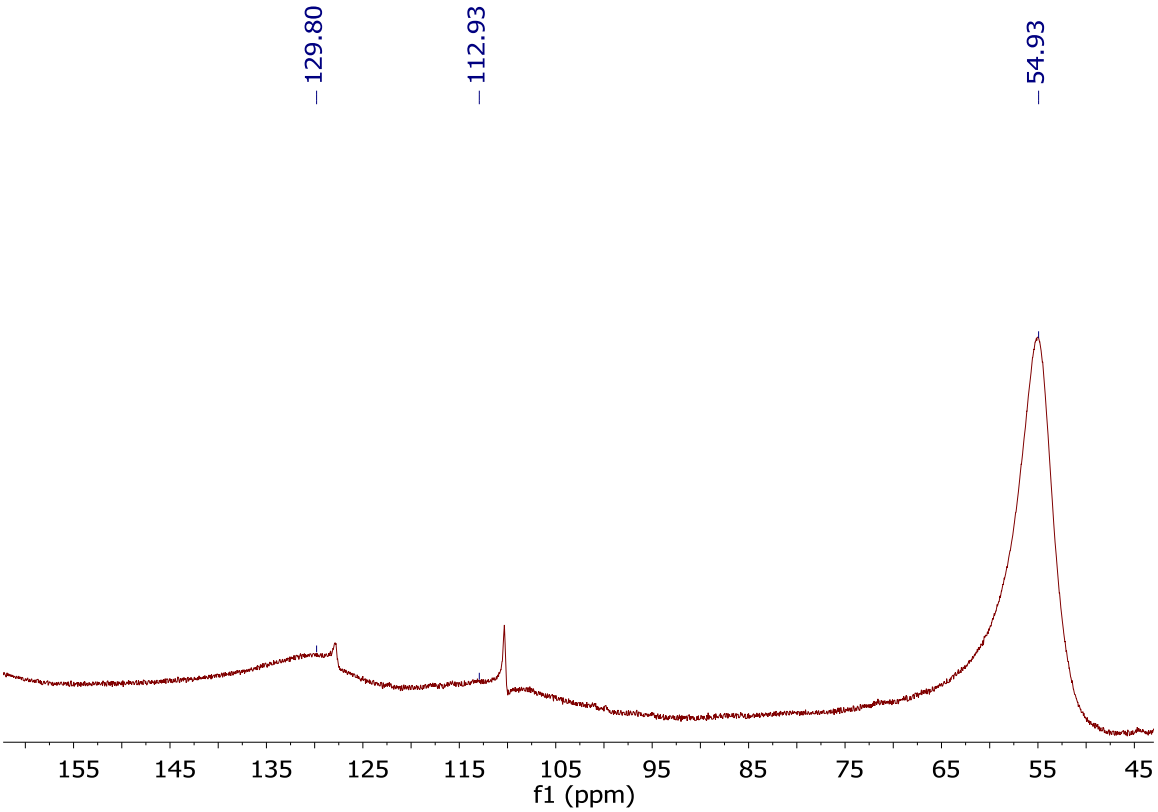

S-4.1 ^{1}H NMR of **4** (300 MHz, d_8-THF) showing broad extremely downfield mesityl resonances.

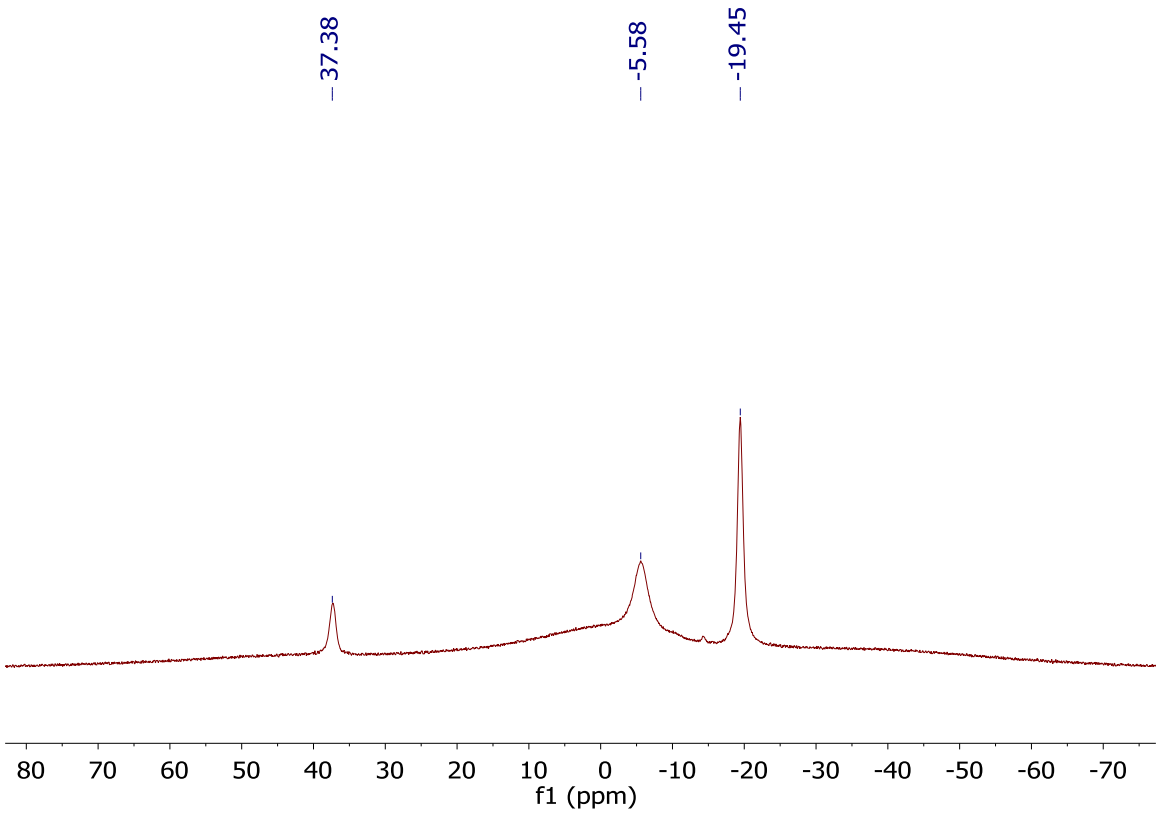

S-4.2 ^{11}B-(^{1}H-dec) NMR (96 MHz, d_8-THF).

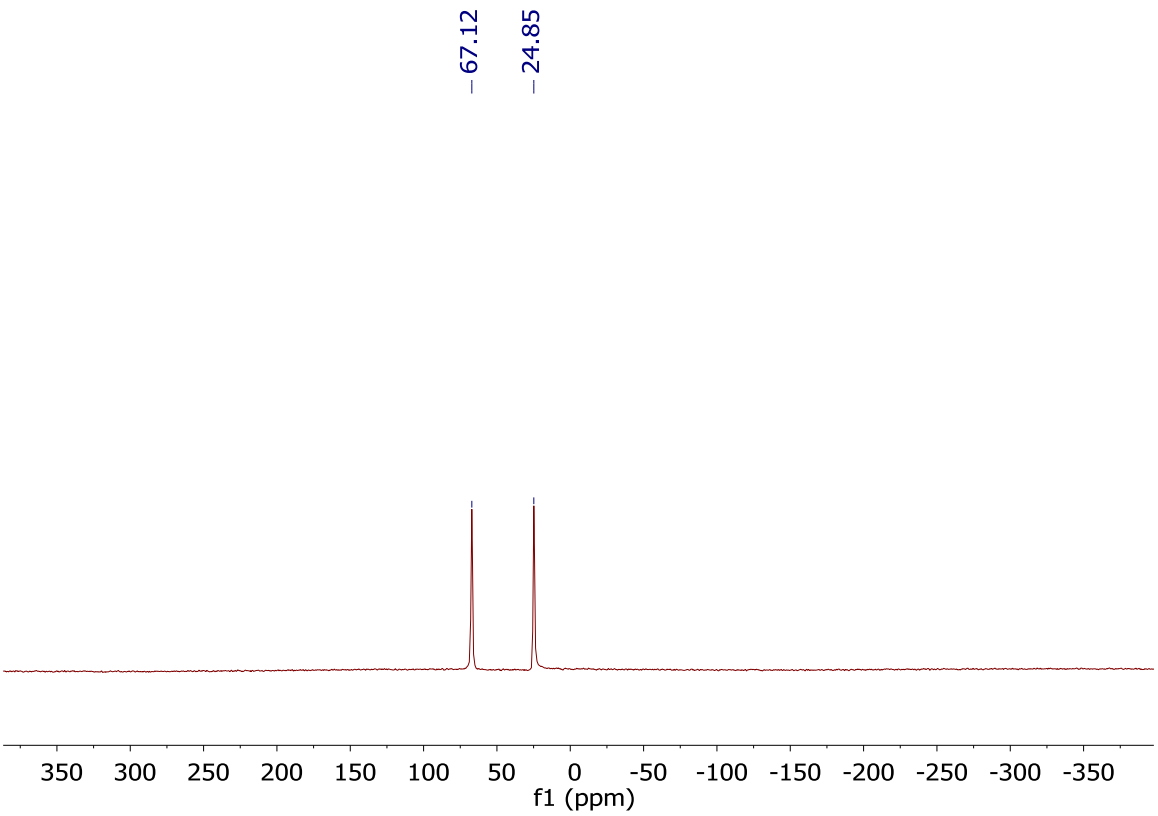

S-4.3 ^{13}C-(^{1}H-dec) NMR of **4** (101 MHz, d_8-THF) displaying no signals, only residual protio solvent observed.

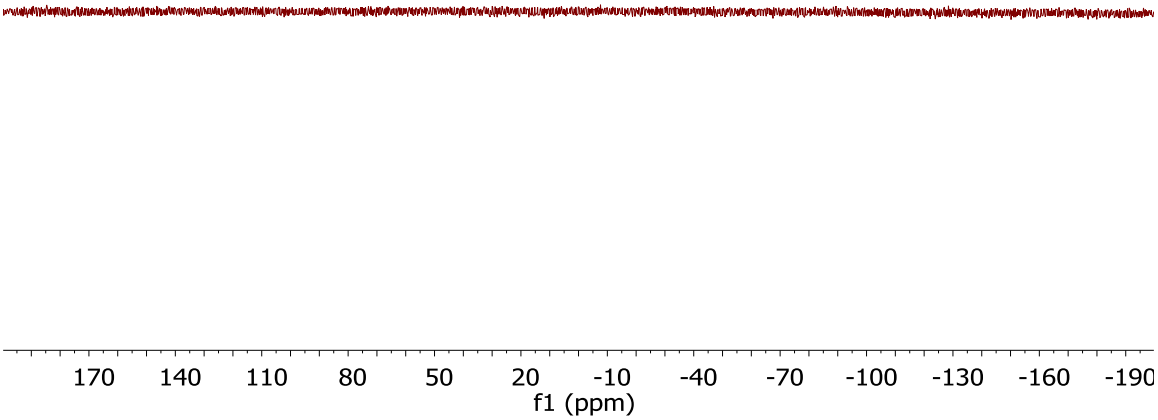

S-4.4 ^{31}P-(^{1}H-dec) NMR of **4** (121 MHz, C_6D_6) displaying no trace of starting phosphine **3**.

4.5.2 Synthesis of **5**

A solution of Compound **4** (100 mg, 0.15 mmol) and THF (4 mL) was added to a 20 mL scintillation vial to which methyl acrylate (39 mg, 0.47 mmol) was added slowly. After 1 hour of stirring the solution was precipitated with pentanes (13mL). Solvent was decanted and washed with pentanes (3 x 4 mL) and then subsequently dried under under reduced pressure to afford 101 mg of **5** as a yellow solid. Crystals were obtained by layering a solution of ^{11}B-(^{1}H-dec) NMR (96 MHz, d_8-THF, 25 °C) δ = 46.74, -12.61, -20.44. ^{31}P-(^{1}H-dec) NMR (121 MHz, d_8-THF, 25 °C). δ = 39.2.

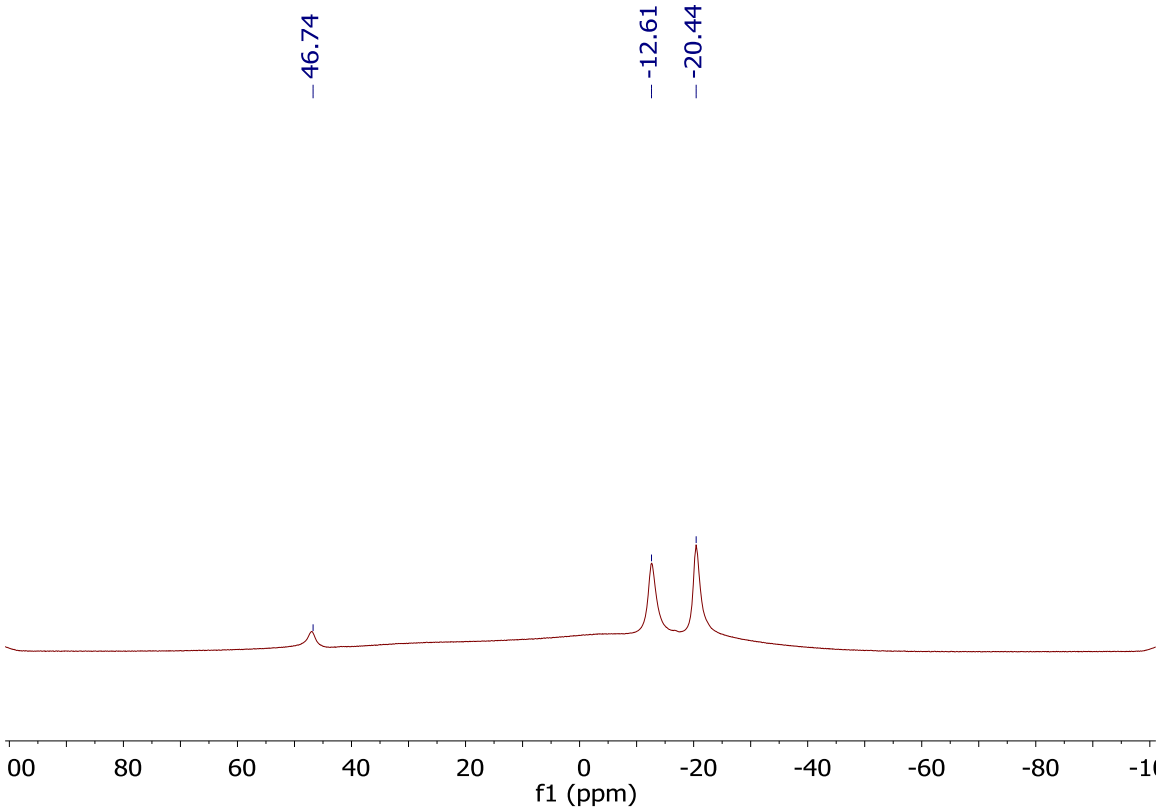

S-4.5 ^{11}B-(^{1}H-dec) NMR of **5** (96 MHz, d_8-THF).

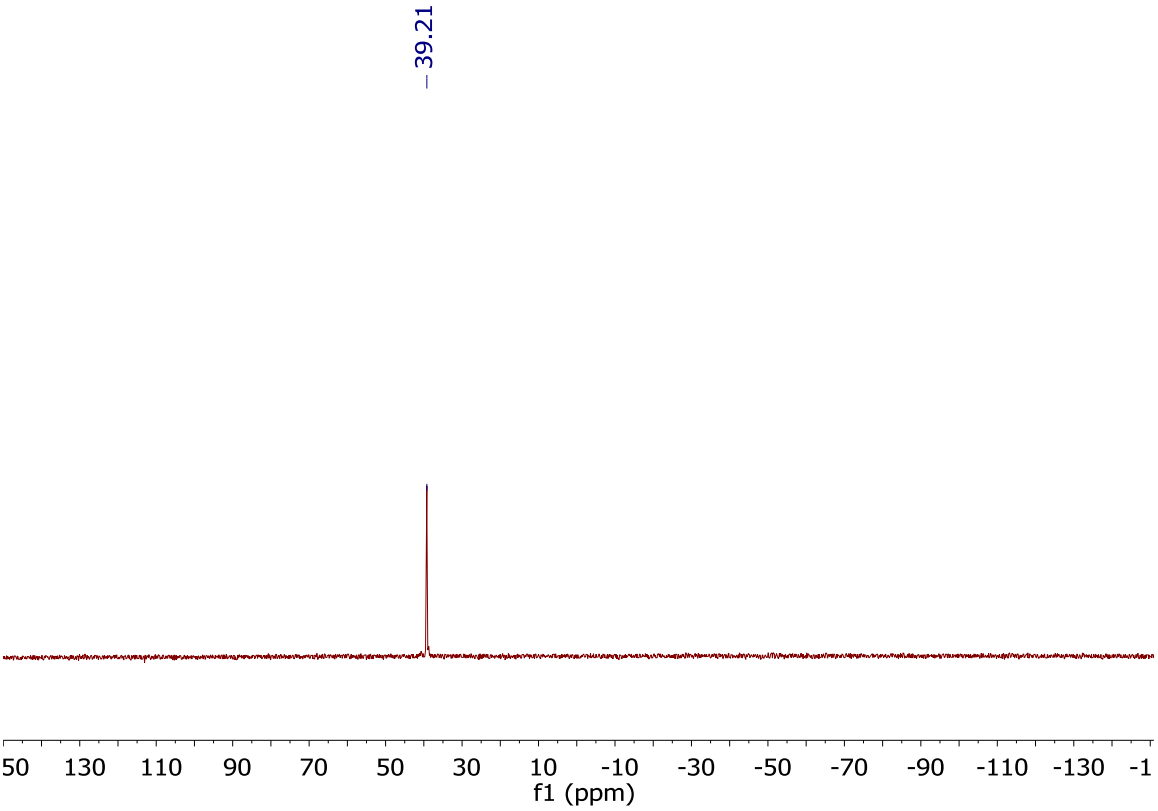

S-4.6 ^{31}P-(^{1}H-dec) NMR of **5** (121 MHz, d_8-THF).

4.5.3 Synthesis of **7**

A solution of **3[Li$^+$]** (27 mg, 0.070 mmol) and THF (1 mL) was prepared. To this aqueous HCl was added to give the protonated phosphonium zwitterion which was filtered, washed with water and hexanes, and dried under vacuum. This white powder was then dissolved in THF (2 mL) in a 20 mL scintillation vial and a separate solution of $[FeMes_2]_2$ (12 mg, 0.020 mmol) and THF (2 mL) was also prepared in a 20 mL scintillation vial. The ligand solution was slowly added to the iron solution and stirred for 30 minutes. Crystals immediately formed and reaction vial was placed in the freezer overnight. Solvent was decanted and crystals were washed with pentanes. Subsequent drying under reduced pressure afforded 24 mg silver crystalline powder **7.** ^{11}B-(^{1}H-dec)

NMR (96 MHz, d_8-THF, 25 °C) δ = 50.13.38, -9.28, -17.03. ^{31}P-(^{1}H-dec) NMR (121 MHz, d_8-THF, 25 °C). silent.

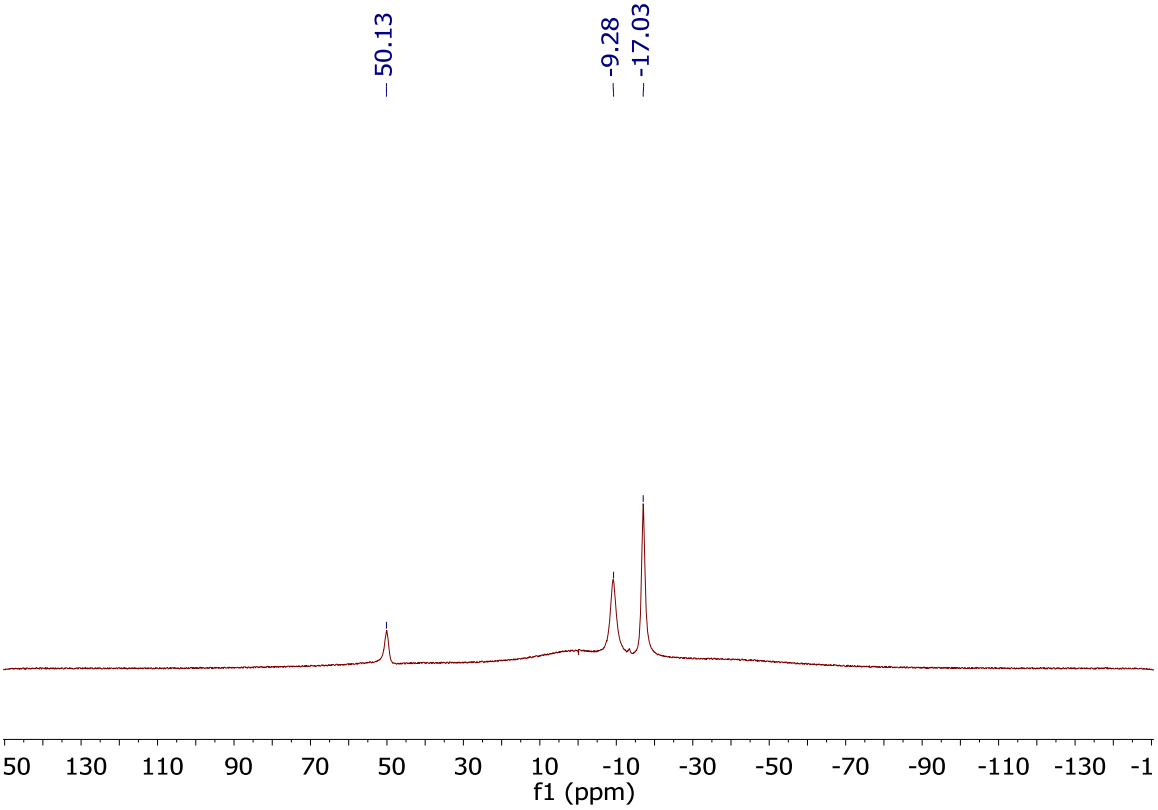

S-4.7 ^{11}B-(^{1}H-dec) NMR of **7** (96 MHz, d_8-THF).

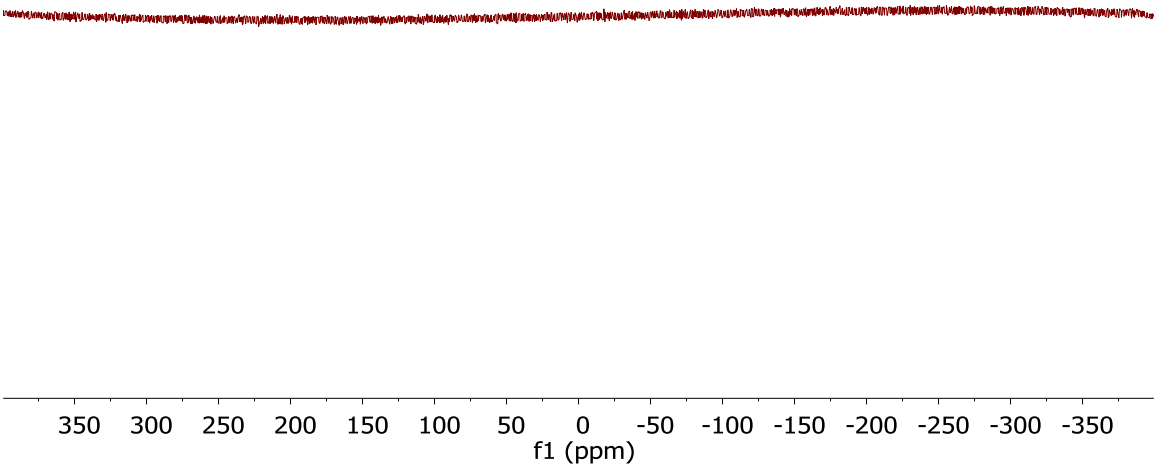

S-4.8 ^{31}P-(^{1}H-dec) NMR of **7** (121 MHz, d_8-THF).

4.6 References

1. M. M. Rauhut and H. Currier, US. Pat. 3,074,999, 1963.

2. (a) J. D. McClure, U.S. Pat. 3,227,745, 1966. (b) J. W. Nemec, R. B. Wuchter, US. Pat. 3,342,853, **1967**. (c) W. Su, D. McLeod, J. G. Verkade, *J. Org. Chem.*, **2003**, *68*, 9499.

3. (a) *J. Chem. Soc., Perkin Trans. 1*, 1979, 0, 2447 (b) N. Nagato, M. Ogawa, T. Naito, Jap. Pat. 7,386,816, 1973.

4. B. A. Feit, *Eur Polym J.*, **1967**, *3*, 523.

5. (a) V. Lavallo, J. H. Wright II, F. S. Tham, and S. Quinlivan, *Angew. Chem. Int. Ed.*, **2013**, *52*, 3172. (b) A. El-Hellani, C. E. Kefalidis, F. S. Tham, L. Maron, V. Lavallo, *Organometallics*, **2013**, *32*, 6887. (c) C. A. Lugo, C. Moore, A. Rheingold, V. Lavallo, *Inorg. Chem.,* **2015**, *54*, 2094. (d) J. Estrada, S.E. Lee, S. McArthur, A. El-Hellani, F.S. Tham, V. Lavallo, *J. Organomet. Chem.,* **2015,** *798*, 214. (e) J. Estrada, D. H. Woen, F. S. Tham, G. M. Miyake, V. Lavallo, *Inorg. Chem.,* **2015**, *54*, 5142. (f) J. Estrada, C.A. Lugo, S.G. McArthur, V. Lavallo, *Chem. Commun.,* **2016,** *52*, 1824. (g) A.L. Chan, J. Estrada, C.E Kefalidis, V. Lavallo, *Organometallics*, **2016,** *35*, 3257.

6. X. F. Zhu, C. E. Henry, O. Kwon, *J. Am. Chem. Soc.*, **2007**, *129*, 6722.

7. R. H. B. Galt, Z. S. Matusiak, *Tetrahedron Lett.*, **1981**, *22*, 2913.

8. S. Matsuoka, S. Namera, A. Washio, K. Takagi, M. Suzuki, *Org. Lett.*, **2013**, *15*, 5916.

Chapter 5: PCl_3 derived 10-vertex carboranyl phosphines

5.1 Abstract

Increasing the versatility of a chemist's synthetic toolbox requires a library of electronically and sterically diverse ligands. Utilization of novel frameworks also opens up an avenue for development of undiscovered reaction pathways. We pursue this goal through utilizing the unique anionic carborane substituent to produce an array of phosphine ligands. Reactions with the dianions of the $HCB_9H_9^-$ and $HCB_9Cl_9^-$ clusters showed similar reactivity with PCl_3 to generate mono and disubstituted carboranyl phosphines. The phosphines produced with the $HCB_9Cl_9^-$ cluster demonstrated increased stability and allowed for stepwise alkylation with MeMgCl and formation of an isolated dianionic dicarboranylphosphine as a lithium or trityl salt.

5.2 Introduction

Production of a broad range of ligands frameworks is essential to the discovering of novel and more effective catalysts. Varying electronic and steric parameters enables tuning of the properties of a metal complex as best suited for the relevant reaction. Mono dentate phosphines are ubiquitous in the realm of catalysis, with a plethora of alkyl and aryl derivatives commercially available. A unique alternative to hydrocarbon substituents that has begun to garner more recent attention is the carborane cluster. Phosphines have been synthesized incorporating the neutral *closo*-$H_2C_2B_{10}H_{10}$ **1** although cataltytic applications have been hindered due to cyclometalation side reactions[1] and facile boron extrusion in basic conditions.[2] More success has been achieved with substitution utilizing anionic clusters such as the monoanionic $HCB_{11}H_{11}^-$ cluster **2** and its derivatives, with

recent applications in hydroamination,[3] polymerization,[4] and palladium cross-coupling reactions.[5] Phosphines bearing 10-vertex anionic $HCB_9H_9^-$ cluster **3** have been produced and also paired with subsequent ligation to a metal center,[6] but further development into its potential as a ligand substituent is lacking. Recent advances in the synthesis of the 10-vertex cluster have been improved,[7] making it readily available, and we sought to take advantage of this to expand our ligand library with **3** and its derivatives, specifically the $HCB_9Cl_9^-$ **4** cluster.

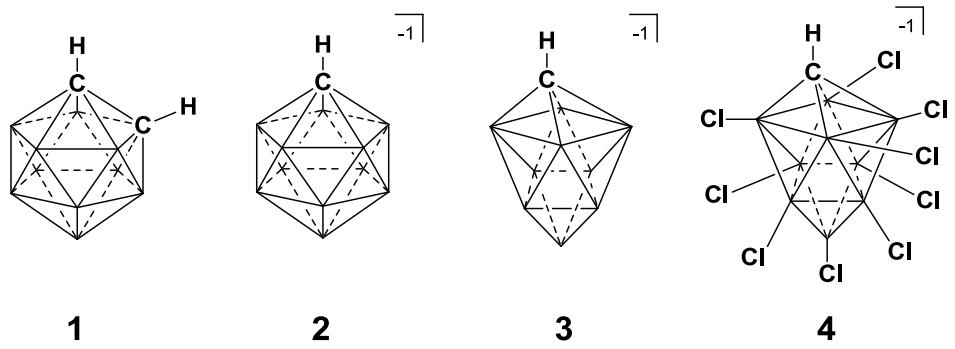

Figure 5.1- Representations of carborane clusters **1** ($H_2C_2B_{10}H_{10}$), **2** ($HCB_{11}H_{11}^-$), **3** ($HCB_9H_9^-$), and **4**($HCB_9Cl_9^-$).

Synthesis of carboranyl phosphines commonly begin with deprotonation of the carboranyl C-H proton to produce a nucleophile that can react with a suitable monochlorophosphine electrophile, replacing the chloride with the carboranyl substituent. If instead PCl_3 is used, multiple substitutions could occur, appending more than one carborane to the phosphorus atom. After at least one carborane has been substituted, alkyl and aryl groups can replace remaining chlorides adding another layer of diversity to the potential ligand library accessible through this method. With this in mind, we explored the reactivity of PCl_3 with **3** and **4** in hopes of developing novel dianionic and/or trianionic carboranyl phosphine ligands.

5.3 Results and discussion

Deprotonation of the **[$HNMe_3^+$]3** to its nucleophilic dianion was achieved with *n*-BuLi. Reaction with PCl_3 was monitored by ^{11}B and ^{31}P NMR spectroscopy after 1, 2, 3, and excess equivalents of the dianion were added (**Scheme 5.1**). Immediately after addition of one equivalent, a major resonance at 193.86 ppm was observed in the ^{31}P NMR (upfield shift from 222.24 ppm of PCl_3) corresponding to single substitution. Presence of a minor resonance at 134.00 ppm suggested a second substitution and was supported by its increase in signal height after a second equivalent of dianion was added. Additional equivalents produced no new species, suggesting the disubstitued product **5** and no formation of a trisubstituted species. ^{11}B NMR resonances at 1, 2, and 3 display maintained local C_{4v} symmetry of the carborane cages. Unfortunately isolation was not achieved as the compound is easily hydrolyzed upon attempted workup, giving a doublet in the $^{31}P(^1H$-coup) spectrum with an extremely large coupling constant (^1J = 510.8 Hz) typical of a hydrogen with a direct bond to a phosphorus atom in the +4 or +5 oxidation state.[8] Single crystal X-ray diffraction data was obtained which further corroborated the identity of the hydrolyzed product **6**. Data was not sufficient enough for bond length discussion, but connectivity could be established as the phosphorus atom has two **3** moieties attached in addition to an oxygen atom.

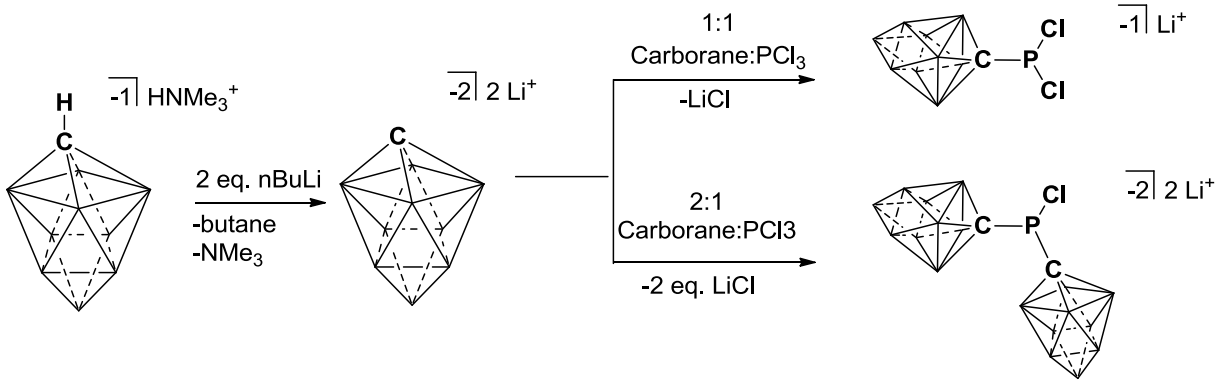

Scheme 5.1- General method for generating mono and di substituted carboranyl phosphines starting from **3** or **4.**

Halogenated derivates of **2** have been shown to demonstrate enhanced stability, in comparison to their hydridic parent clusters. We hoped that **4** would also display similar properties in hopes of isolating a stable dianionic dicarboranyl phosphine ligand. The same procedure that was applied for **3** was used for **4** in its reaction with PCl_3 (**Scheme 5.1**). To our gratification **4** was more controlled in comparison to **3**, where one equivalent of dianion afforded clean formation of the mono substituted product **7** (^{31}P NMR = 180.46) in 1 hour with no traces of any disubstituted or hydrozlyed species. A second equivalent was added which produced a resonance at 121.52 ppm. This upfield shift of roughly 60ppm follows the same trend as with **5** transforming to **6**. This new product **8** was cleanly isolated and further characterized by multi-nuclear NMR spectroscopy as well as single-crystal X-ray diffraction studies.

In the solid state the bond lengths around the phosphorus atom are as expected for typical P-C and P-Cl single bonds (1.859 Å and 1.874 Å for the two P-C bonds, and 2.021 Å for the P-Cl bond). There are two lithium countercations present each with four coordinated THF molecules. The fact that there are no strong interactions of the anionic

cage with the lithium atoms demonstrates how halogenated derivatives are more weakly coordinating then their hydridic cluster. A slight comparison can be seen with a previously reported rhodium dicarbonyl complex containing a diisopropyl phosphine with one **3** substituent showed an evident interaction between the cage and the lithium cation (Li-H distance l.997 Å, and only two coordinating THF molecules). The two C-P-Cl bond angles are nearly identical (99.85 ° and 99.61 °) while the C-P-C angle is significantly larger 112.80°. This can be rationalized by the steric bulk of the carborane cages repelling each other.

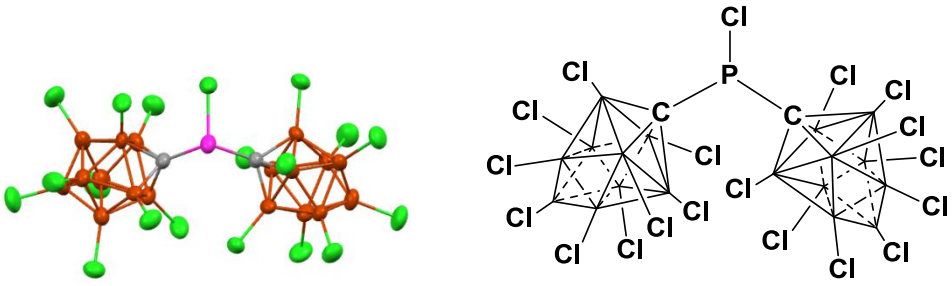

Figure 5.2- Solid state structure (left) with corresponding representation (right) of **8**. Unlabled verticies are B-Cl bonds. Color code: C, gray; B, brown; P, violet; Cl, green. Lithium cations with four coordinated THFmolecules omitted for clarity.

Phosphines **7** and **8** open up a platform for further derivitization as their remaining chlorine atoms allow for substitution for other substituents. As a proof of concept, **7** was initially treated with a stepwise addition of MeLi. This reagent proved too harsh, as P-$C_{carborane}$ bond cleavage resulted, evidenced by production of PMe_3 (^{31}P NMR = -55 ppm) and the dianion of **4** (^{11}B NMR = 18.56 and -5.39). A softer reagent was found in MeMgCl, which after adding one equivalent cleanly shifted the single phosphorus resonance upfield approximately 65 ppm to 115.40 ppm suggesting a replacement of an electron withdrawing chloride group with an electron donating methyl

group. Upon addition of another equivalent the signal shifted to -8.14 ppm for the disubstituted product **9**. To our delight, no trace of PMe_3 was detected suggesting no P-$C_{carborane}$ bond cleavage. The ^1H NMR spectrum revealed an upfield resonance for the two methyl substituents at 2.21 and 2.22 ppm and also coordinating THF molecules at 3.74 ppm and 1.91 ppm. The identity of compound **9** was further proved by X-ray crystal data, though the quality of the data obtained prohibits discussion of bond lengths. Synthesis of **9** demonstrates that **7** can serve as a platform from which a library of carboranyl ligands can be produced.

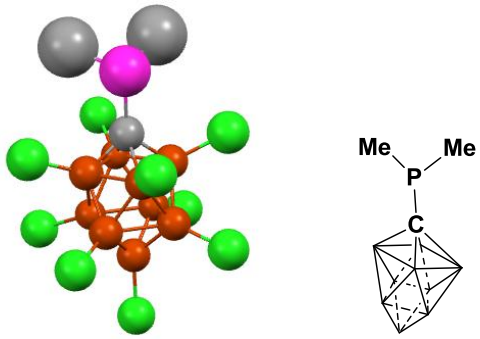

Figure 5.3- Solid state structure (left) with corresponding representation (right) of **9**. Color code: C, gray; B, brown; P, violet; Cl, green. Hydrogens omitted for clarity. Magnesium cation omitted for clarity.

We next turned our attention to **8** with hopes of abstracting the remaining chloride to produce a novel and likely highly reactive carboranyl phosphenium cation. Halogenated carboranes have already been deemed effective at stabilizing reactive species.[9] Phosphenium cations are known, typically derived from N-heterocylic phosphinochlorides.[10] These molecules have two adjacent nitrogen atoms that can stabilize the cationic phosphorus atom. In a similar manner we hoped the adjacent carboranes would protect the phosphorus atom through their weakly coordinating

properties, as well as through their bulky steric profile. From this, we reacted **8** with a variety of silver salts in hopes of abstracting the chloride and cleanly generating the subsequent phosphenium cation. Unfortunately the desired product was never isolated, as reactions did not occur or did not give chloride abstracted products. In the case of AgOTf, addition to **8** produced new slightly shifted ^{31}P and ^{11}B NMR signals (101.67 ppm and 24.02, -4.52, -7.43 respectively). An isolated crystal revealed a silver-phosphine adduct, **10**, in which the chlorine atom is still attached to the phosphorus (**Figure 5.4**).

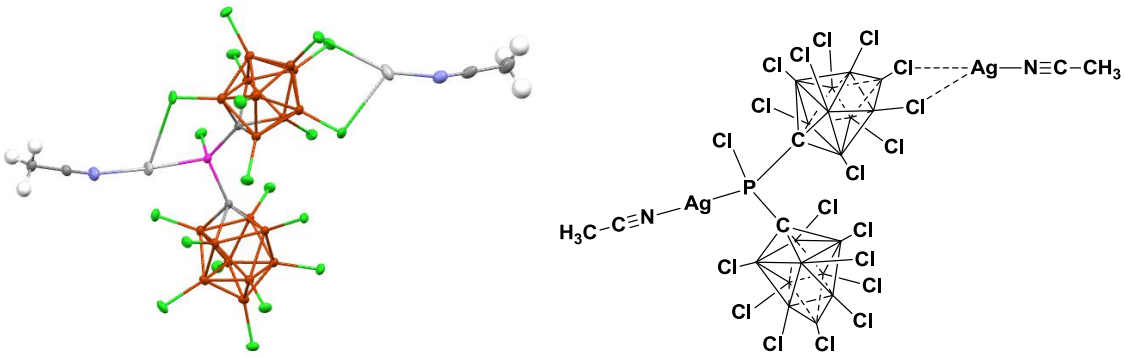

Figure 5.4- Solid state structure (left) with corresponding representation (right) of **10**. Color code: C, gray; B, brown; P, violet; Cl, green; Ag, silver; N, light blue.

The resistance to silver salts prompted us to try the more exotic silylium cation. In situ generation of a silyium cation can be obtained by reacting a trialkyl silane with a trityl cation. From this, we sought to synthesize a trityl salt of compound **8** to undergo a chloride abstraction via an in situ silylium cation. Production of 8 initially provides it with THF molecules coordinating to the lithium cations, which are detrimentally reactive towards trityl cations. To circumvent this we took **8** and replaced THF with acetonitrile by successive addition of acetonitrile and removing of solvent by placing under reduced pressure to produce $\mathbf{8}_{\mathbf{ACN}}$. This species was then reacted with an excess of trityl chloride to precipitate off lithium chloride and give the desired trityl salt **11**. While the ^{31}P and ^{11}B

NMR remain unchanged, the ^{1}H NMR reveals the disappearance of acetonitrile (suggesting complete removal of lithium) and appearance of the three downfield trityl resonances. To unambiguously verify the correct structure, single-crystal X-ray data (**Figure 5.5**) was obtained and gratifyingly corresponded to the expected product **11**.

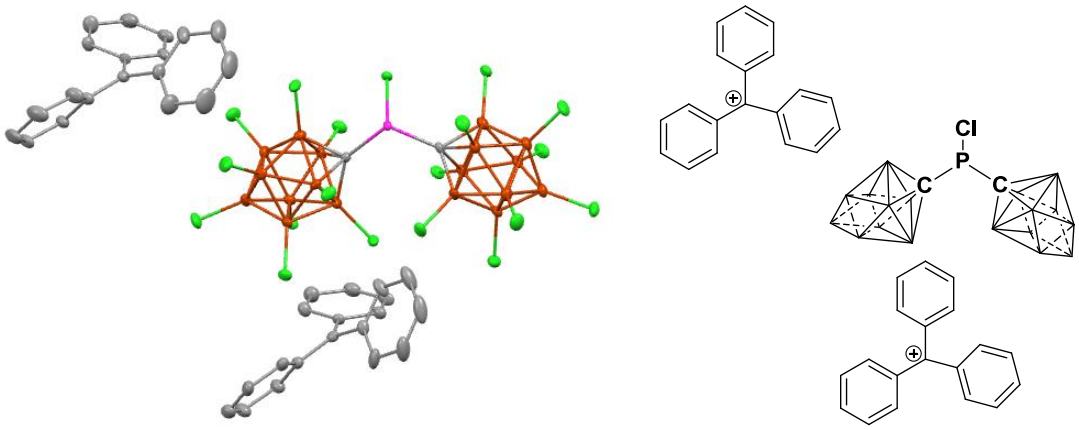

Figure 5.5- Solid state structure (left) with corresponding representation (right) of **11**. Color code: C, gray; B, brown; P, violet; Cl, green. Hydrogens omitted for clarity.

We were then able to add the trityl salt to triethyl silane in attempt to produce the desired phosphenium cation. Immediately after addition, multiple new phosphorus resonances occur upfield at 48.20 and 28.35, 15.76, and -26.53 respectively. The species at 15.76 ppm also displays a doublet in the ^{31}P(^{1}H-coup) spectrum (^{1}J = 544.1 Hz), suggesting a hydrogen directly bound to the phosphorus atom. A single product could not be isolated, and the only crystals obtained showed a protonated **8** with one trityl cation and with the chlorine atom still intact. The difficulty in obtaining a chloride abstracted species speaks to the likely high instability of the subsequent phosphenium cation to be produced.

5.4 Conclusion

The above investigations have not only served to expand upon the library of carboranyl phosphines, but have also opened up a new platform of ligands that help to elucidate the properties from one carborane to the next. The more localized charge of **3** likely produces excessive electron density to the phosphorus atom, therefore increasing its susceptibility to hydrolysis when compared to **4.** Reactions of **4** with PCl_3 produce the monoanionic **7** and the dianionic **8**. Ligand tunability was demonstrated by sequential substitution of the chlorine atoms on **7** with methyl substituents to produce **9**. Since addition of alkyl groups is controlled, production of phosphines containing substituents where R_1 and R_2 are different alkyl substituents can be envisioned. The reactivity of **8** with silver salts highlights the resistance of **8** towards chloride abstraction. Alternatively we sought to remove the chloride by producing trityl salt **11** which would allow in situ generation of a silylium cation. Unfortunately this reaction was unsuccessful and mixtures of products were observed, none of which could be isolated as the desired chloride abstracted phosphenium cation. Regardless, **8** and **11** are unique molecules whose reactivity is still in need of further elucidation.

5.5 Experimental

Unless otherwise stated, all manipulations were carried out using standard Schlenk or glovebox techniques (O_2, H_2O < 1ppm) under a dinitrogen or argon atmosphere. piperdine and ethanol were bubbled with N_2 for 15 minutes prior to use. Solvents were dried on K or CaH_2, and distilled under argon before use. Reagents were purchased from commercial vendors and used without further purification. Compound **3**

was prepared according to literature[6]. NMR spectra were recorded on Bruker Avance 300/600 MHz or Varian Inova 400 MHz spectrometers. NMR chemical shifts are reported in parts per million (ppm). ^{1}H NMR and ^{13}C NMR chemical shifts were referenced to residual solvent. ^{11}B NMR chemical shifts were externally referenced to BF_3OEt_2. ^{31}P NMR chemical shifts were externally referenced to 80% H_3PO_4 in H_2O.

5.5.1 Data for **4** and **5**

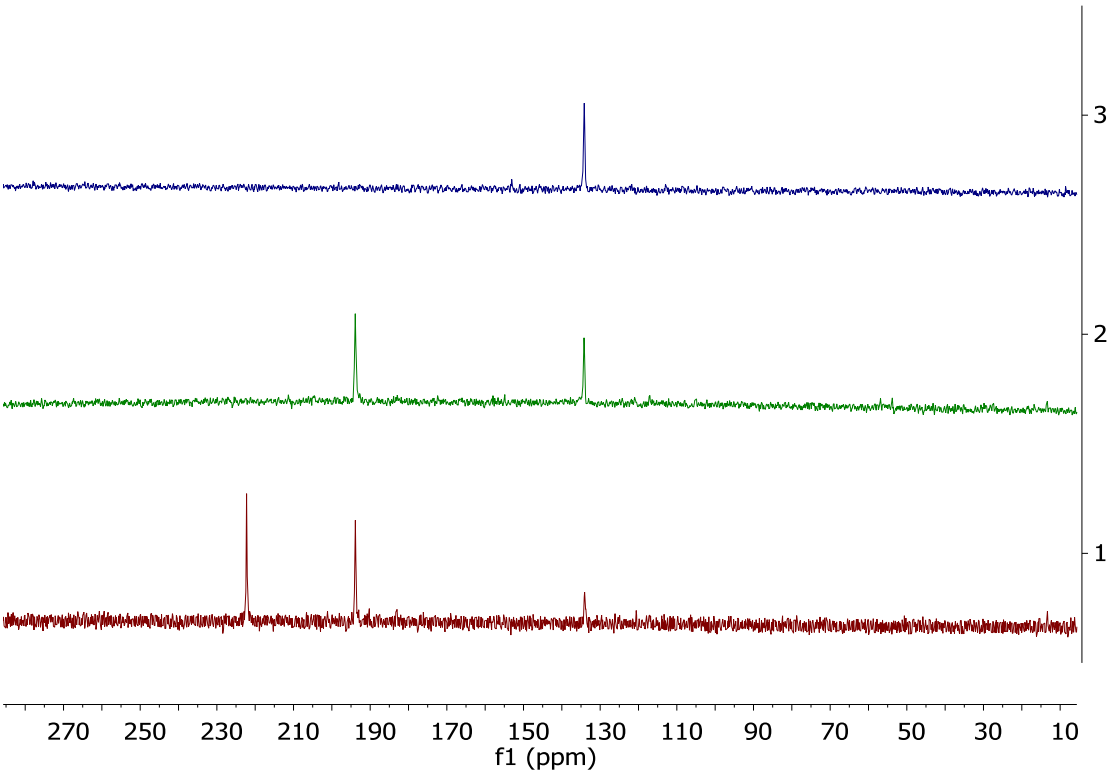

S-5.1 ^{31}P(1H-dec) NMR (300 MHz, THF) progression upon addition of 1, 2, and 3 equivalents. 222.23 ppm = PCl_3, 193.89 ppm = **4**, 134.00 ppm = **5**.

5.5.2 Synthesis of **7**

Compound **4** (52mg, 0.11 mmol) was dissolved in THF (4 mL) inside a 20 mL scintillation vial charged with a magnetic stir bar. *n*-BuLi (2.5M in hexanes, 1 mL) was added slowly and then stirred for 1 hour. Pentane (10mL) was added to precipitate out the dianion, which solvent was decanted and subsequent pentane washes occurred (3 x 10 mL). Precipitate was then dissolved in THF (2mL) and slowly added to a solution of THF (1 mL) and PCl_3 (14 mg, 0.11 mmol). After an 1 hour of stirring, the solution was precipitated in hexanes , extracted with DCM (2 x 4 mL) from LiCl, solvent was then removed under reduced pressure. Compound **7** was isolated as a white powder 47 mg.

^{11}B-(^{1}H-dec) NMR (96 MHz, CH_2Cl_2, 25 °C) δ = 28.06, 0.64, -1.86. ^{31}P-(^{1}H-dec) NMR (121 MHz, CH_2Cl_2, 25 °C). δ = 180.46.

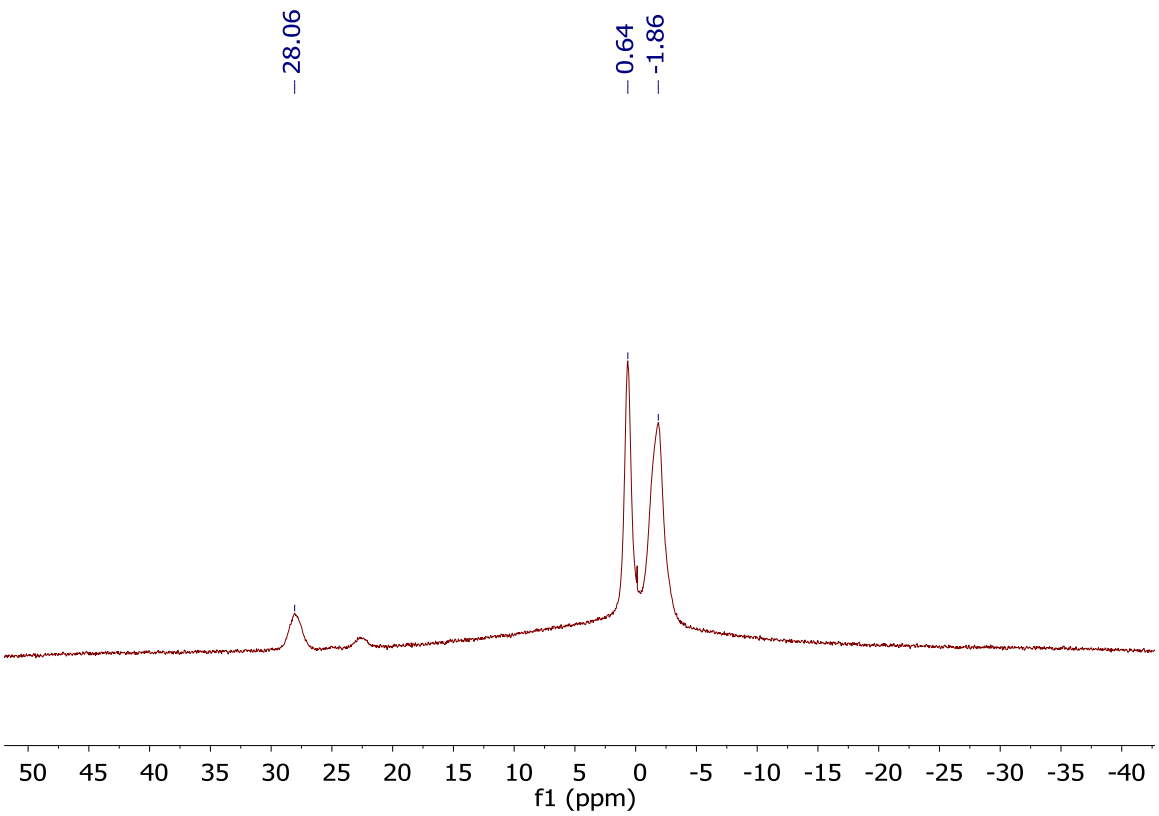

S-5.2 ^{11}B-(^{1}H-dec) NMR of **7** (96 MHz, CH_2Cl_2).

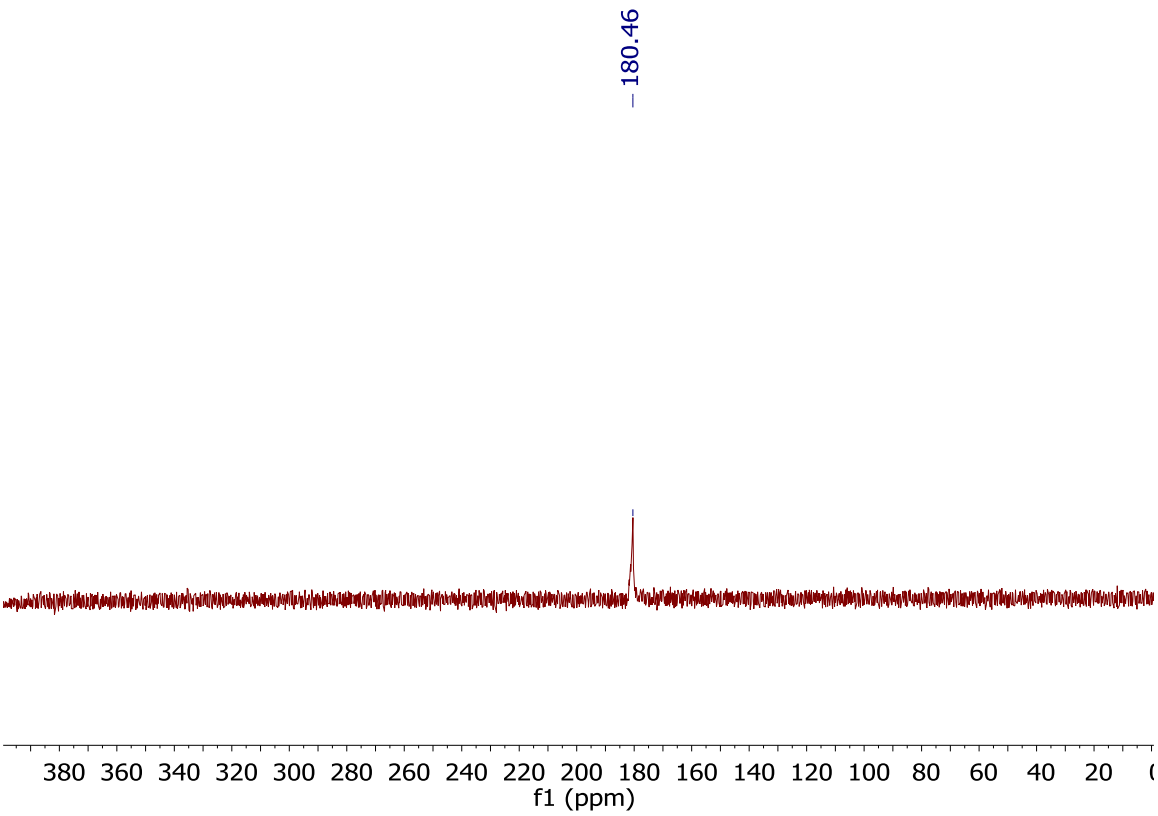

S-5.3 ^{31}P-(^{1}H-dec) NMR of **7** (121 MHz, CH_2Cl_2)

5.5.3 Synthesis of **8**

Compound **4** (520mg, 1.06 mmol) was dissolved in THF (10 mL) inside a 20 mL scintillation vial charged with a magnetic stir bar. *n*-BuLi (2.5M in hexanes, 4 mL) was added slowly and then stirred for 1 hour. Pentane (5mL) was added to precipitate out the dianion, which solvent was decanted and subsequent pentane washes occurred (3 x 10 mL). Precipitate was then dissolved in THF (7mL) and slowly added to a solution of THF (3 mL) and PCl_3 (72 mg, 0.53 mmol). After an 1 hour of stirring, the solution was precipitated in hexanes, extracted with CH_2Cl_2 from LiCl, solvent was then removed under reduced pressure (Note: depending on amount of protonation of dianion, washing with ether can slowly remove this side product). Compound **8** 450mg was isolated as a

white powder (47mg). ^{1}H NMR (400 MHz, CD_2Cl_2, 25 °C) δ = 3.78 (br s, 4H, THF), 1.95 (br s, 4H, THF). ^{11}B-(^{1}H-dec) NMR (128 MHz, CD_2Cl_2, 25 °C) δ = 24.34, -2.07, -4.66. ^{13}C-(^{1}H-dec) NMR (101 MHz, CD_2Cl_2 δ = 70.39 (THF), 27.22 (THF). ^{31}P-(^{1}H-dec) NMR (121 MHz, CD_2Cl_2, 25 °C) δ = 120.14.

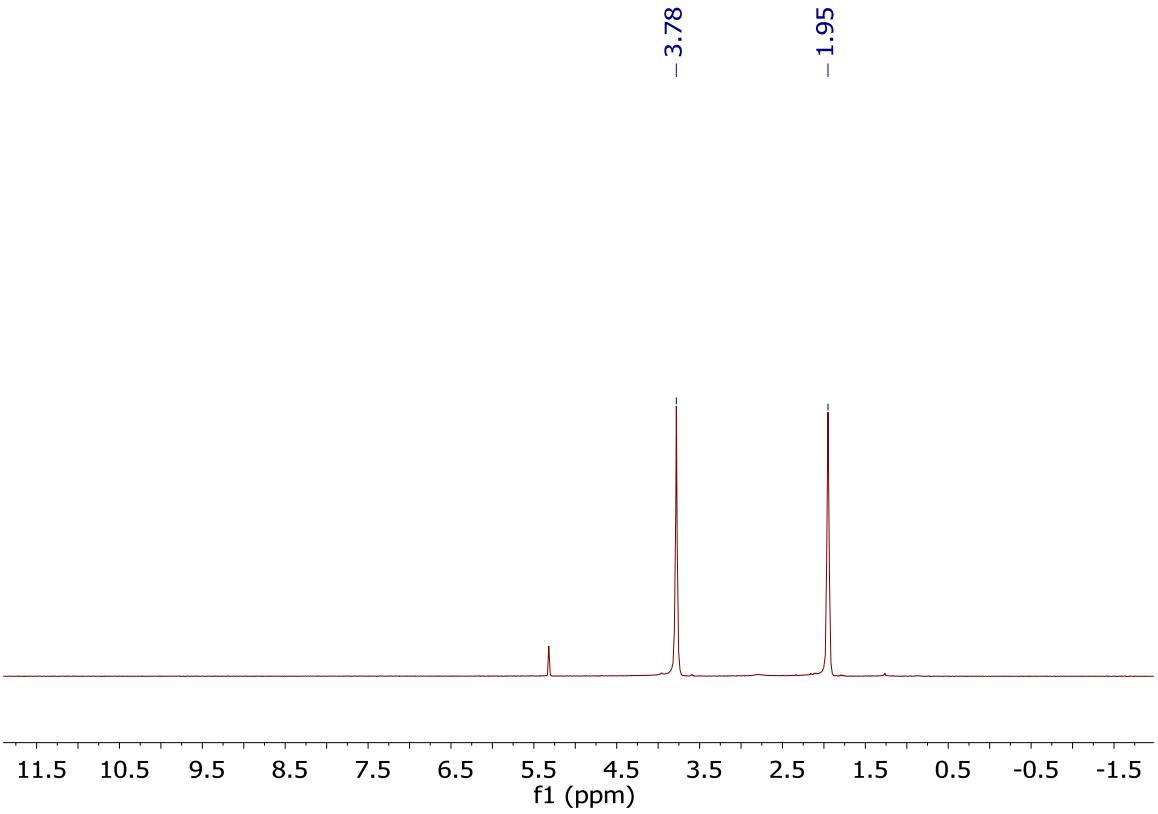

S-5.4 ^{1}H NMR of **8** (400 MHz, CD_2Cl_2)

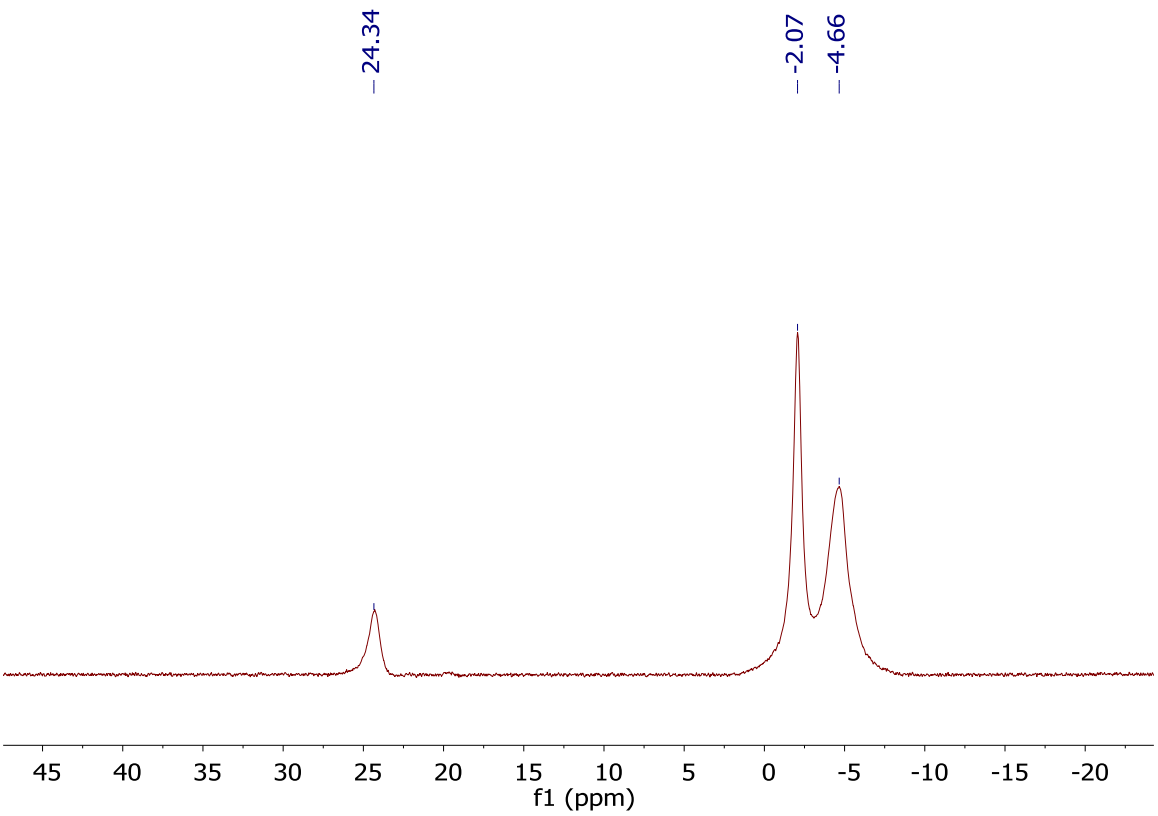

S-5.5 ^{11}B-(^{1}H-dec) NMR of **7** (96 MHz, CH_2Cl_2).

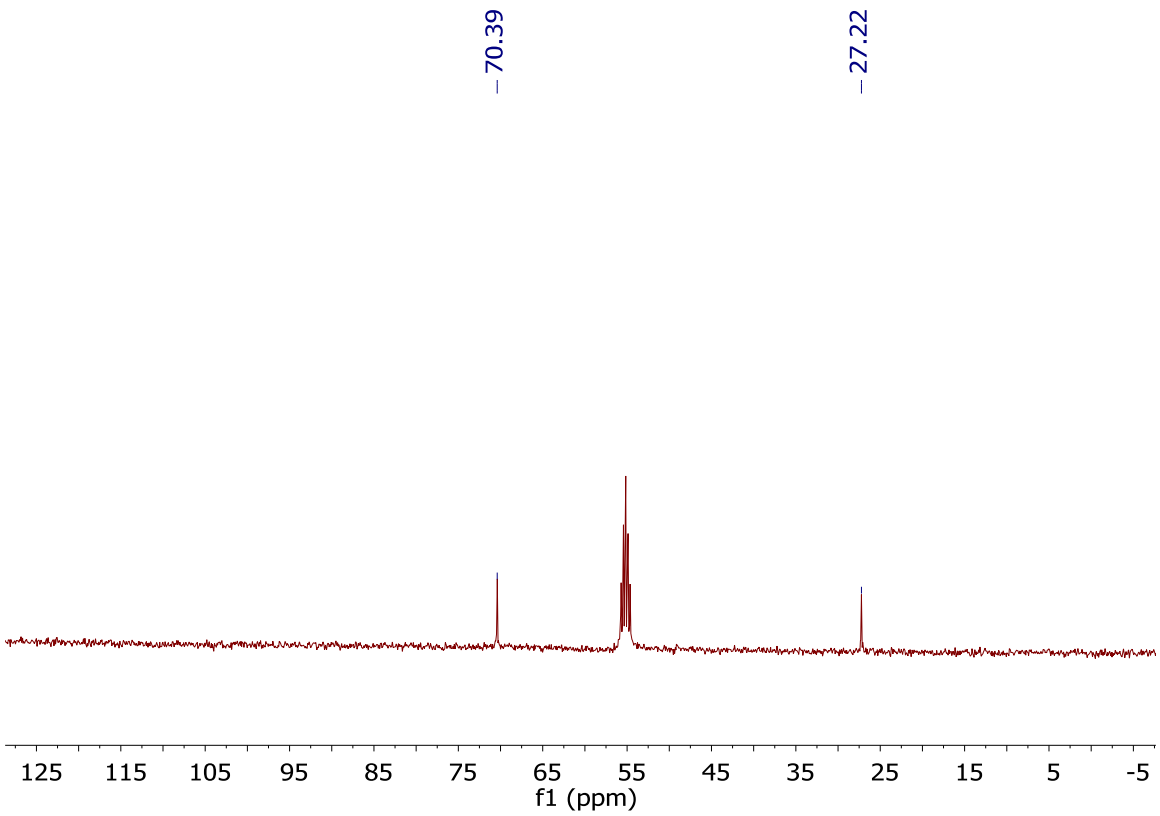

S-5.6 ^{13}C-(^{1}H-dec) NMR of **8** (101 MHz,CD_2Cl_2).

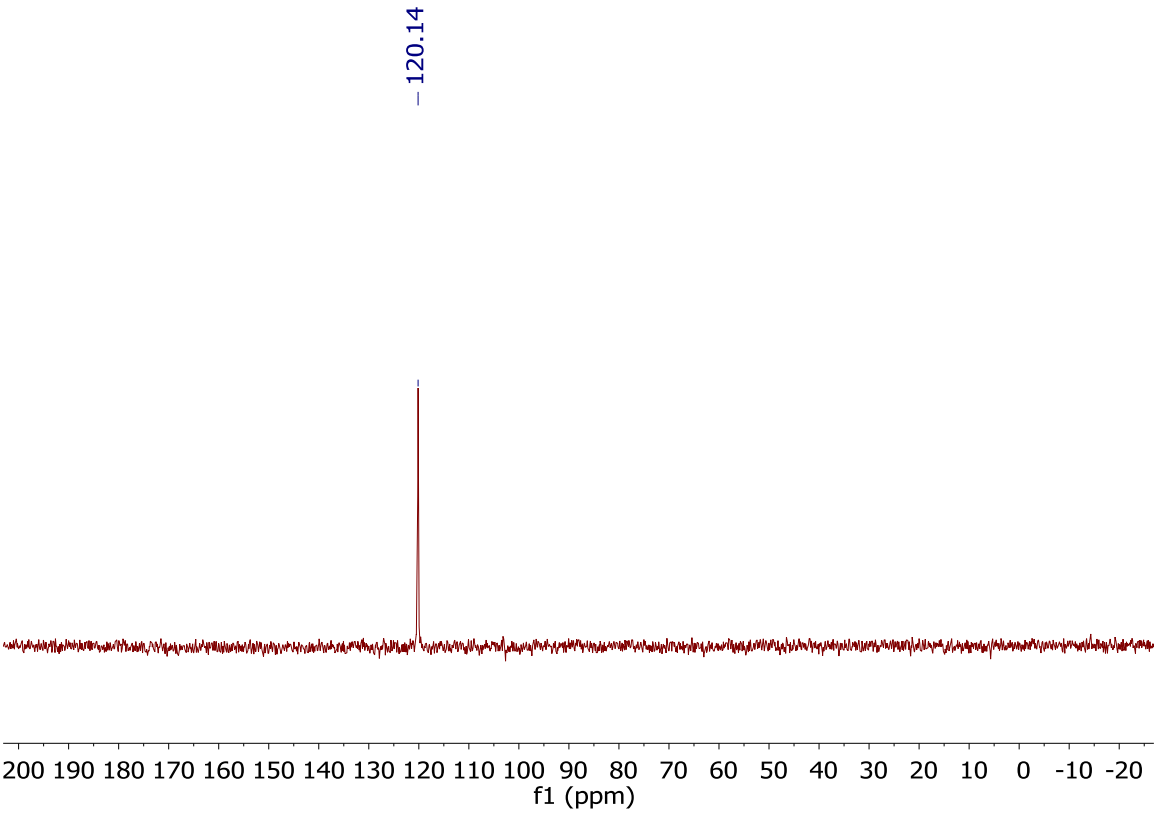

S-5.7 ^{31}P-(^{1}H-dec) NMR of **8** (161 MHz, CD_2Cl_2).

5.5.4 Synthesis of **9**

Compound **7** (11 mg, 0.017 mmol) was dissolved in THF (1mL) inside of a 20mL scintillation vial. To that, a solution of THF (2mL) and MeMgCl (3M in ether, 11.5 µl, 0.034 mmol) added slowly. After 1 hour of stirring, solvent was removed under reduced pressure followed by extraction with CH_2Cl_2. Compound **9** was observed to be a white powder. ^{1}H NMR (400 MHz, CD_2Cl_2, 25 °C) δ = 3.74 (br s, 4H, THF), 2.22 (s, 3H, CH_3), 2.21 (s, 3H, CH_3), 1.91 (br s, 4H, THF). ^{11}B-(^{1}H-dec) NMR (96 MHz, CD_2Cl_2, 25 °C) δ = 20.61, -4.05, -5.84. ^{31}P-(^{1}H-dec) NMR (121 MHz, CD_2Cl_2, 25 °C) δ = -8.16.

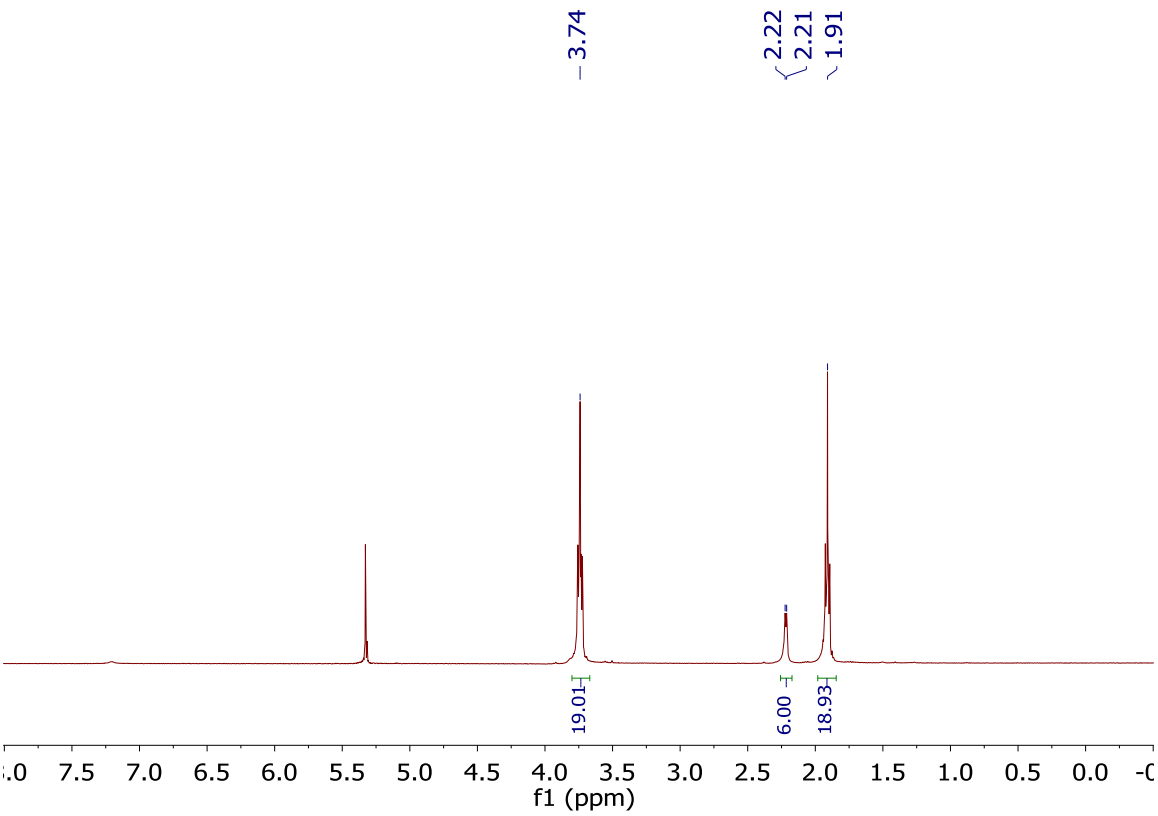

S-5.8 ^{1}H NMR of **9** (400 MHz, CD_2Cl_2).

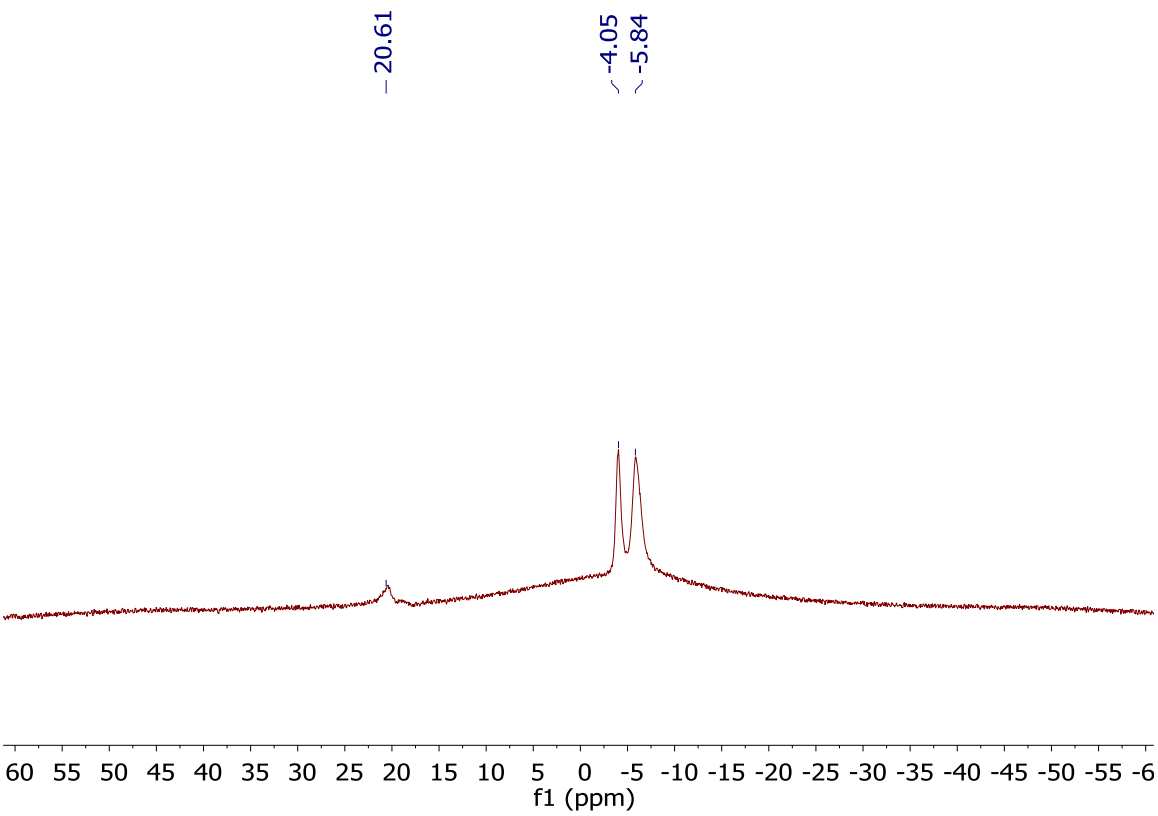

S-5.9 ^{11}B-(^{1}H-dec) NMR of **9** (96 MHz, CD_2Cl_2).

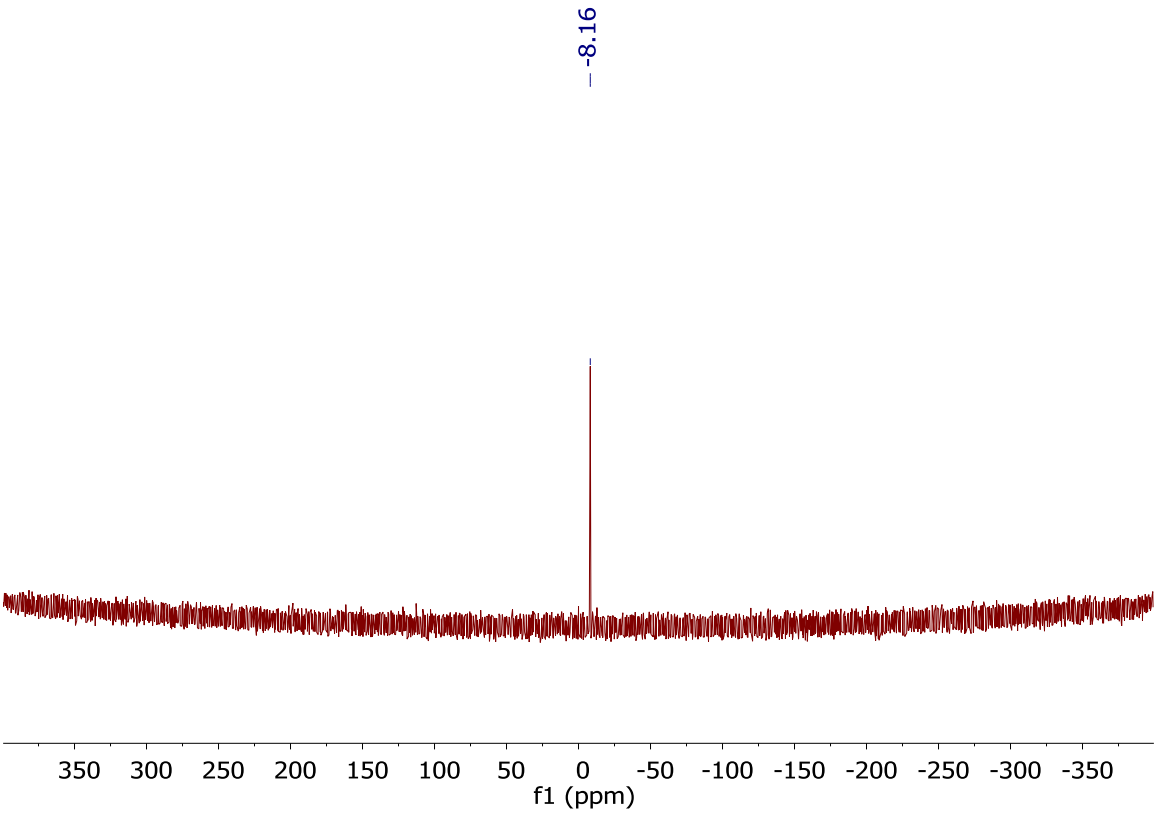

S-5.10 ^{31}P-(^{1}H-dec) NMR of **9** (121 MHz, CD_2Cl_2).

5.5.5 Synthesis of **10**

A solution of CH_2Cl_2 (1 mL) and Compound **8** (30 mg, 0.020 mmol) was added to a solution of CH_2Cl_2 (1 mL) and AgOTf (5mg, 0.020 mmol). After stirring for 2 hours, the mixture was filtered and solvent was then removed in vacuo. Crystallization of the compound was achieved by addition dissolving in acetonitrile and placing in the freezer overnight. ^{11}B-(^{1}H-dec) NMR (96 MHz, CD_2Cl_2, 25 °C) δ = 24.02, -4.52, -7.43. ^{31}P-(^{1}H-dec) NMR (121 MHz, CD_2Cl_2, 25 °C) δ = 101.67.

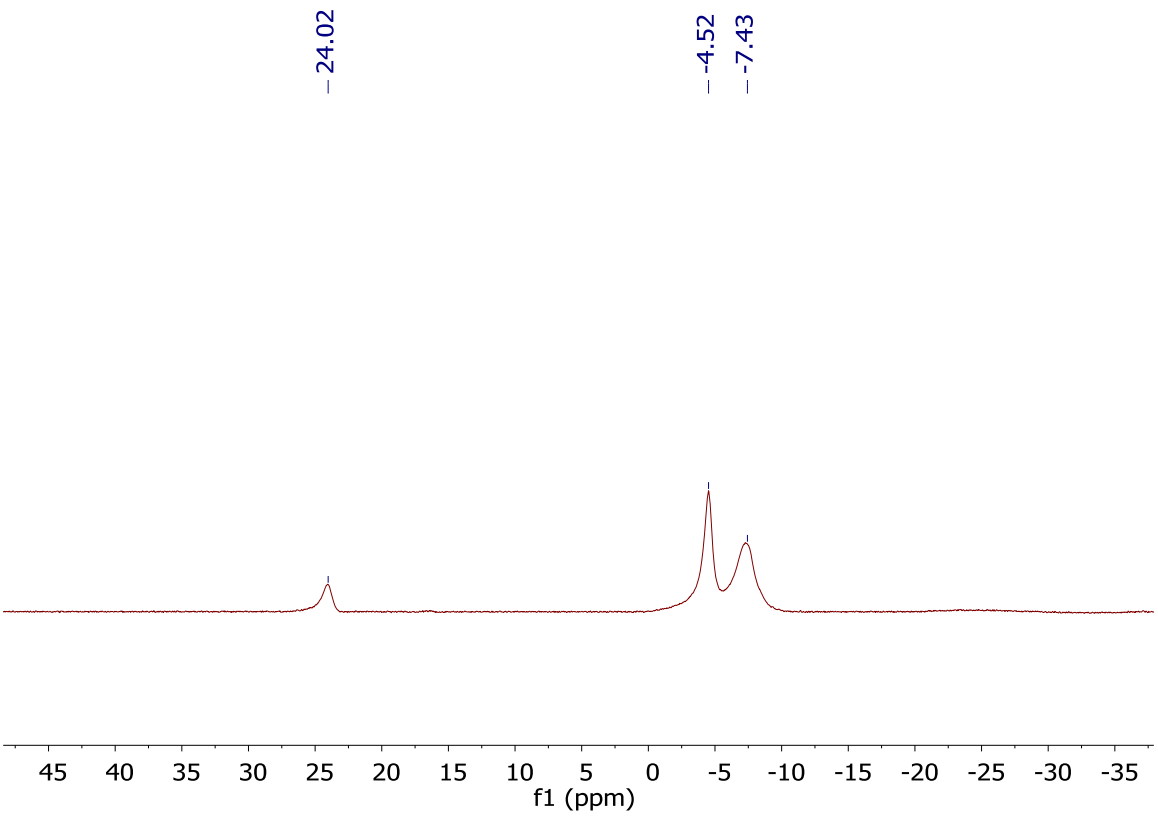

S-5.11 ^{11}B-(^{1}H-dec) NMR of **10** (96 MHz, CD_2Cl_2).

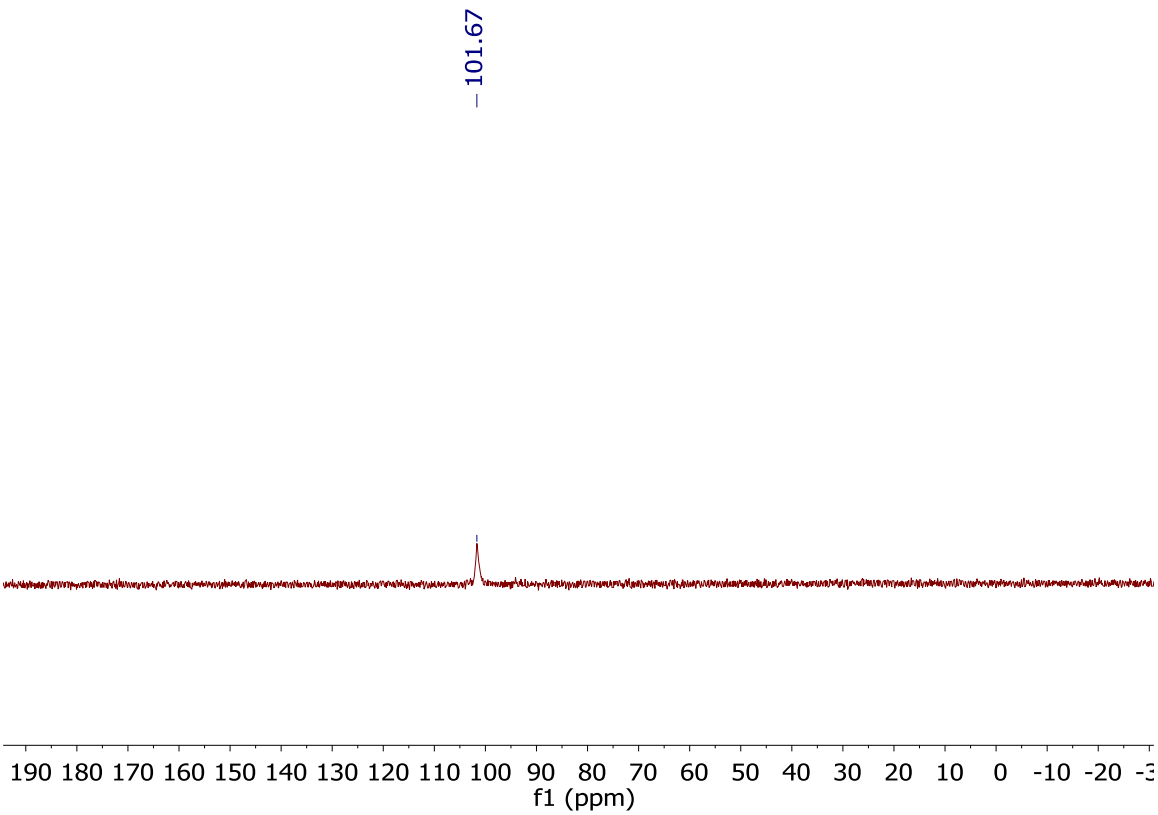

S-5.12 ^{31}P-(^{1}H-dec) NMR of **10** (121 MHz, CD_2Cl_2).

5.5.6 X-ray crystallographic data for compound **10**

A colorless needle fragment (0.307 x 0.232 x 0.080 mm^3) was used for the single crystal x-ray diffraction study of $[CB_9Cl_9]_2Ag_2ClP[CH_3CN]_2.CH_2Cl_2$ (sample vL304CL_0m). The crystal was coated with paratone oil and mounted on to a cryo-loop glass fiber. X-ray intensity data were collected at 100(2) K on a Bruker APEX2[11]platform-CCD x-ray diffractometer system (fine focus Mo-radiation, λ = 0.71073 Å, 50KV/30mA power). The CCD detector was placed at a distance of 5.0600 cm from the crystal.

A total of 3600 frames were collected for a sphere of reflections (with scan width of 0.3° in ω, starting ω and 2θ angles of –30°, and ϕ angles of 0°, 90°, 120°, 180°, and 270° for every 600 frames, 10 sec/frame exposure time). The frames were integrated using the Bruker SAINT software package[12] and using a narrow-frame integration algorithm. Based on a monoclinic crystal system, the integrated frames yielded a total of 98722 reflections at a maximum 2θ angle of 61.016° (0.70 Å resolution), of which 12767 were independent reflections (R_{int} = 0.0336, R_{sig} = 0.0193, redundancy = 7.7, completeness = 100%) and 11176 (87.5%) reflections were greater than 2σ(I). The unit cell parameters were, **a** = 12.5621(4) Å, **b** = 13.3068(4) Å, **c** = 25.1613(8) Å, **β** = 95.4893(5)°, V = 4186.7(2) $Å^3$, Z = 4, calculated density D_c = 2.072 g/cm^3. Absorption corrections were

applied (absorption coefficient μ = 2.332 mm^{-1}; max/min transmission = 0.835/0.535) to the raw intensity data using the SADABS program.[13]

The Bruker SHELXTL software package[14] was used for phase determination and structure refinement. The distribution of intensities (E^2-1 = 0.961) and systematic absent reflections indicated one possible space group, P2(1)/n. The space group P2(1)/n (#14) was later determined to be correct. Direct methods of phase determination followed by two Fourier cycles of refinement led to an electron density map from which most of the non-hydrogen atoms were identified in the asymmetric unit of the unit cell. With subsequent isotropic refinement, all of the non-hydrogen atoms were identified. There was one polymeric molecule of $[CB_9Cl_9]_2Ag_2ClP[CH_3CN]_2$ and one disordered solvent of CH_2Cl_2 (disordered site occupancy ratio was 81.3%/9.4%/9.3%) present in the asymmetric unit of the unit cell.

Atomic coordinates, isotropic and anisotropic displacement parameters of all the non-hydrogen atoms were refined by means of a full matrix least-squares procedure on F^2. The H-atoms were included in the refinement in calculated positions riding on the atoms to which they were attached. The refinement converged at R1 = 0.0252, wR2 = 0.0586, with intensity I>2σ (I). The largest peak/hole in the final difference map was 1.205/-0.906 e/$Å^3$. The highest peak/hole in difference electron density map near the Ag-atom is probably due to absorption correction errors.

Table 1. Crystal data and structure refinement for vL304CL_0m.

Identification code	vL304CL_0m	
Empirical formula	C7 H8 Ag2 B18 Cl21 N2 P	
Formula weight	1305.89	
Temperature	100(2) K	
Wavelength	0.71073 Å	
Crystal system	Monoclinic	
Space group	P 21/n	
Unit cell dimensions	a = 12.5621(4) Å	α= 90°.
	b = 13.3068(4) Å	β= 95.4893(5)°.
	c = 25.1613(8) Å	γ = 90°.
Volume	4186.7(2) $Å^3$	
Z	4	
Density (calculated)	2.072 Mg/m^3	
Absorption coefficient	2.332 mm^{-1}	
F(000)	2480	

Crystal size	0.307 x 0.232 x 0.080 mm^3
Theta range for data collection	1.626 to 30.508°.
Index ranges	-17<=h<=17, -19<=k<=19, -35<=l<=35
Reflections collected	98722
Independent reflections	12767 [R(int) = 0.0336]
Completeness to theta = 25.242°	100.0 %
Absorption correction	Semi-empirical from equivalents
Refinement method	Full-matrix least-squares on F^2
Data / restraints / parameters	12767 / 142 / 501
Goodness-of-fit on F^2	1.037
Final R indices [I>2sigma(I)]	R1 = 0.0252, wR2 = 0.0586
R indices (all data)	R1 = 0.0315, wR2 = 0.0614
Extinction coefficient	n/a
Largest diff. peak and hole	1.205 and -0.906 e.$Å^{-3}$

Table 2. Atomic coordinates (x 10^4) and equivalent isotropic displacement parameters ($Å^2$x 10^3) for vL304CL_0m. U(eq) is defined as one third of the trace of the orthogonalized U^{ij} tensor.

	x	y	z	U(eq)
Ag(1)	4644(1)	11906(1)	6892(1)	24(1)
N(1)	6460(1)	4991(2)	9123(1)	25(1)
C(2)	6661(2)	4161(2)	9155(1)	24(1)
C(3)	6946(2)	3104(2)	9196(1)	35(1)
Ag(2)	6324(1)	6619(1)	9289(1)	29(1)
N(2)	4341(2)	13468(1)	6876(1)	25(1)
C(4)	4312(2)	14305(1)	6950(1)	18(1)
C(5)	4290(2)	15374(1)	7056(1)	21(1)
P(1)	5132(1)	10176(1)	6884(1)	13(1)
Cl(1)	6302(1)	9942(1)	6406(1)	19(1)
C(1A)	4008(1)	9440(1)	6557(1)	12(1)
B(2A)	2776(2)	9893(1)	6513(1)	12(1)
B(3A)	3600(2)	9860(2)	5950(1)	13(1)
B(4A)	3996(2)	8532(1)	6115(1)	12(1)
B(5A)	3153(2)	8567(1)	6691(1)	12(1)
B(6A)	1832(2)	8884(2)	6357(1)	13(1)
B(7A)	2149(2)	9783(2)	5832(1)	14(1)
B(8A)	3016(2)	8833(2)	5550(1)	13(1)
B(9A)	2694(2)	7918(2)	6066(1)	13(1)
B(10A)	1752(2)	8595(2)	5699(1)	14(1)
Cl(1A)	2432(1)	10972(1)	6873(1)	16(1)
Cl(2A)	4224(1)	10884(1)	5658(1)	19(1)
Cl(3A)	5119(1)	7799(1)	5998(1)	18(1)
Cl(4A)	3167(1)	7858(1)	7282(1)	17(1)
Cl(5A)	685(1)	8770(1)	6719(1)	18(1)
Cl(6A)	1429(1)	10827(1)	5540(1)	19(1)
Cl(7A)	3399(1)	8652(1)	4891(1)	18(1)
Cl(8A)	2627(1)	6584(1)	6042(1)	18(1)
Cl(9A)	634(1)	8144(1)	5283(1)	18(1)

C(1B)	5713(1)	9694(1)	7530(1)	13(1)
B(2B)	6975(2)	9504(2)	7768(1)	15(1)
B(3B)	5888(2)	8570(2)	7770(1)	15(1)
B(4B)	4993(2)	9594(2)	8033(1)	14(1)
B(5B)	6113(2)	10487(2)	8016(1)	14(1)
B(6B)	7156(2)	9917(2)	8468(1)	15(1)
B(7B)	6972(2)	8564(2)	8302(1)	16(1)
B(8B)	5578(2)	8623(2)	8469(1)	16(1)
B(9B)	5758(2)	9979(2)	8651(1)	15(1)
B(10B)	6626(2)	9077(2)	8875(1)	16(1)
Cl(1B)	8084(1)	9552(1)	7387(1)	21(1)
Cl(2B)	5763(1)	7493(1)	7365(1)	23(1)
Cl(3B)	3627(1)	9918(1)	7972(1)	19(1)
Cl(4B)	6105(1)	11800(1)	7910(1)	20(1)
Cl(5B)	8301(1)	10645(1)	8695(1)	21(1)
Cl(6B)	7856(1)	7508(1)	8354(1)	24(1)
Cl(7B)	4765(1)	7642(1)	8708(1)	24(1)
Cl(8B)	5145(1)	10772(1)	9099(1)	22(1)
Cl(9B)	7044(1)	8689(1)	9533(1)	23(1)
C(1S)	8642(3)	671(3)	302(2)	59(1)
Cl(1S)	9827(1)	1362(1)	359(1)	72(1)
Cl(2S)	7599(1)	1273(1)	582(1)	81(1)
C(1D)	8460(15)	820(20)	586(14)	59(1)
Cl(1D)	7143(11)	1243(10)	608(7)	72(1)
Cl(2D)	9170(9)	1573(11)	175(5)	81(1)
C(1E)	7909(17)	1810(40)	486(16)	97(9)
Cl(1E)	7858(15)	2645(9)	1022(6)	112(6)
Cl(2E)	6661(14)	1287(10)	267(5)	101(5)

Table 3. Bond lengths [Å] and angles [°] for vL304CL_0m.

Ag(1)-N(2)	2.1129(18)
Ag(1)-P(1)	2.3837(5)
N(1)-C(2)	1.134(3)
N(1)-Ag(2)	2.2152(19)
C(2)-C(3)	1.453(3)
C(3)-H(3A)	0.9800
C(3)-H(3B)	0.9800
C(3)-H(3C)	0.9800
Ag(2)-Cl(7B)	2.6981(5)
Ag(2)-Cl(9A)#1	2.7432(5)
Ag(2)-Cl(7A)#1	2.9094(5)
N(2)-C(4)	1.130(3)
C(4)-C(5)	1.448(3)
C(5)-H(5A)	0.9800
C(5)-H(5B)	0.9800
C(5)-H(5C)	0.9800
P(1)-C(1B)	1.8316(19)
P(1)-C(1A)	1.8465(18)
P(1)-Cl(1)	2.0104(6)
C(1A)-B(5A)	1.639(3)
C(1A)-B(4A)	1.640(3)
C(1A)-B(2A)	1.655(3)
C(1A)-B(3A)	1.660(3)
B(2A)-Cl(1A)	1.774(2)
B(2A)-B(6A)	1.809(3)
B(2A)-B(7A)	1.822(3)
B(2A)-B(3A)	1.832(3)
B(2A)-B(5A)	1.870(3)
B(3A)-Cl(2A)	1.767(2)
B(3A)-B(8A)	1.810(3)
B(3A)-B(7A)	1.822(3)
B(3A)-B(4A)	1.871(3)

B(4A)-Cl(3A)	1.7630(19)
B(4A)-B(9A)	1.822(3)
B(4A)-B(8A)	1.834(3)
B(4A)-B(5A)	1.876(3)
B(5A)-Cl(4A)	1.760(2)
B(5A)-B(6A)	1.837(3)
B(5A)-B(9A)	1.838(3)
B(6A)-B(10A)	1.694(3)
B(6A)-Cl(5A)	1.781(2)
B(6A)-B(7A)	1.854(3)
B(6A)-B(9A)	1.875(3)
B(7A)-B(10A)	1.681(3)
B(7A)-Cl(6A)	1.777(2)
B(7A)-B(8A)	1.853(3)
B(8A)-B(10A)	1.695(3)
B(8A)-Cl(7A)	1.787(2)
B(8A)-B(9A)	1.854(3)
B(9A)-B(10A)	1.691(3)
B(9A)-Cl(8A)	1.777(2)
B(10A)-Cl(9A)	1.775(2)
Cl(7A)-Ag(2)#2	2.9095(5)
Cl(9A)-Ag(2)#2	2.7434(5)
C(1B)-B(3B)	1.620(3)
C(1B)-B(4B)	1.630(3)
C(1B)-B(5B)	1.656(3)
C(1B)-B(2B)	1.659(3)
B(2B)-Cl(1B)	1.766(2)
B(2B)-B(7B)	1.835(3)
B(2B)-B(6B)	1.837(3)
B(2B)-B(5B)	1.844(3)
B(2B)-B(3B)	1.847(3)
B(3B)-Cl(2B)	1.758(2)
B(3B)-B(7B)	1.815(3)
B(3B)-B(8B)	1.837(3)

B(3B)-B(4B)	1.923(3)
B(4B)-Cl(3B)	1.762(2)
B(4B)-B(8B)	1.805(3)
B(4B)-B(9B)	1.823(3)
B(4B)-B(5B)	1.846(3)
B(5B)-Cl(4B)	1.768(2)
B(5B)-B(6B)	1.816(3)
B(5B)-B(9B)	1.830(3)
B(6B)-B(10B)	1.694(3)
B(6B)-Cl(5B)	1.783(2)
B(6B)-B(7B)	1.858(3)
B(6B)-B(9B)	1.859(3)
B(7B)-B(10B)	1.689(3)
B(7B)-Cl(6B)	1.787(2)
B(7B)-B(8B)	1.842(3)
B(8B)-B(10B)	1.698(3)
B(8B)-Cl(7B)	1.796(2)
B(8B)-B(9B)	1.870(3)
B(9B)-B(10B)	1.682(3)
B(9B)-Cl(8B)	1.773(2)
B(10B)-Cl(9B)	1.766(2)
C(1S)-Cl(2S)	1.741(4)
C(1S)-Cl(1S)	1.744(4)
C(1S)-H(1A)	0.9900
C(1S)-H(1B)	0.9900
C(1D)-Cl(2D)	1.746(9)
C(1D)-Cl(1D)	1.754(9)
C(1D)-H(1C)	0.9900
C(1D)-H(1D)	0.9900
C(1E)-Cl(1E)	1.754(9)
C(1E)-Cl(2E)	1.754(9)
C(1E)-H(1E)	0.9900
C(1E)-H(1F)	0.9900

N(2)-Ag(1)-P(1)	175.11(6)
C(2)-N(1)-Ag(2)	163.55(19)
N(1)-C(2)-C(3)	178.5(2)
C(2)-C(3)-H(3A)	109.5
C(2)-C(3)-H(3B)	109.5
H(3A)-C(3)-H(3B)	109.5
C(2)-C(3)-H(3C)	109.5
H(3A)-C(3)-H(3C)	109.5
H(3B)-C(3)-H(3C)	109.5
N(1)-Ag(2)-Cl(7B)	117.16(5)
N(1)-Ag(2)-Cl(9A)#1	108.77(5)
Cl(7B)-Ag(2)-Cl(9A)#1	99.180(16)
N(1)-Ag(2)-Cl(7A)#1	84.00(5)
Cl(7B)-Ag(2)-Cl(7A)#1	155.851(16)
Cl(9A)#1-Ag(2)-Cl(7A)#1	83.396(14)
C(4)-N(2)-Ag(1)	167.09(18)
N(2)-C(4)-C(5)	178.7(2)
C(4)-C(5)-H(5A)	109.5
C(4)-C(5)-H(5B)	109.5
H(5A)-C(5)-H(5B)	109.5
C(4)-C(5)-H(5C)	109.5
H(5A)-C(5)-H(5C)	109.5
H(5B)-C(5)-H(5C)	109.5
C(1B)-P(1)-C(1A)	115.66(8)
C(1B)-P(1)-Cl(1)	102.99(6)
C(1A)-P(1)-Cl(1)	102.84(6)
C(1B)-P(1)-Ag(1)	114.35(6)
C(1A)-P(1)-Ag(1)	109.23(6)
Cl(1)-P(1)-Ag(1)	110.94(2)
B(5A)-C(1A)-B(4A)	69.77(12)
B(5A)-C(1A)-B(2A)	69.20(11)
B(4A)-C(1A)-B(2A)	105.95(14)
B(5A)-C(1A)-B(3A)	106.12(14)
B(4A)-C(1A)-B(3A)	69.07(12)

B(2A)-C(1A)-B(3A)	67.12(12)
B(5A)-C(1A)-P(1)	140.51(13)
B(4A)-C(1A)-P(1)	130.52(12)
B(2A)-C(1A)-P(1)	120.50(12)
B(3A)-C(1A)-P(1)	112.82(11)
C(1A)-B(2A)-Cl(1A)	122.18(13)
C(1A)-B(2A)-B(6A)	109.51(13)
Cl(1A)-B(2A)-B(6A)	121.62(13)
C(1A)-B(2A)-B(7A)	110.58(14)
Cl(1A)-B(2A)-B(7A)	116.19(12)
B(6A)-B(2A)-B(7A)	61.40(11)
C(1A)-B(2A)-B(3A)	56.57(11)
Cl(1A)-B(2A)-B(3A)	126.74(13)
B(6A)-B(2A)-B(3A)	102.82(13)
B(7A)-B(2A)-B(3A)	59.80(11)
C(1A)-B(2A)-B(5A)	55.00(10)
Cl(1A)-B(2A)-B(5A)	135.15(13)
B(6A)-B(2A)-B(5A)	59.87(11)
B(7A)-B(2A)-B(5A)	103.13(13)
B(3A)-B(2A)-B(5A)	90.80(12)
C(1A)-B(3A)-Cl(2A)	122.12(13)
C(1A)-B(3A)-B(8A)	109.31(13)
Cl(2A)-B(3A)-B(8A)	121.55(13)
C(1A)-B(3A)-B(7A)	110.35(14)
Cl(2A)-B(3A)-B(7A)	116.86(13)
B(8A)-B(3A)-B(7A)	61.37(11)
C(1A)-B(3A)-B(2A)	56.31(10)
Cl(2A)-B(3A)-B(2A)	127.47(13)
B(8A)-B(3A)-B(2A)	102.65(13)
B(7A)-B(3A)-B(2A)	59.81(11)
C(1A)-B(3A)-B(4A)	54.98(10)
Cl(2A)-B(3A)-B(4A)	134.56(13)
B(8A)-B(3A)-B(4A)	59.73(11)
B(7A)-B(3A)-B(4A)	102.95(13)

B(2A)-B(3A)-B(4A)	90.53(12)
C(1A)-B(4A)-Cl(3A)	124.40(13)
C(1A)-B(4A)-B(9A)	109.05(14)
Cl(3A)-B(4A)-B(9A)	117.86(12)
C(1A)-B(4A)-B(8A)	109.05(13)
Cl(3A)-B(4A)-B(8A)	118.69(13)
B(9A)-B(4A)-B(8A)	60.94(11)
C(1A)-B(4A)-B(3A)	55.96(11)
Cl(3A)-B(4A)-B(3A)	133.29(13)
B(9A)-B(4A)-B(3A)	101.02(13)
B(8A)-B(4A)-B(3A)	58.47(11)
C(1A)-B(4A)-B(5A)	55.08(10)
Cl(3A)-B(4A)-B(5A)	131.47(13)
B(9A)-B(4A)-B(5A)	59.60(11)
B(8A)-B(4A)-B(5A)	101.97(13)
B(3A)-B(4A)-B(5A)	89.46(12)
C(1A)-B(5A)-Cl(4A)	126.96(14)
C(1A)-B(5A)-B(6A)	108.89(13)
Cl(4A)-B(5A)-B(6A)	116.45(12)
C(1A)-B(5A)-B(9A)	108.33(14)
Cl(4A)-B(5A)-B(9A)	116.55(12)
B(6A)-B(5A)-B(9A)	61.36(11)
C(1A)-B(5A)-B(2A)	55.79(10)
Cl(4A)-B(5A)-B(2A)	133.72(13)
B(6A)-B(5A)-B(2A)	58.40(10)
B(9A)-B(5A)-B(2A)	100.74(13)
C(1A)-B(5A)-B(4A)	55.15(10)
Cl(4A)-B(5A)-B(4A)	132.76(13)
B(6A)-B(5A)-B(4A)	101.76(13)
B(9A)-B(5A)-B(4A)	58.74(11)
B(2A)-B(5A)-B(4A)	89.22(12)
B(10A)-B(6A)-Cl(5A)	120.33(13)
B(10A)-B(6A)-B(2A)	110.87(14)
Cl(5A)-B(6A)-B(2A)	119.86(13)

B(10A)-B(6A)-B(5A)	111.19(14)
Cl(5A)-B(6A)-B(5A)	119.06(13)
B(2A)-B(6A)-B(5A)	61.72(11)
B(10A)-B(6A)-B(7A)	56.37(11)
Cl(5A)-B(6A)-B(7A)	131.17(13)
B(2A)-B(6A)-B(7A)	59.64(11)
B(5A)-B(6A)-B(7A)	103.20(13)
B(10A)-B(6A)-B(9A)	56.28(11)
Cl(5A)-B(6A)-B(9A)	131.77(13)
B(2A)-B(6A)-B(9A)	101.65(13)
B(5A)-B(6A)-B(9A)	59.35(11)
B(7A)-B(6A)-B(9A)	89.60(12)
B(10A)-B(7A)-Cl(6A)	121.54(14)
B(10A)-B(7A)-B(3A)	110.96(14)
Cl(6A)-B(7A)-B(3A)	119.05(13)
B(10A)-B(7A)-B(2A)	110.82(14)
Cl(6A)-B(7A)-B(2A)	118.91(13)
B(3A)-B(7A)-B(2A)	60.38(11)
B(10A)-B(7A)-B(8A)	57.07(11)
Cl(6A)-B(7A)-B(8A)	131.99(13)
B(3A)-B(7A)-B(8A)	59.00(11)
B(2A)-B(7A)-B(8A)	101.37(13)
B(10A)-B(7A)-B(6A)	57.00(11)
Cl(6A)-B(7A)-B(6A)	131.56(13)
B(3A)-B(7A)-B(6A)	101.50(13)
B(2A)-B(7A)-B(6A)	58.96(11)
B(8A)-B(7A)-B(6A)	90.40(12)
B(10A)-B(8A)-Cl(7A)	121.39(14)
B(10A)-B(8A)-B(3A)	110.88(14)
Cl(7A)-B(8A)-B(3A)	119.14(13)
B(10A)-B(8A)-B(4A)	111.16(14)
Cl(7A)-B(8A)-B(4A)	118.03(12)
B(3A)-B(8A)-B(4A)	61.79(11)
B(10A)-B(8A)-B(7A)	56.35(11)

Cl(7A)-B(8A)-B(7A)	131.84(13)
B(3A)-B(8A)-B(7A)	59.63(11)
B(4A)-B(8A)-B(7A)	103.18(13)
B(10A)-B(8A)-B(9A)	56.69(11)
Cl(7A)-B(8A)-B(9A)	131.16(13)
B(3A)-B(8A)-B(9A)	102.13(13)
B(4A)-B(8A)-B(9A)	59.21(11)
B(7A)-B(8A)-B(9A)	90.27(12)
B(10A)-B(9A)-Cl(8A)	119.00(14)
B(10A)-B(9A)-B(4A)	111.97(14)
Cl(8A)-B(9A)-B(4A)	119.36(12)
B(10A)-B(9A)-B(5A)	111.27(14)
Cl(8A)-B(9A)-B(5A)	120.60(13)
B(4A)-B(9A)-B(5A)	61.66(11)
B(10A)-B(9A)-B(8A)	56.93(11)
Cl(8A)-B(9A)-B(8A)	130.17(13)
B(4A)-B(9A)-B(8A)	59.85(11)
B(5A)-B(9A)-B(8A)	102.65(13)
B(10A)-B(9A)-B(6A)	56.43(11)
Cl(8A)-B(9A)-B(6A)	132.14(13)
B(4A)-B(9A)-B(6A)	102.37(13)
B(5A)-B(9A)-B(6A)	59.29(11)
B(8A)-B(9A)-B(6A)	89.72(12)
B(7A)-B(10A)-B(9A)	102.38(14)
B(7A)-B(10A)-B(6A)	66.63(12)
B(9A)-B(10A)-B(6A)	67.29(12)
B(7A)-B(10A)-B(8A)	66.58(12)
B(9A)-B(10A)-B(8A)	66.39(12)
B(6A)-B(10A)-B(8A)	101.82(14)
B(7A)-B(10A)-Cl(9A)	129.66(14)
B(9A)-B(10A)-Cl(9A)	127.96(14)
B(6A)-B(10A)-Cl(9A)	128.51(13)
B(8A)-B(10A)-Cl(9A)	129.66(14)
B(8A)-Cl(7A)-Ag(2)#2	101.11(7)

B(10A)-Cl(9A)-Ag(2)#2	101.37(7)
B(3B)-C(1B)-B(4B)	72.51(13)
B(3B)-C(1B)-B(5B)	106.95(15)
B(4B)-C(1B)-B(5B)	68.35(12)
B(3B)-C(1B)-B(2B)	68.52(12)
B(4B)-C(1B)-B(2B)	106.80(15)
B(5B)-C(1B)-B(2B)	67.58(12)
B(3B)-C(1B)-P(1)	133.05(13)
B(4B)-C(1B)-P(1)	120.88(12)
B(5B)-C(1B)-P(1)	119.90(12)
B(2B)-C(1B)-P(1)	131.27(13)
C(1B)-B(2B)-Cl(1B)	125.04(15)
C(1B)-B(2B)-B(7B)	107.45(14)
Cl(1B)-B(2B)-B(7B)	118.59(13)
C(1B)-B(2B)-B(6B)	109.06(14)
Cl(1B)-B(2B)-B(6B)	118.52(13)
B(7B)-B(2B)-B(6B)	60.78(12)
C(1B)-B(2B)-B(5B)	56.11(11)
Cl(1B)-B(2B)-B(5B)	132.57(14)
B(7B)-B(2B)-B(5B)	101.21(14)
B(6B)-B(2B)-B(5B)	59.13(11)
C(1B)-B(2B)-B(3B)	54.74(11)
Cl(1B)-B(2B)-B(3B)	130.42(14)
B(7B)-B(2B)-B(3B)	59.07(11)
B(6B)-B(2B)-B(3B)	102.81(14)
B(5B)-B(2B)-B(3B)	91.02(12)
C(1B)-B(3B)-Cl(2B)	122.30(15)
C(1B)-B(3B)-B(7B)	110.15(14)
Cl(2B)-B(3B)-B(7B)	116.27(13)
C(1B)-B(3B)-B(8B)	106.79(14)
Cl(2B)-B(3B)-B(8B)	124.83(13)
B(7B)-B(3B)-B(8B)	60.56(12)
C(1B)-B(3B)-B(2B)	56.74(11)
Cl(2B)-B(3B)-B(2B)	124.86(14)

B(7B)-B(3B)-B(2B)	60.13(11)
B(8B)-B(3B)-B(2B)	101.63(14)
C(1B)-B(3B)-B(4B)	53.98(11)
Cl(2B)-B(3B)-B(4B)	138.97(13)
B(7B)-B(3B)-B(4B)	99.96(14)
B(8B)-B(3B)-B(4B)	57.34(11)
B(2B)-B(3B)-B(4B)	88.95(12)
C(1B)-B(4B)-Cl(3B)	121.37(14)
C(1B)-B(4B)-B(8B)	107.83(14)
Cl(3B)-B(4B)-B(8B)	124.42(13)
C(1B)-B(4B)-B(9B)	110.67(14)
Cl(3B)-B(4B)-B(9B)	115.81(13)
B(8B)-B(4B)-B(9B)	62.06(12)
C(1B)-B(4B)-B(5B)	56.47(11)
Cl(3B)-B(4B)-B(5B)	125.36(13)
B(8B)-B(4B)-B(5B)	101.99(13)
B(9B)-B(4B)-B(5B)	59.86(11)
C(1B)-B(4B)-B(3B)	53.50(11)
Cl(3B)-B(4B)-B(3B)	137.75(14)
B(8B)-B(4B)-B(3B)	58.95(12)
B(9B)-B(4B)-B(3B)	102.38(13)
B(5B)-B(4B)-B(3B)	88.61(12)
C(1B)-B(5B)-Cl(4B)	121.50(14)
C(1B)-B(5B)-B(6B)	110.25(14)
Cl(4B)-B(5B)-B(6B)	120.01(13)
C(1B)-B(5B)-B(9B)	109.13(14)
Cl(4B)-B(5B)-B(9B)	119.83(13)
B(6B)-B(5B)-B(9B)	61.31(11)
C(1B)-B(5B)-B(2B)	56.31(11)
Cl(4B)-B(5B)-B(2B)	130.25(14)
B(6B)-B(5B)-B(2B)	60.27(11)
B(9B)-B(5B)-B(2B)	103.49(13)
C(1B)-B(5B)-B(4B)	55.18(11)
Cl(4B)-B(5B)-B(4B)	130.29(13)

B(6B)-B(5B)-B(4B)	102.83(13)
B(9B)-B(5B)-B(4B)	59.44(11)
B(2B)-B(5B)-B(4B)	91.42(12)
B(10B)-B(6B)-Cl(5B)	121.07(14)
B(10B)-B(6B)-B(5B)	110.67(14)
Cl(5B)-B(6B)-B(5B)	119.04(13)
B(10B)-B(6B)-B(2B)	111.22(15)
Cl(5B)-B(6B)-B(2B)	119.45(13)
B(5B)-B(6B)-B(2B)	60.61(11)
B(10B)-B(6B)-B(7B)	56.58(12)
Cl(5B)-B(6B)-B(7B)	132.65(13)
B(5B)-B(6B)-B(7B)	101.38(13)
B(2B)-B(6B)-B(7B)	59.54(11)
B(10B)-B(6B)-B(9B)	56.28(11)
Cl(5B)-B(6B)-B(9B)	130.44(14)
B(5B)-B(6B)-B(9B)	59.72(11)
B(2B)-B(6B)-B(9B)	102.61(14)
B(7B)-B(6B)-B(9B)	89.97(13)
B(10B)-B(7B)-Cl(6B)	117.55(14)
B(10B)-B(7B)-B(3B)	112.96(15)
Cl(6B)-B(7B)-B(3B)	118.40(13)
B(10B)-B(7B)-B(2B)	111.57(14)
Cl(6B)-B(7B)-B(2B)	123.08(14)
B(3B)-B(7B)-B(2B)	60.79(11)
B(10B)-B(7B)-B(8B)	57.29(12)
Cl(6B)-B(7B)-B(8B)	127.85(14)
B(3B)-B(7B)-B(8B)	60.32(12)
B(2B)-B(7B)-B(8B)	101.92(13)
B(10B)-B(7B)-B(6B)	56.82(12)
Cl(6B)-B(7B)-B(6B)	133.02(14)
B(3B)-B(7B)-B(6B)	103.26(13)
B(2B)-B(7B)-B(6B)	59.69(11)
B(8B)-B(7B)-B(6B)	90.41(13)
B(10B)-B(8B)-Cl(7B)	119.37(15)

B(10B)-B(8B)-B(4B)	110.99(14)
Cl(7B)-B(8B)-B(4B)	120.77(13)
B(10B)-B(8B)-B(3B)	111.46(15)
Cl(7B)-B(8B)-B(3B)	118.14(13)
B(4B)-B(8B)-B(3B)	63.71(12)
B(10B)-B(8B)-B(7B)	56.85(12)
Cl(7B)-B(8B)-B(7B)	129.02(13)
B(4B)-B(8B)-B(7B)	103.44(14)
B(3B)-B(8B)-B(7B)	59.12(12)
B(10B)-B(8B)-B(9B)	56.00(11)
Cl(7B)-B(8B)-B(9B)	132.69(15)
B(4B)-B(8B)-B(9B)	59.42(11)
B(3B)-B(8B)-B(9B)	103.87(14)
B(7B)-B(8B)-B(9B)	90.12(13)
B(10B)-B(9B)-Cl(8B)	121.28(15)
B(10B)-B(9B)-B(4B)	110.90(15)
Cl(8B)-B(9B)-B(4B)	119.00(13)
B(10B)-B(9B)-B(5B)	110.55(15)
Cl(8B)-B(9B)-B(5B)	119.55(13)
B(4B)-B(9B)-B(5B)	60.70(11)
B(10B)-B(9B)-B(6B)	56.89(11)
Cl(8B)-B(9B)-B(6B)	131.46(14)
B(4B)-B(9B)-B(6B)	102.06(14)
B(5B)-B(9B)-B(6B)	58.97(11)
B(10B)-B(9B)-B(8B)	56.81(12)
Cl(8B)-B(9B)-B(8B)	132.88(14)
B(4B)-B(9B)-B(8B)	58.52(11)
B(5B)-B(9B)-B(8B)	100.12(14)
B(6B)-B(9B)-B(8B)	89.48(13)
B(9B)-B(10B)-B(7B)	102.39(16)
B(9B)-B(10B)-B(6B)	66.83(13)
B(7B)-B(10B)-B(6B)	66.60(13)
B(9B)-B(10B)-B(8B)	67.19(13)
B(7B)-B(10B)-B(8B)	65.87(13)

B(6B)-B(10B)-B(8B)	101.42(15)
B(9B)-B(10B)-Cl(9B)	130.32(15)
B(7B)-B(10B)-Cl(9B)	127.21(14)
B(6B)-B(10B)-Cl(9B)	131.39(14)
B(8B)-B(10B)-Cl(9B)	127.12(14)
B(8B)-Cl(7B)-Ag(2)	98.14(7)
Cl(2S)-C(1S)-Cl(1S)	113.2(2)
Cl(2S)-C(1S)-H(1A)	108.9
Cl(1S)-C(1S)-H(1A)	108.9
Cl(2S)-C(1S)-H(1B)	108.9
Cl(1S)-C(1S)-H(1B)	108.9
H(1A)-C(1S)-H(1B)	107.8
Cl(2D)-C(1D)-Cl(1D)	111.8(8)
Cl(2D)-C(1D)-H(1C)	109.3
Cl(1D)-C(1D)-H(1C)	109.3
Cl(2D)-C(1D)-H(1D)	109.3
Cl(1D)-C(1D)-H(1D)	109.3
H(1C)-C(1D)-H(1D)	107.9
Cl(1E)-C(1E)-Cl(2E)	113.3(9)
Cl(1E)-C(1E)-H(1E)	108.9
Cl(2E)-C(1E)-H(1E)	108.9
Cl(1E)-C(1E)-H(1F)	108.9
Cl(2E)-C(1E)-H(1F)	108.9
H(1E)-C(1E)-H(1F)	107.7

Symmetry transformations used to generate equivalent atoms:
#1 x+1/2,-y+3/2,z+1/2 #2 x-1/2,-y+3/2,z-1/2

5.5.7 Synthesis of **11**

Compound **8** (153 mg, 0.10 mmol) was repeatedly dissolved in acetonitrile followed by removal of solvent under reduced pressure (4 mL x 6). The residue was then

dissolved in CH_2Cl_2 and excess trityl chloride was added to the solution which immediately turned a vibrant yellow color with precipitation quickly visible. After stirring the reaction overnight, the mixture was filtered and then crashed out in pentane. Washing with pentane (15 mL x 1) and then benzene (15 mL x 4) was followed with drying on high vac overnight. 130mg of a yellow powder **11** (92.3 % yield) was isolated. ^{1}H NMR (600 MHz, CD_2Cl_2, 25 °C) δ = 8.28 (tt, 6H, CH_{aryl}, ^{3}J (*H-H*) = 7.4 Hz, ^{4}J (*H-H*), δ = 7.90 (tt, 12H, CH_{aryl}, ^{3}J (*H-H*) = 7.6 Hz, ^{4}J (*H-H*), = 1.4 Hz), δ = 7.68 (m, 12H, CH_{aryl}). ^{11}B-(^{1}H-dec) NMR (192 MHz, CD_2Cl_2, 25 °C) δ = 23.00, -3.36, -5.85. ^{13}C-(^{1}H-dec) NMR (151 MHz,CD_2Cl_2) δ = 210.9 (C_{trityl}), 143.8 (CH$_{aryl}$), 143.0 (CH$_{aryl}$), 140.2 (C_{aryl}), 130.9 (CH$_{aryl}$). ^{31}P-(^{1}H-dec) NMR (243 MHz, CD_2Cl_2, 25 °C) δ = 120.10.

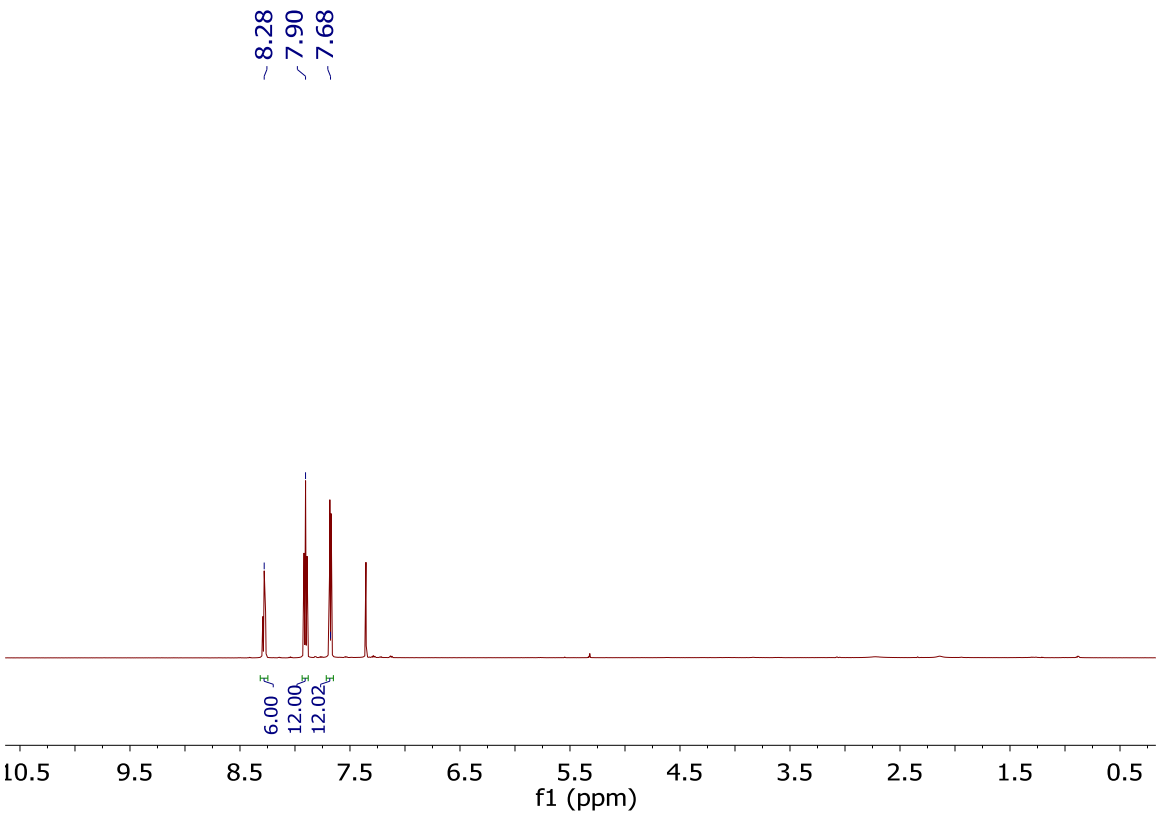

S-5.13 ^{1}H NMR of **11** (600 MHz, CD_2Cl_2).

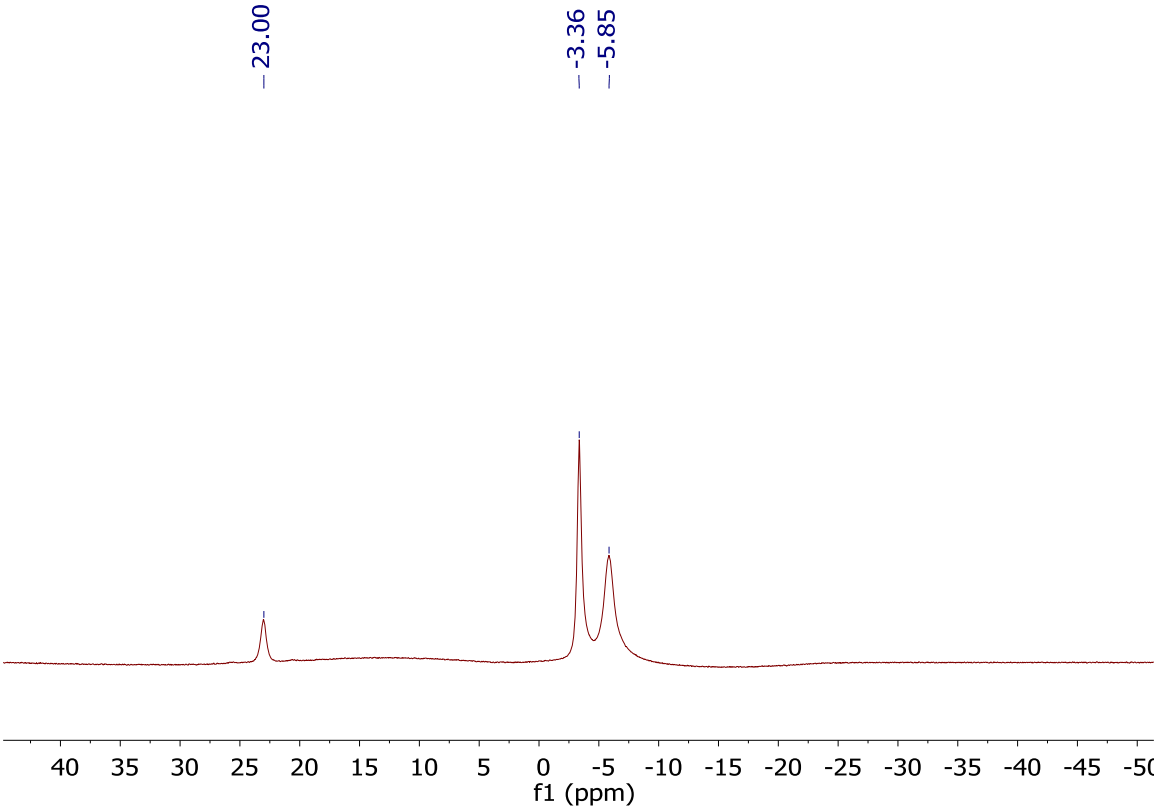

S-5.14 ^{11}B-(^{1}H-dec) NMR of **11** (192 MHz, CD_2Cl_2).

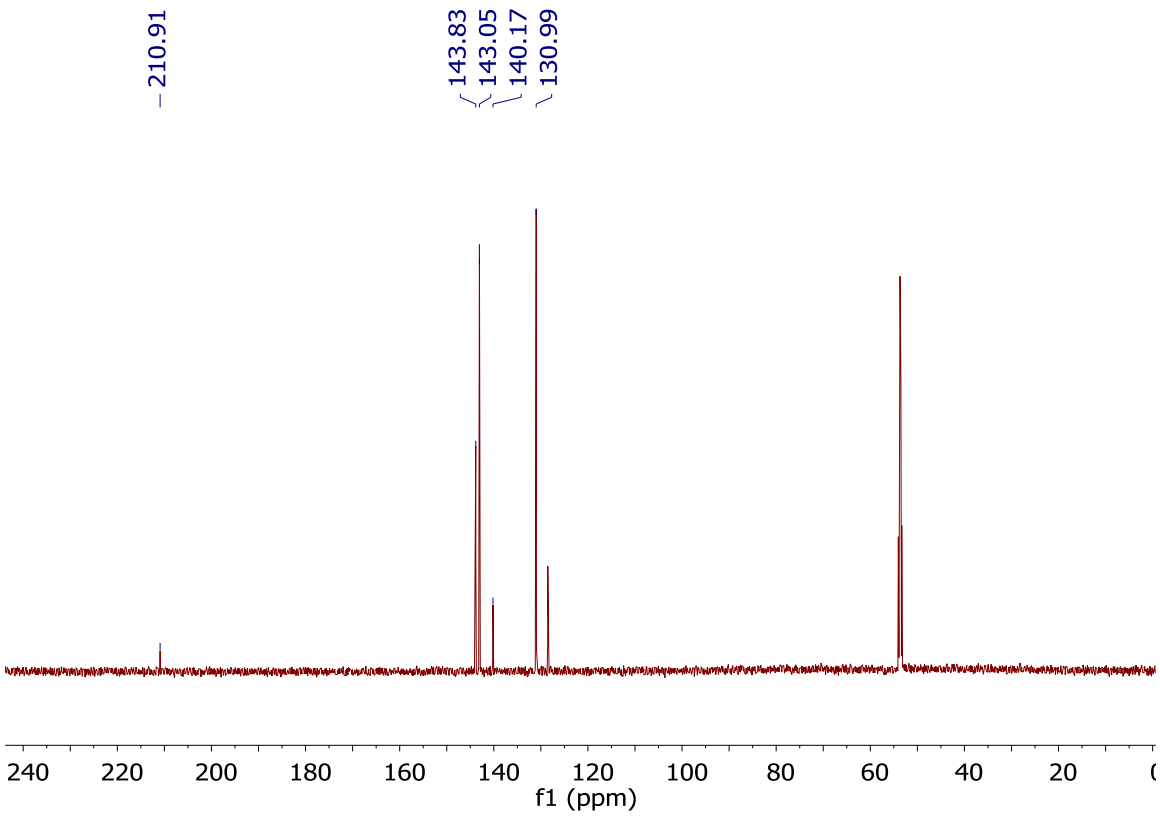

S-5.15 ^{13}C-(^{1}H-dec) NMR of **11** (151 MHz,CD_2Cl_2).

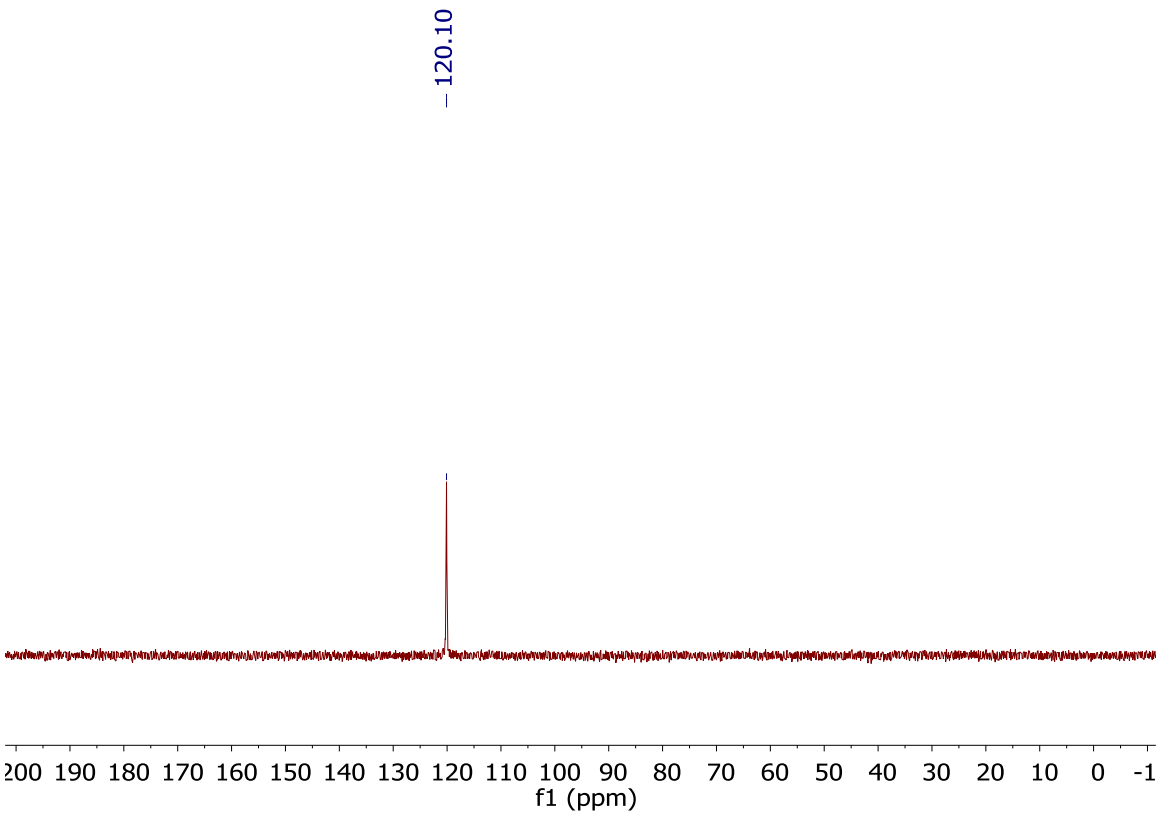

S-5.16 ^{31}P-(^{1}H-dec) NMR of **11** (243 MHz, CD_2Cl_2).

5.6 References

1. E. L. Hoel, M. F. Hawthorne, *J. Am. Chem. Soc.,* **1975,** *97*, 6388.

2. R. Wiesbock, M. F. Hawthorne, *J. Am. Chem. Soc.,* **1964**, *86*, 1962.

3. J. H. Wright II, C. E. Kefalidis, F. S. Tham, L. Maron, V. Lavallo, *Inorg. Chem.,* **2013**, 52, 6223.

4. J. Estrada, D. H. Woen, F. S. Tham, G. M. Miyake, V. Lavallo, *Inorg. Chem*., **2015**, 54, 5142.

5. A. L. Chan, J. Estrada, C. E Kefalidis, V. Lavallo, *Organometallics*, **2016,** 35, 3257.

6. J. Estrada, C. A. Lugo, S. G. McArthur, V. Lavallo, *Chem. Commun.,* **2016,** 52, 1824.

7. A. Franken, C. A. Kilner, M. Thornton-Pett, J. D. Kennedy, *Chem. Commun.,* **2002,** *18*, 2048.

8. K. Moesdritzer, L. Maier, L. C. D. Groenweghe, *J. Chem. Eng. Data*, **1962**, *7*, 307.

9. (a) M. Nava, I. V. Stoyanova, S. Cummings, E. S. Stoyanov, C. A. Reed, *Angew. Chem., Int. Ed.,* **2014**, *53*, 1131. (b) A. S. Jalilov, L. Han, S. F. Nelsen, I. A. Guzei, *J. Org. Chem.,* **2013**, *78*, 11373. (c) K. C. Kim, F. Hauke, A. Hirsch, P. D. W. Boyd, E. Carter, R. S. Armstrong, P. A. Lay, C. A. Reed, *J. Am. Chem. Soc.,* **2003**, *125*, 4024. (d) R. H. Xie, G. W. Bryant, G. Y. Sun, M. C. Nicklaus, D. Heringer, T. Frauenheim, M. R. Manaa, V. H. Smith, Y. Araki, O. Ito, *J. Chem. Phys.,* **2004**, *120*, 5133.

10. (a) M. K. Denk, S. Gupta, A. J. Lough, *Eur. J. Inorg. Chem.,* **1999**, 41. (b) M. K. Denk, S. Gupta, R. Ramachandran, *Tetrahedron Lett.,* **1996***, 37,* 9025. (c) C. J. Carmalt, V. Lomeli, B. G. McBurnett, A. H. Cowley, *Chem. Commun*. **1997**, 2097.

11. *APEX 2,* version 2014.1-1, Bruker (2014), Bruker AXS Inc., Madison, Wisconsin, USA.

12. *SAINT,* version V8.34A, Bruker (2012), Bruker AXS Inc., Madison, Wisconsin, USA.

13. *SADABS,* version 2012/1, Bruker (2012), Bruker AXS Inc., Madison, Wisconsin, USA.

14. *SHELXTL,* version 2013/4, Bruker (2013), Bruker AXS Inc., Madison, Wisconsin, USA.